Département de Physique

Université de Fribourg (Suisse)

Dielectric Catastrophe at the Mott Transition

THESE

présentée à la Faculté des Sciences de l'Université de Fribourg (Suisse)
pour l'obtention du grade de *Doctor rerum naturalium*

CHRISTOPHE AEBISCHER

de

La Brillaz

Thèse No. 1367

Mécanographie, Université de Fribourg

2002

Acceptée par la Faculté des Sciences de l'Université de Fribourg (Suisse) sur la proposition de Dionys Baeriswyl, Reinhard Noack et George Japaridze

Fribourg, le 23 janvier 2002

Le directeur de thèse:

D. Baeriswyl

Prof. Dr. Dionys Baeriswyl

Le doyen:

A. v. Zelewsky

Prof. Dr. Alex von Zelewsky

To my parents and

Gabriella

Acknowledgments

C'est tout d'abord mes parents, Danielle et Emile, que j'aimerais remercier chaleureusement pour leur soutien immuable et leur amour qui m'a conduit jusqu'à ce jour. Mia cucciolina bellissima, sono tutto emozionato quando penso a tutto il tuo amore, che mi ha sostenuto duranto questo lavoro e ti invio tantissimi baci, ti amo. Vorrei anche ringraziare i tuoi genitori, Claudia e Vittorio, per la loro amicizia e le loro numerose invitazioni a Genova. Je voudrais également remercier mes amis / meine Freunde möchte ich auch bedanken / vorrei anche ringraziare i miei amici / tak / spassiba for sharing so many moments together during those past four years, including wine and beer tasting and traveling reports: Philippe et Corina, Lars, René, Christoph, Damien, Andrea, Jérôme, Stéphane, Eric, Cédric, Paolo, Mark-Olivier, Uladzimir, Claudio, Yvan, Jessen, Thorsten, Carl-Alex, Anna, Valérie, Marc-Hadrien, Claude.

Of course I would like to warmly thank my thesis advisor, Dionys Baeriswyl, for having this great idea of investigating the *dielectric constant* in the Hubbard model, the starting point of this work, and for intense and enlightening discussions which most notably led to the publication of a "Physical Review Letters". Thanks a lot to Reinhard Noack, post-doc in Fribourg when I began my thesis, who reviewed my thesis as an external expert. A great word of thanks to George Japaridze, external expert as well, for many illuminating discussions during his visits at the Institute and of course for reviewing my thesis. A special $\varepsilon\upsilon\chi\alpha\rho\iota\sigma\tau\omega$ to Xenophon Zotos, who supported me with a couple of enlightening discussions. Another special thanks to Charles Stafford who made his Ph.D. in the same field ten years ago; his invitation for an unforgettable one-month stay at the University of Arizona in Tucson gave a strong momentum to the second part of my thesis. Thanks also to the army of professors at the now defunct Institute of Theoretical Physics: muit'obrigado a Alvaro Ferraz, who shared the office with me more than one year, for many refreshing digressions, merci à Xavier Bagnoud, next door neighbor and all time friend, thanks to Yi-Cheng Zhang, for friendship and "parallel" discussions, muit'obrigado a Cristiane de Morais Smith, all time confident.

I also would like to thank everybody at the Institute (especially Cristiane) for being so patient with my overwhelming use of the shared CPU time. I thank again Reinhard Noack and Charles Stafford for being so generous with their CPU time. I also thank Damien, Reinhard, Andrea for sharing the Linux/Unix system administration and the students for being good learners and good friends as well. A special thank to René Zbinden, who made his diploma thesis partly under my supervision: the theme was an idea of mine, a subject close to the one of my own thesis.

A last weird word of thanks goes to the virus of traveling: this work would *not* have been possible without those refreshing breaks in Holland, Chile, Argentina, Uruguay, Slovenia, Italy, Spain, Germany, Russia, Hawaii, Lebanon and Syria, since theoretical physics is about clear-sighted thinking.

Abstract

The Mott metal-insulator transition is investigated as a quantum phase transition. The $U-t-t'$ model at half-filling is considered as a paradigm; the sign of t' is not relevant and is taken to be positive. The phase diagram presents two Mott insulating phases with distinct symmetries and one global metallic phase which is presumed to be a Luttinger liquid for the charge degrees of freedom. We identify the bond order parameter of the large–t' Mott phase (dimerization). There are intriguing similarities with the phase diagram of the one-dimensional quantum sine-Gordon model.

At $t' \leq \frac{1}{2}$, the critical point is the same as in the simple Hubbard model, $U_c = 0$ and the metallic phase lies exclusively in the negative-U part of the phase diagram. On the other hand, for $t' > \frac{1}{2}$, there exists a metallic phase with *repulsive* U. Using the Density Matrix Renormalization Group (DMRG) we find that the electric susceptibility χ, finite for an insulator and infinite for a metal, diverges continuously as one approaches the critical point from the insulating side. This is the *dielectric catastrophe* predicted by Mott. By application of a detailed fitting procedure, we find that χ always diverges exponentially exactly the same way, whatever the value of t': it is an *infinite-order* transition. Simultaneously we have determined the transition line $U_c(t')$ and further shown that the correlation length ξ is proportional to the fluctuations of polarization, which are determined by the DMRG as well. ξ also diverges, and one finds $\chi \sim \xi^2$. The hyperscaling hypothesis is satisfied, i. e. physical quantities may be expressed in terms of universal functions of L/ξ_∞. In particular $\xi(L) = LS(L/\xi_\infty)$, which means that $\xi(L)/L$ has a *universal jump* at the metal-insulator transition. This latter quantity might be related to the Drude weight itself. This prediction was confirmed by DMRG calculations for several values of t'.

We also investigated analytically the band-insulator-to-metal transition. The electric susceptibility and the correlation length both have a power-law divergence, implying a *second order* transition. Hyperscaling is satisfied and the universal jump can be calculated exactly. We find again that $\chi \sim \xi^2$ as for the Mott transition. This may be a *universal* result, since it is in agreement with many experiments on metal-insulator transitions at zero temperature, where both correlation and disorder have an essential rôle.

Résumé

La transition métal-isolant de Mott est étudiée en tant que transition de phase quantique. Le modèle $U-t-t'$ à demi-remplissage est choisi comme paradigme; le signe de t' n'est pas pertinent et nous le prendrons positif. Le diagramme de phase présente deux phase isolantes de type Mott, avec des symétries distinctes, et une phase métallique globale, pressentie comme liquide de Luttinger pour les degrés de liberté de charge. Nous déterminons le paramètre d'ordre de lien de la phase de Mott à grand t' (dimérisation). Tout porte à croire qu'il s'agit là de la classe d'universalité du modèle de sine-Gordon quantique.

A $t' \leq \frac{1}{2}$, le point critique est le même que dans le modèle de Hubbard standard, $U_c = 0$ et la phase métallique se situe exclusivement dans la partie attractive du diagramme de phase (U négatif). Pour $t' > \frac{1}{2}$ par contre, il y a une phase métallique pour une interaction U *répulsive*. Grâce à GRMD (Groupe de Renormalisation de la Matrice Densité) nous obtenons une susceptibilité χ finie pour un isolant et infinie pour un métal, et qui diverge continûment lorsque l'on approche le point critique depuis la phase isolante. Ce n'est rien d'autre que la *catastrophe diélectrique* prédite par Mott. Une procédure de fit réalisée avec précaution révèle que χ diverge exponentiellement et ce, toujours exactement de la même façon, quelque soit t': il s'agit d'une transition d'*ordre infini*. La ligne de transition $U_c(t')$ est déterminée en même temps. Par la suite, nous montrons que la longueur de corrélation ξ est proportionelle aux fluctuations de polarisation et nous la calculons en utilisant GRMD également. ξ diverge aussi, et $\chi \sim \xi^2$. L'hypothèse de hyperscaling est satisfaite, c'est-à-dire que les quantités physiques peuvent être exprimées en termes de fonctions universelles de L/ξ_∞. En particulier, $\xi(L) = LS(L/\xi_\infty)$, ce qui signifie que $\xi(L)/L$ présentera un *saut universel* à la transition métal-isolant. Cette prédiction fut confirmé par les calculs du GRMD pour de nombreuses valeurs de t'.

Nous étudiâmes également la transition métal-isolant de bande, par des méthodes analytiques cependant. La susceptibilité électrique et la longueur de corrélation divergent toutes deux avec une loi de puissance, ce qui donne une transition de *deuxième ordre*. Le hyperscaling est également satisfait et le saut universel peut cette fois être déterminé exactement. Nous retrouvons la relation $\chi \sim \xi^2$, tout comme pour la transition de Mott. Il pourrait s'agir là d'un résultat universel, puisqu'il est en accord avec de nombreuses expériences sur des transitions métal-isolant à température nulle, où corrélation et désordre jouent tous deux des rôles essentiels.

Contents

Chapter 1

Introduction: Talking about Transitions

At the beginning of the 19th century, science, especially physics, was dominated by a pervasive *positivism*: the outlook that everything can and will be humanly known resonated as a universally acclaimed axiom. The subsequent discovery of quantum mechanics soon shattered this limited world view. In the following hundred years further developments repeatedly played such an iconoclastic role. Physics rediscovered an age-old socratic virtue: science is more about asking the right questions, about fruitful astonishment in the face of intricate puzzles, about opening minds rather than confining them in definitive and sterile solutions.

Such a revolution occurred in the study of *phase transitions* in the 1960s and 1970s. Old questions such as why does a magnet lose its properties when it is sufficiently heated, what is the origin of the liquid-gas transition and what determines the percolation threshold, could be addressed using a new paradigm. A realm of fascinating perspectives had just been opened up: the apparent stillness of a state of matter does not guarantee the immobility of its various properties. Drastic and abrupt changes may occur when the values of some parameters are varied in a particular way. Earlier theories sowed the premises for following ones: scaling ideas were introduced and the renormalization group was borrowed from quantum field theory [1]. While singular flashes of insight were provided by exact solutions, they were rather isolated, providing a lesson of humility for the physicist. However, success stories were plentiful; they kept enriching the fertile soil in which the theory of *classical* phase transitions was growing. Fascinating riddles still abound today: one could mention for example self-organized criticality or critical phenomena far from equilibrium, both domains in their infancy.

On the experimental side, the absolute zero of temperature was being approached. In this limit the entropy vanishes, as predicted by the third law of thermodynamics[1]. The system is in a unique quantum state, namely the ground state of the Hamiltonian $\mathcal{H}$ governing it. Is a phase transition possible at all without thermal fluctuations? However, total quiescence is nonsense at $T = 0$ because *quantum fluctuations* are inevitably present. These quantum

[1] also called the "Nernst theorem"

fluctuations will take over the role of the thermal fluctuations and can trigger a *quantum phase transition*, as introduced by Hertz in his pioneering work of 1975 [2]. The inspiration for the the study of quantum phase transitions came from the theory of classical phase transitions. After a solid basis was built[2], some reviews based on particular points of view and focusing on a few models were published [3, 4, 5]. The first complete presentation of the theory of quantum phase transitions, summarizing the past 20 years of research, was still lacking. A very nice book by Sachdev — which we highly recommend — published quite recently [6] filled this gap: quantum phase transitions are treated comprehensively rather than as cumbersome oddities. They are portrayed in terms of the standard theory of critical phenomena, compared with classical phase transitions. Subsequently, aspects of their quantum nature are investigated deeply.

The metal-insulator transition at zero temperature is one interesting class of quantum critical phenomena. However, it does not completely follow the general trends described above: no order parameter characterizing the metallic "ordered" phase has been identified and the applicability of scaling ideas is still a delicate issue [7]. Very much in the spirit described above, we would now like to try to ask the right questions in order to obtain a deeper understanding of the transition. The most fundamental question is: what distinguishes a metal from an insulator? "Its response to an applied electric field E" would be a starting point for a correct answer. But how is this response expressed? The answer is through the emergence of a *polarization* $\mathcal{P}(E)$, which diverges in a metal and remains finite in an insulator. One may justifiably claim that the introduction of the electric field is artificial and that explicit dependence on it should be removed. How can we then characterize the transition? The answer is by looking at the linear response, valid for a vanishingly small electric field E:

$$\mathcal{P} \;=\; \chi\, E\,. \tag{1.1}$$

The quantity χ is called the *electric susceptibility* and shares some properties with the polarization: it remains finite for an insulating state and is infinite in the thermodynamic limit for a metal. However, unlike the polarization, it is not explicitly dependent on the applied electric field. How does the transition occur? Does the system go abruptly from an insulator with a finite χ to a metal with an infinite one? The transition would then be discontinuous, e.g. first-order. Or will χ grow and eventually diverge in the insulating phase when approaching the metal? Mott put forward such a continuous scenario for the metamorphosis, which he named the *dielectric catastrophe* [8].

What now complicates the understanding is that experimental realizations of *continuous* $T = 0$ metal-insulator transitions are quite scarce [7]. Doped semi-conductors like Si:P are among the best studied systems: experiments are plentiful and quite exhaustive. Both the electric susceptibility and the correlation length have been measured. The results are in accordance with the dielectric catastrophe hypothesis (as will be seen in Eqs. 2.15 and 2.13). Unfortunately for the theoretician, materials like Si:P are extremely delicate to deal

[2]Note that the advent of computational physics freed this emerging field of research from the iron collar of the usual analytic approaches

with: both disorder (Anderson) and electronic interactions (Mott) play distinct and equally important roles in the transition. The metal-insulator in these materials *should* thus be of the *Anderson-Mott* type [9] and a first real understanding is still far away, not to mention a determination of the electric susceptibility. Even the "simpler" Mott transition still lacks a complete and concise description in any dimension, despite numerous claims found here and there in the literature. The issue of the dielectric catastrophe itself has never been properly addressed, and calculations of the electric susceptibility are unheard of. This is exactly the point we would like to focus our attention on. Strongly correlated electron systems — the Hubbard model and certain avatars — will be thoroughly investigated in *one dimension* to determine the behavior of the electric susceptibility and of its companion, the correlation length. The Density Matrix Renormalization Group (DMRG) will be extensively used to reach this goal.

Our results will confirm Mott's intuition: there is a *dielectric catastrophe* at the Mott transition in one dimension. The transition will be found to be *infinite order*, irrespective of the microscopic details of the underlying Hamiltonian. Thus evidence for a possible unique universality class will be provided. Deeper investigation will reveal that *hyperscaling* is satisfied, which is far from obvious for metal-insulator transitions [7].

The results covered in Chapters 3 and 6 have already been published [10, 11], while Chapter 7 contains the material of a forthcoming publication [12].

Chapter 2

Metal-to-Insulator Transition: a Critical Phenomenon

Metal-insulator transitions form a broad class of fascinating problems that have attracted a lot of attention in the past century, and in fact, still do today as many relevant questions remain unresolved. While there are many intriguing aspects of this problem for the interested physicist, the fact that intuition won in the study of one type of transition is often of little use in understanding another type can be discouraging. A serious reader interested in learning more about this vast field should consider *investigating* in detail Mott's own contribution [8] which reviews a life-long study of the problem, as well as an extensive review by Imada et al. [13].

Rather than getting lost in a jungle of material-related details, one should concentrate on extracting the general features characterizing possibly quite dissimilar metal-insulator transitions: this means searching for *universal* behavior, which is usually found close to the transition, in the critical region. Should success occur, there is hope that *simple* theoretical models, i.e. without superfluous features, may be relevant to the understanding of many metal-insulator transitions, which in turn could be divided into a limited number of *universality classes*. Finding such a classification may be thought of as the Holy Grail of phase transition theory.

2.1 The Transition in Si:P

We devote ourselves here to the study of the metal-to-insulator transition driven by *quantum*, rather than *thermal*, fluctuations [6]: this means the transition occurs at $T = 0$. A confrontation with any experiment may seem at first awkward, if not impossible altogether, since the absolute zero of temperature is clearly out of reach! However, experimentalists can deal with extremely low temperatures[1], where many physical quantities, such as the zero-frequency (di)electric susceptibility on the insulating side or the zero-frequency conductivity on the metallic side, have already attained asymptotic behavior [6]. A convincing example

[1] in the millikelvin range; the relevant scale here is $k_B T$ (energy of low-lying excitations).

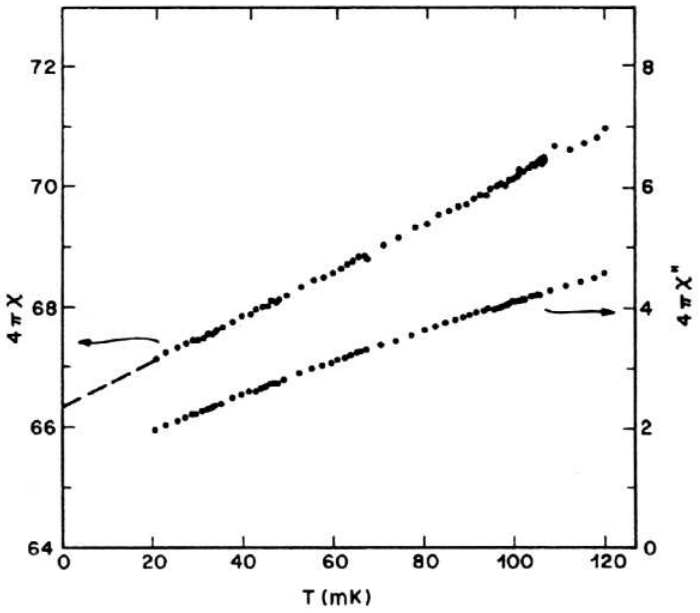

Figure 2.1: Real and imaginary parts of the electric susceptibility as a function of temperature for the insulating Si:P. This material is Silicon doped with randomly distributed Phosphorus atoms that act as donors; $n = 3.110^{18}\ cm^{-3}$ is their concentration.

is given in Fig. 2.1 (taken from [14]).

A linear extrapolation from low-temperature data then yields the $T = 0$ value, a procedure called *finite-temperature scaling*.[2] From now on, we shall restrict ourselves to $T = 0$ values, and concentrate on the experimental observation of quantum phase transitions and on their interpretation.[3] We are interested in quantities which separately characterize the metallic and the insulating phases: an insulator, also called a *dielectric*, has a finite dielectric constant ε [15], which is related to the (real part of the zero-frequency) electric susceptibility χ

$$\varepsilon = 1 + 4\pi\chi, \tag{2.1}$$

but a vanishing conductivity [15], whereas a metal has a finite (zero-frequency) conductivity $\sigma(0)$ and an infinite dielectric constant. How does the transition occur? Does the electric susceptibility diverge continuously when approaching the transition from the insulating side and does the electric conductivity drop continuously to zero when coming from the other side? Or is there any discontinuity? This can be answered, provided that one can measure sufficiently close to the transition point — i.e. enter the critical region. (Here, however, finite-temperature scaling may become impossible [16, 17, 14, 18, 6].) Early experiments in

[2]It is closely related to *finite-size scaling* [6] which consists of extrapolating large-size data to obtain the infinite-size value, a procedure mainly used to obtain relevant bulk quantities out from numerical simulations of finite-size systems. See Chapter 5.

[3]Of course, the discussion of finite-temperature effects is extremely interesting in its own right, see [6].

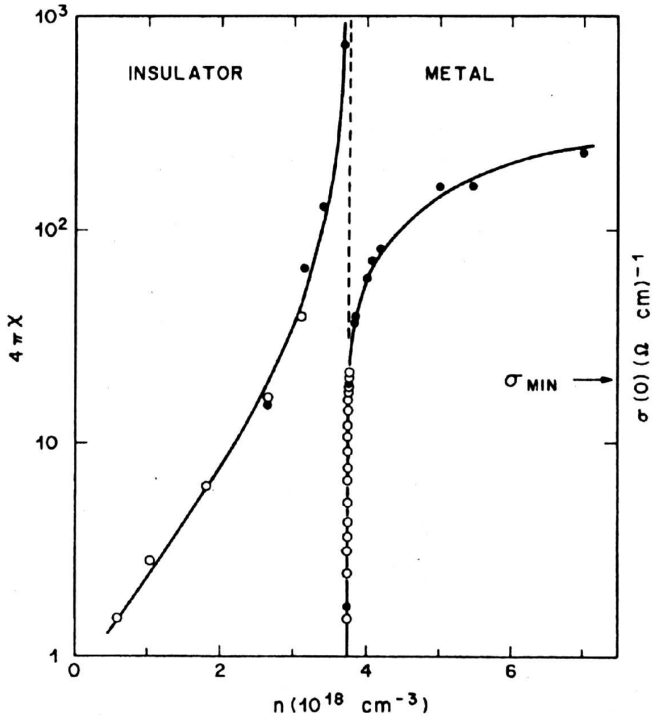

Figure 2.2: Divergence of the $T = 0$ electric susceptibility $4\pi\chi$ for Si:P in the insulator (solid circles from [14]; open circles from [17]; solid line: fit from Eq. 2.2) and the $T = 0$ conductivity $\sigma(0)$ in the metal (solid circles from [20, 22]; open circles from [21]; solid line, fit from Eq. 2.3) as a function of P donor density n. Figure taken from [14].

1956 [19] were only able to demonstrate a large enhancement in χ at microwave frequencies and at 4.2 K for doped Ge. Fortunately, in a series of more recent experiments, beginning in the 1970's [16, 17, 20, 14, 21] (for a short review, see [18]), the critical behavior of a metal-insulator transition could be observed. The material used was Si doped with a donor like P, As or Sb [16]. At $T = 0$, pure Si is an insulator.[4] In Si:P (or equivalently in Si:As, Si:Sb), the donors are randomly distributed. Let $n \equiv N_D$ be their concentration: as n is increased, the wave functions of the "free" donor electrons begin to overlap, until metallic coherence can be achieved throughout the material (and not only at a smaller length scale) at a *critical concentration* n_c beyond which the system remains metallic. However, it is not a simple band-insulator-to-metal transition. As soon as Si is doped, the band theory picture breaks down and electrons cannot be treated as non-interacting anymore. Disorder as well certainly plays a major role. In any case we face here a pretty complex transition that has not been very well understood yet, even though the metamorphosis of Si into a metal through doping may seem intuitively clear. The summarized measurements are presented in Fig. 2.2 [14].

[4]Due to filled bands which correspond to closed atomic shells

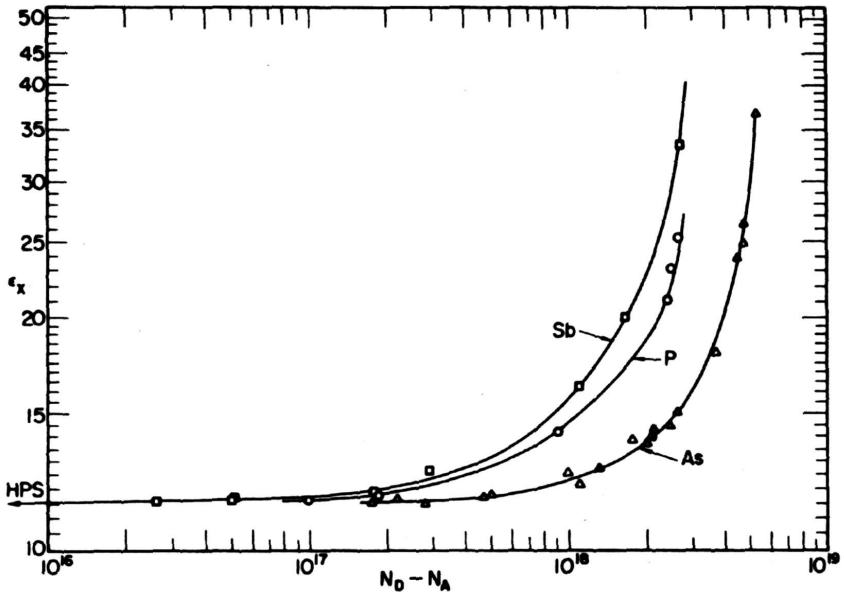

Figure 2.3: Electric susceptibility of Si doped with Sb, P and As as a function of donor concentration.

The electric susceptibility diverges as n approaches n_c from below, following a power-law

$$\chi \sim (n_c - n)^{-\gamma} \tag{2.2}$$

with $\gamma \simeq 1.15$ according to the fit in Fig. 2.2. This divergence was termed the *dielectric catastrophe* by Mott [8] and the *dielectric anomaly* by Imry [23]. The replacement of P by other donors like As or Sb changes only the value of n_c without affecting the strength of the divergence, as can be seen in Fig. 2.3 [16]. The same holds for doping with acceptors like Boron [24].

The conductivity $\sigma(0)$ goes continuously to zero, following a different power-law

$$\sigma(0) \sim (n - n_c)^{\nu} \tag{2.3}$$

with $\nu \simeq 0.5$ according to the fit in Fig. 2.2. There is no *minimum metallic conductivity* (see the position of the hypothetical $\sigma_{\min}$ on Fig. 2.1), contradicting Mott's conjecture for metal-insulator transitions in general [8].

A similar transition may also be triggered by applying an uniaxial stress S at fixed donor concentration. The transition would then occur at a critical value S_c [21, 14, 18, 25]. The finite-temperature conductivity in the critical region may then even be described by a scaling form [25]

$$\sigma(S,T) = \sigma_c(T)\, \mathcal{F}[(S - S_c)^{z\nu}/T] \tag{2.4}$$

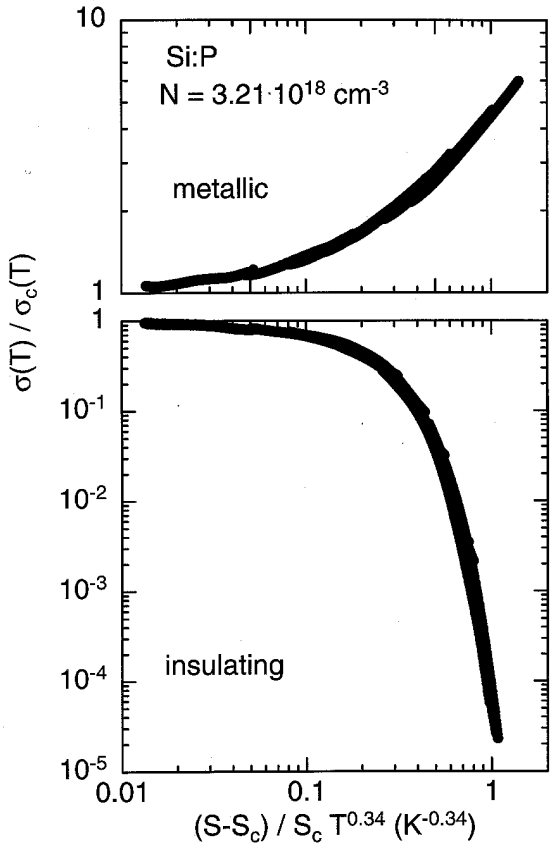

Figure 2.4: Scaling plot of $\sigma(S,T)/\sigma(S_c,T)$ vs $|S-S_c|/(S_cT^{1/z\nu})$ with $S_c = 1.75$ kbar and $1/(z\nu) = 0.34$. N is the P concentration and S is the applied uniaxial stress.

where $\sigma_c(T) = \sigma(S_c,T) \sim T^{1/z}$ and $\mathcal{F}$ is a universal function. In Fig. 2.4 [25] values of $\sigma(S,T)/\sigma_c(T)$ measured at several stresses S and temperatures T are plotted against $|S-S_c|/(S_cT^{1/z\nu})$, where $z\nu \simeq 2.94$ has been chosen to achieve the best collapse of all the data onto a single curve.

Note that similar scaling is observed in Si:B (acceptor doped Si), although with different exponents [26, 27, 28]. See also [29] for Si:Nb. Eq. 2.4 enables us to identify an elementary energy scale

$$\Delta \sim |S-S_c|^{z\nu} \tag{2.5}$$

which vanishes at the transition [6]. Thus, there is a unique relevant energy scale, or, equivalently, a *unique relevant length scale* close to the transition: this means that *hyperscaling* should be valid [6]. In that case, the electric susceptibility can also be expressed directly in terms of Δ close to the transition. This relation was indeed observed quite early in the donor-concentration-driven transition, and the corresponding relation is [17]

$$\chi \sim \frac{1}{\Delta^2}. \tag{2.6}$$

(See also Ref. [24] for more details on Si:B). This transition thus appears to be completely continuous, with well-developed critical behavior.

2.2 A Universal relation?

In the beginning of this chapter, we evoked the quest for universal relations, which can arise for example between the exponents characterizing the divergence of various physical quantities [1, 6]. Such a relation may then exist between γ and ν, the exponents of χ and $\sigma(0)$, respectively (see (2.2) and (2.3))

$$\gamma = 2\nu \,, \tag{2.7}$$

and it has been indeed experimentally probed for some metal-insulator transitions, including Si:P [14, 18], Si:B [24], Ge:As [30] and Ge:Ga [31].

This relation has also been observed in the Anderson model in three dimensions [32, 33], where increasing disorder localizes the wave functions of the independent electrons, eventually turning the system into an insulator at a critical disorder strength. It is tempting to try this model to understand the metal-insulator transition in Si:P. Disorder certainly plays a major role (the donors are randomly distributed). But it should be kept in mind that, unlike in the Anderson model, in Si:P an increase of the disorder (the donor concentration) turns the insulating semi-conductor into a metal! We will nevertheless outline the interpretation of Si:P [18] with the scaling theory of Anderson localization [34]. In the localization problem, it can be shown that [33, 35, 23]

$$\sigma(0) \sim 1/\xi \tag{2.8}$$

where ξ is the unique relevant length scale of the system, also called *localization* (or *correlation*) length. This readily gives [8, 33, 35, 23]

$$\chi \sim \xi^2 \tag{2.9}$$

via

$$\xi \sim |g - g_c|^{-\nu}, \tag{2.10}$$

where g is the tuning parameter and g_c its critical value. While the scaling theory predicts $\nu = 1$ [34, 33], there is little consensus for experimental values in doped semi-conductors: ν ranges from ~ 0.3 [31] to ~ 0.5 [20, 21, 14, 30, 18, 36] and even to 1.3 [25] and 1.6 [26, 27, 28]. This is in clear contradiction with the elementary scaling theory of localization and highlights the following point: the metal-insulator transition in Si:P (and related doped semi-conductors) is far more complicated than a problem of independent disordered electrons. Interactions should clearly be treated on equal footing with the disorder [9]. However, this just turns the problem into a very difficult one.

2.3 Critical behavior

Maybe you noticed that the transitions we reviewed in the previous sections all share a common feature: the singular behavior (either divergence or vanishing) of physical quantities in a parameter regime surrounding the transition point. This zone is called the *critical region* and the singular behavior is called the *critical behavior*.

Generalizing this concept, Sachdev [6] identifies any point of non-analyticity (read: singularity) g_c in the ground state energy of a system as a *quantum critical point*. In general, g is a set of parameters $g = (g_1, g_2, \ldots)$ in the Hamiltonian governing the system that can be tuned, e.g. the interaction strength or the density of electrons. For a *continuous* transition, there is a characteristic energy scale of fluctuations above the ground state that vanishes as $g \to g_c$. We name it Δ, which correctly suggests you that this energy scale is nothing but a *gap* in the excitation spectrum[5]. In the critical region, the gap behaves as a power-law, provided the transition is *second order*:

$$\Delta \sim |g - g_c|^{z\nu} \tag{2.11}$$

Here $z\nu$ is a *critical exponent*; this matches Eq. 2.5. An *exponential* opening of the gap at g_c

$$\Delta \sim e^{\frac{A}{(g-g_c)^\sigma}} , \tag{2.12}$$

with some constant A and some exponent σ is also possible. In this case we will talk about an *infinite order* transition.

Continuous quantum phase transitions also invariably have a diverging characteristic length scale, the *correlation length* [6]

$$\xi \sim |g - g_c|^{-\nu} . \tag{2.13}$$

(See Eqs. 2.8 and 2.10.) The scales of energy and length are related by

$$\xi \sim \Delta^z , \tag{2.14}$$

where z is called the *dynamical critical exponent*: $z = 1$ corresponds to a system in which energy — i.e. time — and space are on equal footing, i.e. where *relativistic invariance* is satisfied. The susceptibility then diverges as well with the form

$$\chi \sim |g - g_c|^{-\gamma} \tag{2.15}$$

for a second-order transition. In the particular case of the metal-insulator transition, χ is the electric susceptibility, and Eq. 2.15 is the *dielectric catastrophe*, that we already came in contact with in the experiments (see Eqs. 2.2, 2.6 and 2.9).

All the other well-known critical exponents may be defined in analogy with their classical counterpart. The whole set of critical exponents are expected to be *universal* and exceptions to this rule can be explained by well tested theories in the context of classical phase transitions.[6]

[5] for non-critical gapless systems see [6]

[6] Like the effect of marginal operators for instance.

Chapter 3

Electric Susceptibility: Theoretical Basics

As emphasized in the previous chapter, the *electric susceptibility* χ is ideal for experimental investigation of the insulating side of the transition. On the other side many theoreticians have concentrated their efforts on the conductivity

$$\sigma(\omega) \;=\; 2\pi D\delta(\omega) + \sigma_{\rm reg}(\omega) \tag{3.1}$$

both on the insulating (see e.g. [37, 38, 39, 40]) and on the metallic (see e.g. [41, 42, 43, 44, 45]) sides. In the metal, a non-vanishing *Drude weight* D characterizes an ideal conductor and is per force absent in experiments, while it represents, for theoreticians, *the* static quantity to study a perfectly metallic phase. It can be determined via Kohn's formula [46, 47]

$$D \;=\; \frac{L}{2}\frac{\partial^2 E_o}{\partial\Phi^2}\bigg|_{\Phi=0} . \tag{3.2}$$

Here the system forms a ring of length L with ground state energy E_o and is pierced by a magnetic flux Φ: this is equivalent to probing the sensitivity of the *wavefunction* in the ring towards a change in the boundary conditions. D has thus also been named *charge stiffness*.

On the other hand, theoretical studies of the electric susceptibility are scarce: one finds scaling theories of disorder-driven transitions [35, 48] and numerical investigations (the classical Coulomb gas in 2D [49], the Anderson insulator with Coulomb — i. e. long-ranged — interactions in 3D [50]). These studies are the first of their kind and have the great merit of emphasizing that χ is the susceptibility relevant for the metal-insulator transition [50] rather than the *charge susceptibility* that nearly everybody has in mind [51, 47]. Indeed, the charge susceptibility is proportional to the charge compressibility and vanishes identically in an incompressible insulating state [13].

3.1 Open boundary conditions

Let us take as a starting point a crystal of L^d atoms (lattice constant $a = 1$) whose electronic degrees of freedom are described by a Hamiltonian $\mathcal{H}$. We consider *open boundary conditions* (OBC), i.e. the connections terminate at the edges. We point out that this is the natural choice for a direct comparison with the experiments. Our system should undergo a quantum metal-insulator transition if one or more parameters of $\mathcal{H}$ are properly tuned. Our purpose is to study how this occurs.

Following standard classical electrodynamics [15], the (static) electric susceptibility χ of a medium is defined as

$$\chi \ := \ \left.\frac{\partial P}{\partial E}\right|_{E=0} \tag{3.3}$$

where P is its polarization and E is the applied electric field which is constant in time and space. In a quantum world, Eq. 3.3 remains valid if one replaces P with the ground state expectation value of the polarization operator $\mathcal{P}$

$$\chi \ := \ \left.\frac{\partial \langle \mathcal{P} \rangle}{\partial E}\right|_{E=0} . \tag{3.4}$$

Here $\mathcal{P}$ is called *macroscopic bulk polarization* and is the sum of all the elementary dipoles. After proper normalization one gets [52] (we set $e = a = 1$)

$$\mathcal{P} \ = \ \frac{1}{L^d} \sum_i x_i n_i \ = \ \frac{1}{L^d} X \tag{3.5}$$

where X is the one-body *position operator* and L is the size of the system or, equivalently, the number of atoms ("sites"). The quantity n_i is the local density operator and x_i denotes the position of the lattice sites. Putting the origin in the middle of the lattice ensures that the polarization (Eq. 3.5) will be zero in the absence of electric field,[1] due to reflection symmetry.

In order to determine χ we need to know the ground state wave function as a function of the applied electric field. This means we have to couple the Hamiltonian $\mathcal{H}$ describing the transition to the electric field E. We take E to be along the x-direction, yielding an electric potential $\Phi(\mathbf{r}) = -Ex$. We can then readily write down what must be added to $\mathcal{H}$:

$$\mathcal{H}_{\rm ext} \ = \ \int d^d r \Phi(\mathbf{r}) n(\mathbf{r}). \tag{3.6}$$

The new total Hamiltonian then becomes $\mathcal{H}_{\rm tot} = \mathcal{H} + \mathcal{H}_{\rm ext}$ and $n(\mathbf{r})$ is the continuous density operator

$$n(\mathbf{r}) \ = \ \sum_{ij\sigma} \phi^\star(\mathbf{r} - \mathbf{r}_i) \phi(\mathbf{r} - \mathbf{r}_j) c^\dagger_{i\sigma} c_{j\sigma} \tag{3.7}$$

[1] This is only a matter of convenience, since putting the origin elsewhere will give a non-vanishing but constant zero-field contribution to the polarization that will disappear when differentiated with respect to the electric field.

where the ϕ's are Wannier orbitals. In the tight-binding scheme, their overlap is negligible and one can write

$$\int d^d r\ \Phi(\mathbf{r})\phi^\star(\mathbf{r}-\mathbf{r}_i)\phi(\mathbf{r}-\mathbf{r}_j)\ \simeq\ \Phi(\mathbf{r}_i)\delta_{ij} \tag{3.8}$$

provided that the potential Φ varies sufficiently slowly. This eventually leads to the discrete form

$$\mathcal{H}_{\text{ext}}\ =\ -E\sum_i x_i n_i\ =\ -EL^d\mathcal{P}, \tag{3.9}$$

where the electric field directly couples to the polarization. We can write the following equation

$$\mathcal{P}\ =\ -\frac{1}{L^d}\frac{\partial\mathcal{H}_{\text{tot}}}{\partial E} \tag{3.10}$$

that together with Eq. 3.4 and the Hellmann-Feynman theorem will give

$$\chi\ =\ -\frac{1}{L^d}\frac{\partial^2 E_0^{\text{tot}}(E)}{\partial E^2}\bigg|_{E=0}. \tag{3.11}$$

For $E\to 0$ we may apply second-order non-degenerate perturbation theory and write

$$\chi\ =\ \frac{2}{L^d}\sum_{\nu\neq 0}\frac{|\langle\Psi_\nu|X|\Psi_0\rangle|^2}{E_\nu-E_0} \tag{3.12}$$

where the $|\Phi_\nu\rangle$ are eigenstates of $\mathcal{H}$ and E_ν the corresponding eigenenergies. Here $\nu=0$ denotes the ground state.

As mentioned earlier, $\langle\mathcal{P}\rangle=\text{const}$ and may be set to zero in the absence of electric field. However this in no way means that, as Mother Nature becomes quantum, the fluctuations of the polarization will vanish at the same time, i.e.

$$\langle X^2\rangle-\langle X\rangle^2\ \neq\ 0. \tag{3.13}$$

Kudinov, whose work is not very well known, was the first to notice the importance of the variance of the polarization [53]. Other groups ([54] and [55] for non-interacting electrons) then followed. Since the fluctuations of the polarization measure the degree of localization, it is intuitive that Eq. 3.13 should be finite for an insulator and divergent for a perfect metal, if it is properly normalized [53]:

$$\tilde{\xi}\ =\ \frac{1}{L^d}(\langle X^2\rangle-\langle X\rangle^2)\,, \tag{3.14}$$

or equivalently

$$\tilde{\xi}\ =\ \frac{1}{L^d}\sum_{ij}x_i x_j(\langle n_i n_j\rangle-\langle n_i\rangle\langle n_j\rangle) \tag{3.15}$$

We will see that the quantity $\tilde{\xi}$ is complementary to the electric susceptibility χ in characterizing the metal-insulator transition. It may be thought of as a "second moment" of the polarization, with $\mathcal{P}$ being the first. The *fluctuation-dissipation theorem* relates them in a very elegant way, but only at a finite temperature T [50]

$$\chi \;=\; \frac{\tilde{\xi}}{T}\,. \tag{3.16}$$

Unfortunately, the equivalent theorem for $T = 0$ is not so easy to deal with [6] and no relation corresponding to Eq. 3.16 has yet been found. However, a $T = 0$ inequality may be derived from Eq. 3.12: let Δ be the lowest excitation energy for which the dipole matrix element $\langle\Phi_\nu|X|\Phi_0\rangle$ does not vanish (Δ is called the *charge gap*). We immediately get

$$\chi \;\leq\; \frac{2\tilde{\xi}}{\Delta}\,. \tag{3.17}$$

Let θ be the exponent of the divergence of $\tilde{\xi}$. Eq. 3.17 then yields the inequality

$$\gamma \;\leq\; \theta + z\nu\,. \tag{3.18}$$

between exponents (see Eqs.2.11 and 2.15). While the interpretation of $\tilde{\xi}$ in arbitrary dimension d is awkward, $\tilde{\xi}$ has the dimension of a length in $d = 1$. As is well known from the theory of classical [1, 56] and quantum [6] phase transitions, there is a unique relevant length scale in the vicinity of the critical point below the upper critical dimension d_c. We might hope[2] that $d_c^+ > 1$, in which case any divergent length must be the correlation length itself, at least in the critical region. This guess will be confirmed in the Chapter 6. Thus in $d = 1$, we will remove the tilde on ξ. Since $\theta = \nu$ (see Eq. 2.13), Eq. 3.18 becomes

$$\gamma \;\leq\; (1 + z)\nu\,. \tag{3.19}$$

3.2 Linear vs non-linear responses

Since we expect the ground state polarization $\langle\mathcal{P}\rangle$ to be an analytic function of E in principle, we can consider its Taylor expansion

$$\langle\mathcal{P}\rangle \;=\; \sum_{n=0}^{\infty} \chi^{(n)} E^n\,. \tag{3.20}$$

Since the polarization should change its sign when $E \to -E$, all the terms with an even power of E must vanish and we get

$$\langle\mathcal{P}\rangle \;=\; \chi^{(1)}E + \chi^{(3)}E^3 + \ldots \quad . \tag{3.21}$$

[2]We do not know of a model for which it does not hold; it is for example $d_c^+ = 6$ for the Anderson-Mott transition [57].

By definition, $\chi^{(1)}$ is nothing but the electric susceptibility χ. If the electric field is small enough, we enter the *linear response* regime where

$$\chi \;=\; \frac{\langle \mathcal{P} \rangle}{E} \,. \tag{3.22}$$

This expression will reveal itself to be a very useful alternative way of determining χ. A sufficiently large third-order non-linear susceptibility $\chi^{(3)}$ could, however, mask the linear behavior even at very small electric fields. Thus care has to be taken when one makes use of Eq. 3.22. Certain materials, like polydiacetylenes, indeed show a very large $\chi^{(3)}$ [58]. Non-linear response is a very interesting, if delicate, issue in its own right and has been recently investigated by various analytical and numerical methods [58, 59, 60].

3.3 Periodic boundary conditions

Unfortunately open boundary conditions break the translational invariance on a finite lattice, thus making the analytic treatment of a given model much more difficult, or even impossible. One often has to switch to *periodic boundary conditions* (PBC), turning a chain into a ring, a square into a torus and so on. The bad news is that the definition of the polarization itself becomes awkward because the system lacks edges where the polarization is sustained in a real material [15]. One has to resort to a few technical tricks in order to deal with this problem. In particular, one can define a quantity which will tend to the macroscopic bulk polarization as the size of the system grows towards infinity (in $d = 1$ only [61, 52, 62, 63, 64]). Another annoyance is that a constant electric field gives a sawtooth periodic potential, which leads to an ill-defined thermodynamic limit. Instead, one has to use a periodic electric field defined so that one period spans the system size. In $d = 1$, we can choose $E(x) = E\cos(qx)$ with $q = \frac{2\pi}{L}$. As $q \to 0$, we would then get back $E(x) \to E$. This yields a potential

$$\Phi(x) \;=\; -\frac{E}{q}\sin(qx) \,. \tag{3.23}$$

Notice that one must replace x by $\frac{L}{2\pi}\sin(\frac{2\pi}{L}x)$ in $\Phi(x) = -Ex$ in order to get Eq. 3.23. Such a mapping between OBC and PBC is quite general [64] and is reminiscent of conformal mappings, e.g. between quantities at $T = 0$ and $T \neq 0$ [6] or between a system of finite size L and its thermodynamic limit $L \to \infty$ [65, 66]. The coupling to the electric field obeys the same rule

$$\mathcal{H}_{\text{ext}} \;=\; -E\sum_i \frac{\sin(qx_i)}{q} n_i \;=\; -E\tilde{X} \tag{3.24}$$

where we have defined a new position operator $\tilde{X}$ [64]. Note that $\tilde{X}$ is now only a measure of the charge displacement on a ring and no longer represents the polarization, which is instead given by a rather tricky expression [61, 52]

$$P \;=\; \lim_{L\to\infty} \frac{1}{2\pi} \mathrm{Im}\ln\langle e^{\frac{2\pi i}{L}X}\rangle, \tag{3.25}$$

where X is the OBC position operator.[3] The electric susceptibility, however, may still be defined using Eqs. 3.11 [49]:

$$\chi = \frac{2}{L^d} \sum_{\nu \neq 0} \frac{|\langle \Psi_\nu | \tilde{X} | \Psi_0 \rangle|^2}{E_\nu - E_0} \,. \tag{3.26}$$

The correlation length may also be determined from Eq. 3.14 using $\tilde{X}$ instead of X

$$\xi = \frac{1}{L} \langle \tilde{X}^2 \rangle \tag{3.27}$$

where $\langle \tilde{X} \rangle = 0$ due to translational invariance on the ring in the absence of electric field.

[3] Notice that if one could commute Im ln and the expectation value $\langle \ldots \rangle$ one would recover the expression for OBC.

Chapter 4

Mott Transition

Let us go back to the good old days: in 1931 A.H. Wilson [67] described the difference between the metallic and the insulating states using a model of non-interacting electrons. The *band theory* was born and it sounded roughly as follows: if the atoms building up a regular lattice have a closed outermost shell, it will give rise to *filled* or closed band which corresponds to an insulator. We designate this situation "two electrons per atom", provided there are no degeneracies. If the atoms do not have a closed outermost shell, the band will be *half-filled*, designated "one electron per atom". Because there are free quantum states available for the electrons to move around, they can carry a current and maintain quantum coherence over the volume of the system, which is *de facto* a metal. The reign of this "Brave New World", as oppressing as it was for the majority of materials, was not to last forever. Some troublemakers pointed out that a few systems do not obey the rules [68]: they had the rudeness of being insulating despite being assigned to be metallic.

Non-interacting electrons are the building blocks of this flawed Utopia, as first pointed by Wigner [1] in 1938. Eleven years later, Sir Nevill Mott published a paper [69] which was to become one of the cornerstones of modern many-body physics: the insulating state could be built up from "one-electron atoms". One must just *increase* the lattice constant a. This means, experimentally, to decrease the external pressure and, theoretically, to increase the strength of the Coulomb interaction! At some critical a_c the metal eventually turns into an insulator [69, 70, 8]. This Cinderella-like fairy-tale was not to everybody's taste however: A.H. Wilson's early breakthrough was too enticing. Fifteen years and another cornerstone paper by Kohn [46] — a general study of the insulating state of matter — were needed to change minds.

[1] introduction of the so-called *Wigner crystal*

4.1 Early and recent approaches

In the same year, Hubbard introduced a model [71] now named after him which incorporates Coulomb interactions into Wilson's theory:

$$\mathcal{H} \;=\; -t \sum_{<ij>\sigma} c^{\dagger}_{i\sigma} c_{j\sigma} + U \sum_{i} n_{i\uparrow} n_{i\downarrow} \; . \tag{4.1}$$

The first term is the tight-binding kinetic energy with *hopping parameter* t between nearest neighbors (we set $t = 1$), and the second represents the electronic interactions reduced to their *local* component U, a simplification which is motivated by screening of the long-range part of the Coulomb interaction in the outer shells of transition metals. We will take the band to be half-filled and vary the ratio U/t rather than the lattice constant a — which is set to 1 — to probe the so-called *Mott transition*. In 1968 this model was solved by Lieb and Wu in $d = 1$ using the Bethe Ansatz in a paper [72] fatefully entitled "Absence of Mott Transition in an Exact Solution of the Short-Range, One-Band Model in One Dimension". They find no transition at a finite $U_c > 0$, the system is insulating for any finite interaction strength. This result contradicts Mott's original intuition of a critical interaction strength of the bandwidth order, $U_c \sim t$ [70, 8]. However, since a half-filled band of non-interacting electrons is obviously metallic, a metal-insulator transition occurs at $U_c = 0$ right away.

Unfortunately, no exact solution has been found for the Hubbard model in higher dimensions and only approximation schemes are left for the eager physicists. In the early 1960's, Gutzwiller introduced [73] a variational wave function which is an analytic continuation of the non-interacting case:

$$|\Psi_G\rangle \;=\; e^{-\eta \sum_i n_{i\uparrow} n_{i\downarrow}} |\Psi_0\rangle \; , \tag{4.2}$$

where η is the variational parameter and $|\Psi_0\rangle$ the Fermi sea. Brinkman and Rice [74] investigated the Mott transition within the Gutzwiller approximation[2] in 1970. Their conclusion was that a transition occurs at *finite* U_c and that the double occupancy is an order parameter for the metallic phase. This work was much celebrated and in fact it is *still* today, although it is completely wrong: the transition observed by Brinkman and Rice is an artifact of the variational scheme: because the Gutzwiller wave function grows adiabatically from a metallic state, it cannot correctly describe a phase transition. Perturbative calculations indeed show that the double occupancy is a smoothly decreasing function of U that reaches zero only in the $U \to \infty$ limit [76].

Another variational wave function was defined by Baeriswyl [77], starting this time in the strong coupling limit:

$$|\Psi_B\rangle \;=\; e^{-\eta \sum_{<ij>\sigma} c^{\dagger}_{i\sigma} c_{j\sigma}} |\Psi_\infty\rangle \; , \tag{4.3}$$

where $|\Psi_\infty\rangle$ is the ground state of the Hubbard model for $U \to \infty$. This limit describes the antiferromagnetic Heisenberg model, in which double occupancy is forbidden and which has only spin degrees of freedom. The charges are frozen and $|\Psi_B\rangle$ necessarily describes

[2] which, by the way, becomes exact in the limit $d \to \infty$ [75]

an insulator. A calculation gives a lower energy for $|\Psi_B\rangle$ than for $|\Psi_G\rangle$ in the region of the Brinkman-Rice transition [75], thus showing that the Gutzwiller wave function poorly describes strong coupling! These issues have been discussed by other authors [78, 79]. These two variational wave functions are only valid in the two asymptotic regimes, and cannot be trusted in the vicinity of the transition [80]: but that is the fate of any variational approach.

Approximations that rely on continuously metamorphosing an exactly known limit towards the transition will inevitably fail: one definitely needs (at least asymptotically) exact methods to investigate a quantum phase transition, which corresponds to an abrupt and drastic change of the properties of a system. Approximations that rely on metamorphosing continuously an exactly known limit to approach the transition will inevitably fail. An interesting but ambitious approach is to try to extract the scaling limit of the Mott transition within a renormalization group approach [81]. Numerical simulations provide potentially exact results on finite lattices, but are still in their infancy in $d \geq 2$ (QMC,DMRG): the cluster sizes are small and a reliable finite-size scaling is difficult or impossible [82, 83].

Further simplifications arise if one considers the limit $d \to \infty$, where the dynamical mean-field theory (DMFT) gives the exact solution[3] [84]. But this limit suffers from a serious "bug": the paramagnetic insulator obtained has extensive $T = 0$ entropy. This contradicts the third law of thermodynamics! Nevertheless many groups have focused their attention on the Hubbard model in $d \to \infty$, studying the finite-T transition instead [84]: its order has been a subject of much debate and is still a delicate issue [85, 86, 84].

Meanwhile, substantial progress has been made in investigating experimentally compounds in which a *pure* Mott transition occurs [13]. The most promising among them is $NiS_{2-x}Se_x$. Substitution of S with Se in the Mott insulator NiS_2 makes the system metallic [87, 88, 89, 90, 13]. A $T = 0$ study comparable to the one for Si:P and related materials (see Chap. 2) has yet to be carried out. However, very low temperatures have been reached and the Mott transition may also be induced by applying an external stress S: Husman *et al.* started with insulating $NiS_{1.56}Se_{0.44}$ crystals and drove the system metallic with pressure [88]. This way of tuning the transition by changing the lattice spacing perfectly matches Mott's original viewpoint! A dynamical scaling plot comparable to Fig. 2.4 has also been obtained (Fig. 4.1) on the metallic side of the transition [88]. Note that the x-axis is the inverse of the one on Fig. 2.4, so that the two scaling functions in fact look rather different.

4.2 The one-dimensional case

Experimentalists have also investigated the weird world of quasi-one- spatial dimension: chains of atoms or stacks of molecules weakly coupled to each other. Some of these materials are Mott insulators [91, 92] and some others undergo a pressure-induced Mott transition [93, 94]. The transverse coupling is typically weak enough so that the materials can be considered one-dimensional. However the fate of this coupling when one lowers the temperature is not so clear: the general trend is towards an increase due to the quantum fluctuations until the

[3] which has to be evaluated numerically though

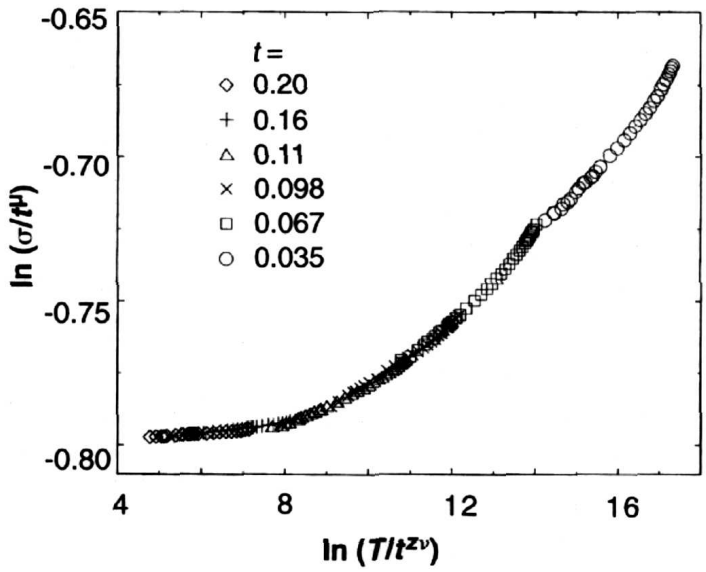

Figure 4.1: Scaling plot of $\sigma(S,T)/\sigma(S_c,T)$ ($t = (S - S_c)/S_c$ and $\sigma(S_c,T) = t^{\mu}$) vs $T/t^{z\nu}$ with $S_c = 1.6 \pm 0.16$ kbar, $\mu = 1.1 \pm 0.2$ and $z\nu = 5 \pm 1.3$ for $NiS_{1.56}Se_{0.44}$. The ability to collapse the data onto a universal curve reflects the measurable influence of the quantum critical point [88].

material eventually reverts to three-dimensionality at sufficiently low temperatures [95, 96]. It is thus very difficult to observe $T = 0$ phenomena for truly one-dimensional materials [94].

The good news is that in such low dimensional systems, a theorist's life is much easier: many strongly correlated lattice models may be solved exactly and many simplifications arise. Finite temperature studies are extremely enticing, as they allow a direct comparison with experiment: some techniques, both analytical (thermodynamic Bethe Ansatz [97]) and numerical (TMRG [98]) are starting to be used [99, 100]. Their application is quite difficult and still in its infancy but shows promising results which match general predictions from continuous models [6].

Thus far, the vast majority of theoretical investigations in this field have been devoted to $T = 0$: a full understanding of this limiting case is essential for further investigations at a finite temperature. The Lieb and Wu solution for the Hubbard model (4.1) was only a starting point: it has recently been extended to obtain the full spectrum [101]! Unfortunately this method is sufficiently complicated so that an analytic treatment involving excited states is considered very delicate [47] even though substantial progress has been made quite recently. Nevertheless, many ground state properties as well as the low-lying structure of the spectrum may be discussed in detail. Let us now summarize the general picture [47]: At $U = 0$, the system is a half-filled band of non-interacting electrons and is thus metallic and totally

gapless. For any $U > 0$, a *gap*

$$\Delta_c(U) \;=\; \frac{16}{U}\int_1^\infty dy\,\frac{\sqrt{y^2-1}}{\sinh(2\pi y/U)} \tag{4.4}$$

opens for the charge excitations [102] while the spin excitations remain gapless. The system is a Mott insulator with a vanishing charge stiffness $D = 0$. There *is* a *quantum phase transition*, but at $U = 0$ [6]. Lieb and Wu's title [72] should not be misunderstood: it only refers to the fact that there is no transition at a finite U. There is even more: it makes perfect sense to consider a negative U, which leads to the *attractive Hubbard model*. At *half-filling* a particle-hole canonical transformation on the down-spins electrons only,

$$\left\{\begin{array}{lcl} c_{i\uparrow} & \rightarrow & \tilde{c}_{i\uparrow} \\ c_{i\downarrow} & \rightarrow & \tilde{c}^\dagger_{i\downarrow} \end{array}\right. , \tag{4.5}$$

turns the attractive interaction into a repulsive one, spin into charge and charge into spin [103]: the point $U = 0$ is a two-way mirror. As soon as $U < 0$, a *gap* Δ_s, also given by Eq. 4.4, opens for the spin excitations, while the charge excitations remain gapless. *Another quantum phase transition* occurs at $U = 0$ for the spins, which have mirrored critical behavior. The system is metallic with a finite Drude weight D that increases as $U \rightarrow 0^-$ and makes a jump of $\frac{2}{\pi}$ at $U = 0$ [41].

The critical region is nothing but the region of validity of weak-coupling: for $|U| \lesssim 2$ Eq. 4.4 becomes [47]

$$\Delta_{c,s} \;=\; \frac{8}{\pi}\sqrt{|U|}e^{-\frac{2\pi}{|U|}} \tag{4.6}$$

where $\sqrt{U}$ is a *logarithmic correction* in front of an exponential and may be neglected for $|U| \rightarrow 0$:

$$\Delta_{c,s} \;\sim\; e^{-\frac{2\pi}{|U|}} \;. \tag{4.7}$$

The gap closes faster than any power-law, which means that, technically, $z\nu \rightarrow \infty$ (see Eq. 2.11). Another weak-coupling analysis reveals that the Hubbard model is *Lorentz invariant*, i. e. time and space may be interchanged. The immediate consequence is that $z = 1$ [38], which in turn implies $\nu \rightarrow \infty$. The correlation length should thus diverge faster than any power-law as $U \rightarrow \infty$. This is confirmed by the explicit Bethe Ansatz form [38] for both positive and negative U,

$$\xi_{c,s}(U) \;=\; \frac{|U|}{4}\left(\int_1^\infty dy\,\frac{\ln(y+\sqrt{y^2-1})}{\cosh(2\pi y/|U|)}\right)^{-1} , \tag{4.8}$$

which can be approximated as

$$\xi_{c,s}(U) \;\sim\; \frac{1}{\Delta_{c,s}} \;\sim\; e^{\frac{2\pi}{|U|}} \tag{4.9}$$

for $U \to 0$. This is an example of an *infinite-order* transition for which the paradigm is the classical Berezinskiĭ-Kosterlitz-Thouless (BKT) transition, present in the 2D XY model [104, 105, 106]:

$$\mathcal{H}_{\rm XY} \;=\; -J \sum_{<ij>} (S_i^x S_j^x + S_i^y S_j^y) \;\; . \tag{4.10}$$

This model has true ferromagnetic long-range order only at $T = 0$, which is destroyed by spin wave excitations as soon as $T > 0$; this is a direct consequence of the Mermin-Wagner theorem. The low temperature phase, however, remains critical with massless excitations, power-law correlations and corresponding quasi-long-range order, up to the *Kosterlitz-Thouless temperature*[4] $T_{\rm KT}$ where the size of the vortex-anti-vortex pairs[5] diverges. Above $T_{\rm KT}$, there is short-range order with free vortices, a finite correlation length

$$\xi(T) \;\sim\; e^{\frac{b}{\sqrt{T - T_{\rm KT}}}} \;, \tag{4.11}$$

where $b \simeq 1.5$ [105], and a susceptibility

$$\chi(T) \;\sim\; \xi^{2-\eta} \tag{4.12}$$

with $\eta = \frac{1}{4}$. The 2D classical Coulomb gas lies in the same universality class [107], when the (anti-)vortices are mapped to (negative) positive charges. The gas is insulating at $T < T_{\rm KT}$ and becomes metallic above the critical temperature [108, 49]. The electric susceptibility has been found to diverge at the transition [49].

May one draw a bridge between the 1d Hubbard model and the Kosterlitz-Thouless transition? Here is the first clue: a quantum-classical mapping is *possible* because the effective classical dimension of the Hubbard model is $D = d + z = 2$. But the situation is quite intricate because there are *two* infinite-order transitions in the Hubbard model, mirrored at $U = 0$. In discussing spins and charges separately we have implicitly referred to a beautiful, yet questioned, property of the electron gas on a one-dimensional lattice: *spin-charge separation* [109, 110]. It is possible to treat spins and charges as separate degrees of freedom; the Hubbard model may thus be treated as a whole or split into its spin and charge components. In the latter case, the gapless phase for either component turns out to be described by the *Gaussian model* [110, 6, 111, 112]. The elementary excitations are free bosons, made up of all spins or all charges. Since the spin and charge correlations decay as power-laws, the phase is *critical*. This is the generic state for a $1d$ massless degree of freedom[6], as intuitively guessed by Haldane [113]. The conjunction of two massless degrees of freedom (one for the spin and one for the charge) makes up a *Luttinger liquid*. The low-temperature phase of the XY model also has the Gaussian model as its scaling limit, while the high-temperature phase corresponds to the massive degrees of freedom of the Hubbard model (above or below U).

[4] The poor Berezinskiĭ is often forgotten, although he was the first one to unravel this transition.

[5] A vortex is a topological excitation where the spins whirl around a common center. An anti-vortex is the same pattern, but with spins whirling in the other direction.

[6] *with a linear spectrum*, see the next section

Even in the latter model, one can reconcile spin and charge by considering a *massive Luttinger model* [114], i.e. by adding a gapped degree of freedom to a gapless one; this yields the *Luther-Emery model*, which fully describes both the negative- and positive-U Hubbard model at half-filling [115]. And guess what? Quite a long while ago, the Luther-Emery model has been shown to be *equivalent* to the 2D Coulomb gas [116, 115], which in turn lies in the same universality class as the XY model! Could the problem be solved? Does the 1d Mott transition lie in the universality class of the XY model, as does the transition for the spins for negative U? Here one must be careful: equivalences between all those models are in general valid in an asymptotic regime of some sort [114, 6], and sometimes even rely on intuitive guesses [114] so that building a chain of correspondences between one model and another model does not ensure that these two models are truly equivalent. A delicate study has to be undertaken anyway. Unfortunately, in the spirit of Lieb and Wu's work, the 1d Mott transition, present in the Hubbard model, has been — and still is — considered *pathological*. A direct comparison with the well known one-dimensional classical Ising model, which lacks a true transition, does not help. This might explain why the issue of the nature of the Mott transition in the Hubbard model has not been fully resolved and only gets out of purgatory by now.

Nevertheless, quantum phase transitions in $(1+1)$ dimensions[7] as well as their mapping to 2D classical phase transitions have attracted a lot of interest [6]. It appears that exponential divergences of critical quantities are actually not that pathological, and are even quite common. Consider for instance the "spinless fermion model" (or $t-V$ model) which is the equivalent of the Hubbard model, but for spinless fermions,

$$\mathcal{H} \;=\; -t \sum_{<ij>} c_i^\dagger c_j + V \sum_{<ij>} n_i n_j \;. \tag{4.13}$$

This model has also been exactly solved using the Bethe Ansatz [117, 118, 119]: the half-filled chain undergoes a *Mott transition* at $V_c = 2t$, with a corresponding jump of the Drude weight [120]. For $V < V_c$ the system is a Luttinger liquid [6, 109, 110], while for $V > V_c$ it is an insulator with a finite correlation length that diverges exponentially [121]

$$\xi(V) \;\sim\; e^{\frac{\pi^2/2\sqrt{2}}{\sqrt{V-2t}}} \tag{4.14}$$

and that is inversely proportional to the charge gap. This transition falls directly into the BKT universality class [6].

After having deprived the electron of its spin, we now consider adding some spin-like degree of freedom to the electron. This leads to the $SU(N)$ Hubbard model, in which each fermion has N spin flavors[8] [122]. For $N = 3$ and 4, Monte-Carlo calculations at half-filling give again a BKT opening of the charge gap, with a $U_c > 0$ of the order of the bandwidth [122].

[7] $d = z = 1$

[8] $N = 2$ is the conventional Hubbard model.

Both types of infinite-order divergences (Eqs. 4.8 and 4.14) may be cast into the form

$$\xi \sim e^{\frac{A}{(g-g_c)^\sigma}} . \tag{4.15}$$

This kind of transition has been found in many other (1+1)D systems with *short-ranged interactions*, with different exponents σ: $\sigma = \frac{1}{2}$ [123], $\sigma = \frac{2}{3}$ [124], $\sigma = 1$ [123, 125, 126, 127, 128, 129]. See also [130, 131, 132, 133, 6]. A classification of these generalized *topological phase transitions*, linking internal symmetries of the underlying model with the value of σ, has been convincingly undertaken by Bulgadaev [134, 135, 136], and subsequently by Itoi et al. [137], who used renormalization group arguments. Application of those ideas to concrete examples is far from trivial, however.

4.3 $1d$ $U - t - t'$ Model

You may have noticed that the Mott transition present in the $t - V$ spinless model and in the $SU(3)$ Hubbard model does not occur at $U_c = 0$ like in the simple Hubbard case, but rather at a $U_c > 0$ of the order of the bandwidth. Why? Let us consider the non-interacting limit in the simple Hubbard model. The Fermi sea contains just two points. A weak interaction will cause scattering processes only between the two Fermi points, so that one can *linearize* the spectrum around them for an effective description of the weak-coupling physics. It turns out that the elementary excitations of such a model will be made up of bosons, collections of the original fermions. Hence the name of this technique: *bosonization* [138, 139]. These scattering processes must conserve momentum modulo a vector of the reciprocal lattice because the original model is on a lattice. Such an *Umklapp process* [47] will eventually turn the system into an insulator [111, 112]. In the simple Hubbard model these processes are fully relevant only at half-filling, [9] where there is a distance 2π between the two Fermi points (perfect nesting) [112]. But they are irrelevant for $SU(3)$ fermions [140] and in the half-filled $t - V$ model.[10]

This is why some pretend that the Umklapp processes *mask* the real Mott transition. To clarify this issue within the Hubbard model, one needs to make them irrelevant in one way or another, still keeping spin-$\frac{1}{2}$ electrons. This is most elegantly achieved by adding a *next-nearest neighbor* hopping t', which results in the $U - t - t'$ model:

$$\mathcal{H} = -\sum_{i\sigma} \left(t\, c^\dagger_{i\sigma} c_{i+1\sigma} + t'\, c^\dagger_{i\sigma} c_{i+2\sigma} \right) + U \sum_i n_{i\uparrow} n_{i\downarrow} . \tag{4.16}$$

Note that the introduction of a t' also relies on experiment [141]. Here we will restrict ourselves to half-filling, where the sign of t' is irrelevant, due to particle-hole symmetry [142]. We set $t = 1$ and consider only positive t'. For $t' \leq \frac{1}{4}$, the non-interacting dispersion relation

$$\varepsilon(k) = -2\cos k - 2t' \cos 2k \tag{4.17}$$

[9] For the relevance of Umklapp processes at commensurate fillings see [112].

[10] In the latter case, half-filling corresponds to a quarter-filled band for electrons with spin. The distance between two Fermi points is thus π.

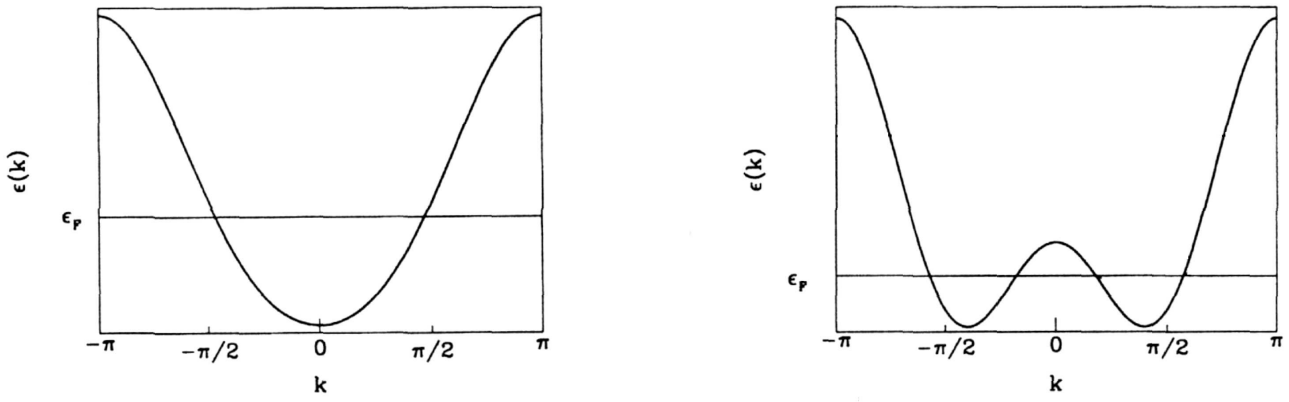

Figure 4.2: Left: energy dispersion relation of the $U-t-t'$ model for $t' < \frac{1}{2}$. Right: energy dispersion relation for $t' > \frac{1}{2}$. Here ϵ_F is the Fermi energy [142].

has one minimum, whereas for $t' > \frac{1}{4}$ it has two. At half-filling the Fermi sea consists of just two points for $t' < \frac{1}{2}$. At $t' = \frac{1}{2}$, there are three Fermi points,[11] while for $t' > \frac{1}{2}$ there are four. The situation is depicted in Fig. 4.2.

When there are two Fermi points, the low-energy behavior, determined by processes in the vicinity of the Fermi points, remains unchanged from that of the simple Hubbard model, while in the four Fermi point regime, the Umklapp processes become irrelevant and for weak *repulsive* interactions, the system is a metal with a spin gap, as predicted by bosonization [142]. As the interaction becomes stronger, the metal is predicted to undergo a Mott transition to a dimerized insulator [142]. This picture has been confirmed confirmed numerically with quantum Monte-Carlo [143] and DMRG [143, 144, 145] simulations. Note that such a tendency to frustrate nesting is generic when one adds a t' even in higher dimensional lattices [146, 147]. A preliminary phase diagram was drawn in [145] with a U_c which was found to be of the order of the bandwidth, but the critical behavior was not investigated at all.

We now turn our attention to the strong-coupling regime. Second-order degenerate perturbation theory[12] in $\frac{t}{U}$ on the $U-t-t'$ model leads to the $J-J'$ model [47]

$$\mathcal{H} = \sum_i \left(J\, \mathbf{S}_i \cdot \mathbf{S}_{i+1} + J'\, \mathbf{S}_i \cdot \mathbf{S}_{i+2} \right) \tag{4.18}$$

where $J = \frac{4}{U}$ and $J' = \frac{4t'^2}{U}$ and we get $J'/J = t'^2$. We are now deep into the insulating phase: the charges are frozen and no double occupancy is allowed anymore. This pure *spin model* has been studied extensively [148, 149, 150, 151, 128, 152]. When $J' = 0$, this is the simple, antiferromagnetic Heisenberg model, with quasi-long-range order. Using the Jordan-Wigner transformation, it can be turned into the spinless fermion model mentioned above, which

[11] The middle one's spectrum cannot be straightforwardly linearized, which makes for an interesting and possibly awkward bosonization scheme.

[12] See forthcoming chapter for further details.

can be further bosonized [6]. It is a critical, gapless system, nothing but a Luttinger liquid [6]! A *positive* J' acts to frustrate the antiferromagnetism, eventually making the system massive at $(J'/J)_c \simeq 0.24$ [151], through a BKT transition [128, 6, 152]. The massive phase has a spin gap and is dimerized [128, 6, 152], perfectly matching Fabrizio's predictions [142] as well as numerical simulations in the strong-coupling regime of the $U - t - t'$ model [145].

Chapter 5

Using the DMRG

Let us now return to the situation up to the late 1980's: approximate analytical methods nearly always have a range of applicability that is confined to limiting cases, like (very) weak or (very) strong coupling, whereas we are interested in phase transitions at intermediate coupling. Anything short of an *exact* result[1] will fail in describing properly the *catastrophes* involved in the critical regime, i. e. the drastic changes affecting the system when for example the insulator metamorphoses into a metal. Exact results are scarce and are quite often regarded as non-generic and pathological [72]. Last bad news: numerical simulations have serious limitations. Hamiltonians on small clusters of up to 30 sites may be exactly diagonalized, but the thermodynamic limit cannot be reached and no true critical behavior may be observed. Quantum Monte Carlo simulations might treat larger clusters, but the price to pay is usually the introduction of finite temperature[2] is the price to pay, once again moving the system away from the quantum criticality.

A few years previously K.G. Wilson invented a *numerical* renormalization group (RG) method specifically to solve the Kondo problem [153]. As a prophet, he was ahead of his time: his method cannot be applied to models that lack an intrinsic separation of energy scales. At the end of the past century his scheme has eventually been generalized by Steven White's *tour de force*[154, 155, 156], the *D*ensity *M*atrix *R*enormalization *G*roup. DMRG was born.

We refer the intrigued reader to the excellent original papers cited above, or to the review in ref. [157]. Let us nevertheless state the basics. We will begin by considering a simplified application of Wilson's original scheme to the particle–in–a–box–problem, an application suggested later by Wilson himself: an initial system of size L is fully diagonalized, and the m lowest-lying states in the energy spectrum are kept to form a new basis. The system of size L is then expressed in this new basis. We now increase the size of the system by putting two blocks of size L together giving a system of size $2L$. The new Hamiltonian is obtained by tensor product and is a matrix of size $2m \times 2m$. Then we go back to the full diagonalization followed by the truncation to m kept states. The system size therefore doubles at each step. The biggest problem is that the boundary conditions are fixed for each diagonalized system.

[1] at least asymptotically exact

[2] Actually QMC can run at $T = 0$ is some special cases.

When we double the size, two boundaries become the center of the new system, which is therefore badly described by the eigenstates. Successive iterations correct this only very slowly.

The DMRG fixes this problem: the idea is to diagonalize a larger system, called a *superblock*, which contains the original *system*, of size L, say. The rest of the superblock, called *the environment*, may be considered as a bath which applies the complete set of possible boundary conditions at the junction with the system. The whole superblock is exactly diagonalized. Depending on how much of the spectrum we finally would like to get, only the ground state and possibly a few excited states are kept at this point. The environment is then treated as a bath and its degrees of freedom are integrated out by forming a *density matrix* which now describes the system alone. As we know from standard quantum mechanics, the system is in a statistical mixture of pure quantum states. The eigenstates of the density matrix give the possible states the system may be in, with the eigenvalues giving the corresponding probability. The density matrix is thus diagonalized and the m states with the greatest eigenvalues are kept, as they are the m most probable states for the system to be in. These m states form the new basis in which we express the Hamiltonian of the system. Then we add one or more lattice sites to the system and repeat the procedure by defining a new environment in a way which depends on the DMRG "flavor" we are using, e.g. by reflecting the system. The reduction of the basis is the crucial point: keeping a small number of states greatly reduces the amount of numerical work in the algorithm, just like in the Wilson case, while keeping all the states turns the DMRG into the good old exact diagonalization.

While few exact mathematical statements exist about the convergence of the DMRG scheme [158], in many cases the energies of the low-lying states converge to the *exact solution exponentially* in the number of states kept [157]. The DMRG can determine the expectation value of any chosen operator in the ground state and in the desired excited states. The most efficient DMRG flavor is the following: one carries out first an *infinite-system* algorithm, i.e. one starts with a system of size $L = 4$, letting it grow by adding pairs of sites and forming the environment by reflecting the system block. Once a given size L is attained, one goes on with the usual DMRG procedure, re-building the system from scratch with the stored systems of the previous step taken now as environments. In this part of the procedure, the size L is kept fixed, therefore we talk about the *finite-system* algorithm. Several *sweeps* with increasing number of states kept m may be necessary. The exact solution is reached at best asymptotically in a *variational* procedure.

However, the DMRG is plagued by a severe drawback: it is basically a one-dimensional algorithm — the superblock is always a chain, that hates long-ranged operators in the Hamiltonian. These will build spiderweb-like bridges between the system and the environment forming the superblock. The two parts of the system become more entangled. Reaching the same accuracy calls for an increase of the number of kept states m, transforming back DMRG into exact diagonalization and its intractable complexity. Two-dimensional systems are thus a far cry from being under good control, as a mapping to a one-dimensional system requires long-range operators! Nevertheless DMRG is a wonderful $1d$ method that can treat *very* large systems without problems, even in their critical regime(s). Investigating critical

properties requires however *extensive* computational resources and the study of quantum phase transition in $1d$, although possible by now, is still a Homeric task that is only now being undertaken [150, 159, 160].

5.1 Testing and tuning the DMRG

Since the DMRG is a variational procedure, it is not truly exact. We therefore need to *test* it by comparing its results to exact solutions. Moreover, the fact that the energy behaves variationally does not imply that other quantities do. Note that this testing procedure is needed for a numerical method, which is *by essence* never exact.

We would like to determine physical quantities such as the electric susceptibility χ (3.4) or the correlation length ξ (3.14) of the $U-t-t'$ model[3] (4.16). We choose open boundary conditions (OBC) as the DMRG works best[4] in that case [157]. In order to calculate χ one could determine the ground state energy of the $U-t-t'$ model (4.16) coupled to the electric field (3.9), and then make use of the second-order perturbation theory formula for χ (3.11), but this would require a numerical evaluation of a second derivative, which is very inaccurate [162]. It is better to utilize the linear response (3.22):

$$\chi(U,t',L) = \frac{\sum_i x_i n_i(U,t',L)}{LE}\,, \tag{5.1}$$

where the x_i are the positions of the lattice sites with the origin chosen to be be in the middle of the chain. The $n_i(U,t',L)$ are the local densities in the ground state $n_i = \langle\Psi_o|\hat{n}_i|\Psi_0\rangle$, and will be determined by the DMRG. Ideally one would take an almost vanishing E and apply Eq. 5.1 straight away; but this is numerically problematic, since one has to divide a very small number by another one. It is fine as long as these numbers are exact, but as soon as they are smeared by errors, the dividing procedure will magnify them and one may end up with a meaningless result. On the other hand, if E is taken too large, the system is outside the linear response regime. Since the potential difference between the two ends of the chain is EL, EL rather than E must be kept small to contain the system in the linear response regime [163]. One has only to hope that the linear response regime begins before numerical complications arise because of the dividing procedure. We were lucky enough that this *was* the case in the $U-t-t'$ model, but keep in mind that this might not always hold. The value $EL = 0.01$ proved to be optimal and was used throughout this work.

In order to determine ξ we use the definition (3.15), with the electric field E set to zero. We do not need to worry about any linear response, we can just determine $\langle\Psi_o|\hat{n}_i\hat{n}_j|\Psi_0\rangle$ for $i \leq j$ with DMRG. The only drawback is that the number of terms grows like L^2, which compared to χ severely limits the maximal size for the calculation.

[3] We have chosen not to consider the charge gap, as it is a *very* tricky quantity to calculate, especially when one considers the thermodynamic limit. See [145, 161]. Also, it has already been calculated, see Ref. [145].

[4] Periodic boundary conditions necessitate the introduction of a *long-range* coupling between the two ends of the chain, thus leading to poorer convergence.

Unfortunately there is no straightforward way of determining the DMRG error. We only know certain trends: the error diminishes exponentially with increasing m [157], and DMRG performs worst when there is no energy scale, i. e. when the system is *gapless* [164, 165]. Using the weight of the discarded states density matrix to quantify the error is often used [157], but this measure is algorithm-dependent and is therefore not universal [166]. Instead we compare the DMRG results in the most unfavorable case, i. e. gapless and without interaction, with the exact result which is of course available. By doing this, we can *tune* the DMRG parameters, the most important of which are the maximum number m of states kept[5] in order to achieve the desired precision. Investigating[6] $U > 0$, we will use exactly the same parameters, knowing that the precision will be at least as good as in the noninteracting case.

At $U = 0$ we have a half-filled band of free electrons, a system that we can solve analytically to get $\chi(U = 0, t', L)$ and $\xi(U = 0, t', L)$; this is done in the appendices A.1 and A.2 respectively. At $t' = 0$ and for large L we obtain the asymptotic behavior

$$\chi(U = 0, t' = 0, L) = \frac{1}{12\pi} L^2 \tag{5.2}$$

$$\xi(U = 0, t' = 0, L) = \frac{7\zeta(3)}{\pi^4} L \,, \tag{5.3}$$

while for nonzero t', we find the same large L dependence:

$$\chi(U = 0, t', L) \propto L^2 \tag{5.4}$$

$$\xi(U = 0, t', L) \propto L \,. \tag{5.5}$$

The constant of proportionality is a function of t'. This is typical for a gapless system: physical quantities will always be finite in a critical system of *finite* size L, *diverging* only with L, while they will remain finite in the thermodynamic limit away from criticality [167]. Note that Eq. 5.5 is pretty much what we expect, on dimensional as well as on physical grounds, since a perfect metal maintains phase coherence throughout the finite lattice, yielding a correlation length spanning the whole system.

DMRG results have been compared to the analytic solution at finite sizes $L = 10, \ldots, 1000$. For small sizes, one has to utilize the exact formulae (3.12) and (A.22) instead of the asymptotic ones. Consider first the calculation of χ. We found that for $t' < \frac{1}{2}$, $m = 800$ was sufficient to obtain 6 significant digits of accuracy, while for $t' > \frac{1}{2}$ we had to increase m greatly, up to 2400, to get the same precision at small sizes, and obtained as few as 4 significant digits at larger ones.[7] To summarize this comparison, we plot the DMRG data $\chi(U = 0, t', L)/L^2$ as a function of $1/L$ in Fig. 5.1 for $t' = 0$ and in Fig. 5.2 for $t' = 0.7$.

A linear fit can be used to extrapolate to $L = \infty$, yielding (the error comes only from the fitting procedure)

[5] as well as the number of sweeps and the way we increase the number of states to reach m

[6] or $U < 0$

[7] Generally, after the infinite-system building-up, we start a first sweep with $m = 50$ and then double m until we reach the maximal number of states that we want to keep. We even went up to $m = 3200$ sometimes.

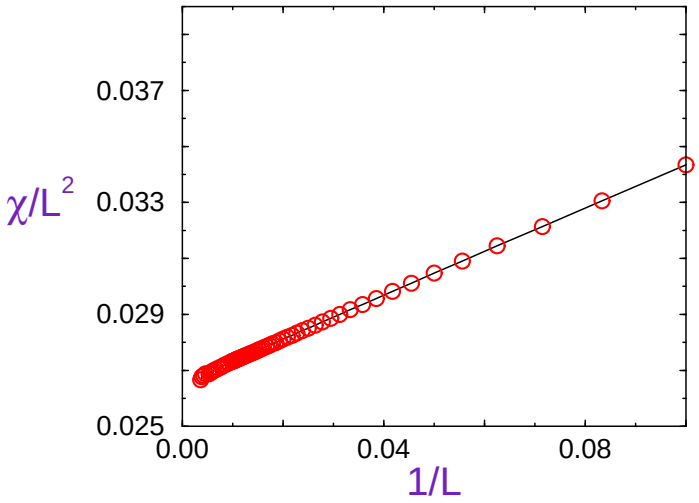

Figure 5.1: Circles: Electric susceptibility divided by L^2 as a function of $1/L$ for L up to 300, according to DMRG, with $U = 0$, $t' = 0$ and $EL = 0.01$. The solid line is a linear fit to the data.

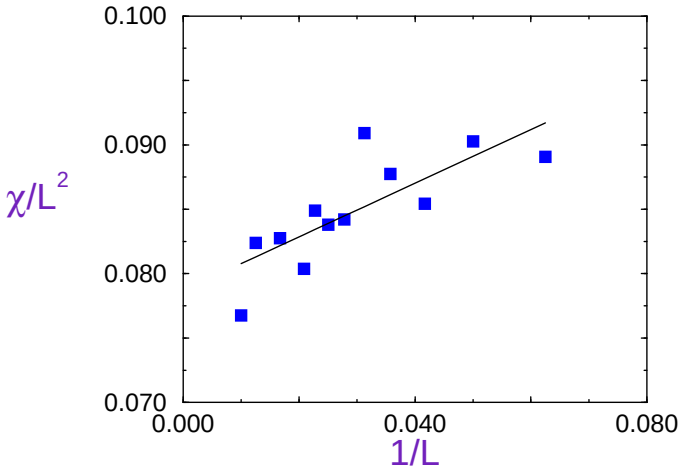

Figure 5.2: Squares: electric susceptibility divided by L^2 for $L = 16$ to 100, as a function of $1/L$, according to DMRG, with $U = 0$, $t' = 0.7$ and $EL = 0.01$. The deviation from a perfect linear behavior, as in Fig. 5.1, is an intrinsic finite-size effect. The solid line is a linear fit to the data.

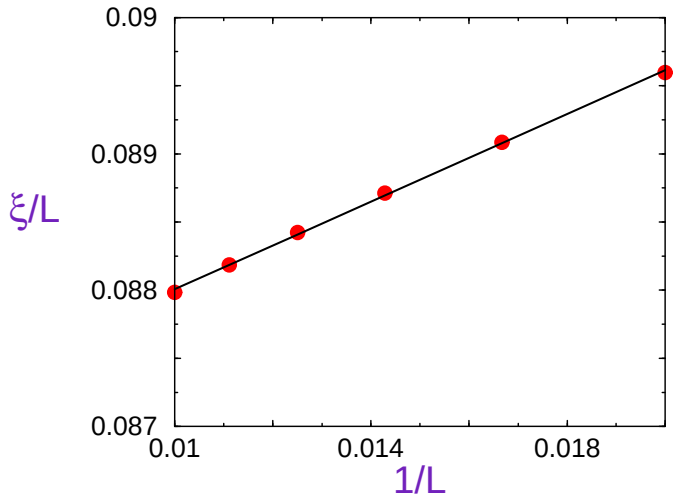

Figure 5.3: Circles: correlation length divided by L as a function of $1/L$, for $L = 50$ to $L = 100$, according to DMRG, with $U = 0$ and $t' = 0$. The solid line is a linear fit to the data.

$$\frac{\chi_{\mathrm{DMRG}}(t'=0,L)}{L^2} \overset{L\to\infty}{\longrightarrow} 0.026650(68) \tag{5.6}$$

$$\frac{\chi_{\mathrm{DMRG}}(t'=0.7,L)}{L^2} \overset{L\to\infty}{\longrightarrow} 0.0786(17)\ , \tag{5.7}$$

whereas the exact values are

$$\frac{\chi(t'=0,L)}{L^2} \overset{L\to\infty}{\longrightarrow} 0.026525\ldots \tag{5.8}$$

$$\frac{\chi(t'=0.7,L)}{L^2} \overset{L\to\infty}{\longrightarrow} 0.0774\ldots\ . \tag{5.9}$$

As can be seen the agreement is quite good. The calculation of ξ is more delicate, since one has to measure long-ranged correlations $\langle \hat{n}_i \hat{n}_j \rangle$. Since such quantities may only be determined with a much lower accuracy within the DMRG, we have to significantly increase the number of states kept m. For $t' < 1/2$, we have kept up to 1200 states in order to obtain 6 significant digits of accuracy, while at $t' > 1/2$, 1600 states were necessary to obtain between 4 and 2 significant digits, depending on the size of the system.[8] We plot the DMRG data $\xi(U = 0, t', L)/L$ as a function of $1/L$ for $t' = 0$ in Fig. 5.3 and for $t' = 0.7$ in Fig. 5.4 We do a linear fit and extrapolate it to $1/L = 0$ (the error comes only from the fitting

[8] We have tried to increase m in order to get a higher precision, but the measurement time proved to be excruciatingly long.

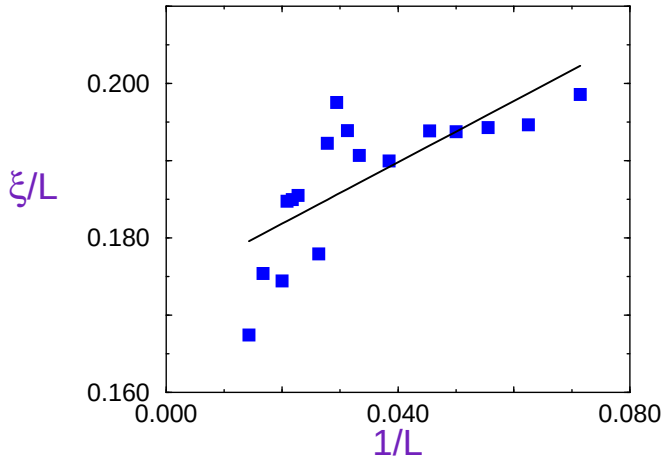

Figure 5.4: Squares: correlation length divided by L as a function of L, for $L = 14$ to $L = 70$, according to DMRG, with $U = 0$ and $t' = 0.7$. The solid line is a linear fit to the data. Note that the deviation from a perfect linear behavior comes partly from intrinsic finite-size effects and partly from the DMRG error.

procedure):

$$\frac{\xi_{\mathrm{DMRG}}(t'=0,L)}{L} \stackrel{L\to\infty}{\longrightarrow} 0.086400(31) \tag{5.10}$$

$$\frac{\xi_{\mathrm{DMRG}}(t'=0.7,L)}{L} \stackrel{L\to\infty}{\longrightarrow} 0.1739(35)\ , \tag{5.11}$$

whereas the exact solution is

$$\frac{\xi_{\mathrm{exact}}(t'=0)}{L} \stackrel{L\to\infty}{\longrightarrow} 0.086382\ldots \tag{5.12}$$

$$\frac{\xi_{\mathrm{exact}}(t'=0.7)}{L} \stackrel{L\to\infty}{\longrightarrow} 0.1727\ldots\quad . \tag{5.13}$$

As can be seen, the agreement is quite good. Note that in Figs. 5.2 and 5.4, there is a lot of scatter in the points, so that it may seem at first not fully convincing that the data are best fit by straight lines. The final justification however is that the values obtained by this extrapolation agree well with the known exact results.

5.2 Strong-coupling limit

To be on the safe side, we would like to compare the DMRG results with some exact results, at $U > 0$ this time, possibly pretty far from $U = 0$. Fortunately this is possible, and even easy: one needs to do a second order degenerate perturbation calculation in $1/U$ on the

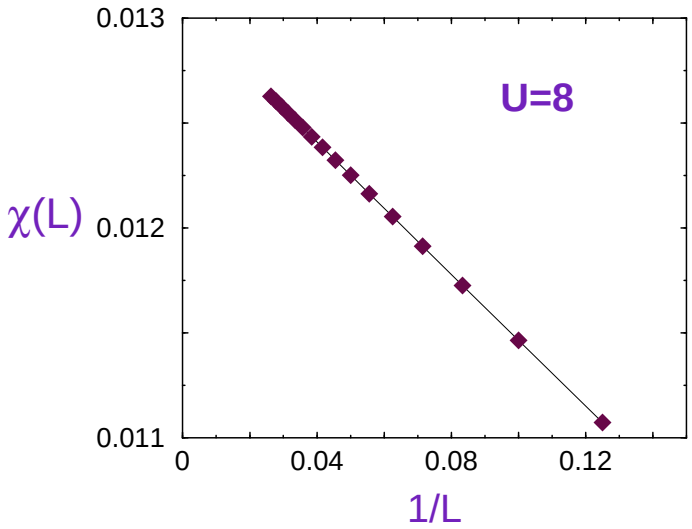

Figure 5.5: Diamonds: electric susceptibility for $U = 8$, $t' = 0$ and L going from 10 to 50. The solid line is a linear fit to the form of Eq. 5.15.

$U - t - t'$ model for χ (appendix B.1) and simply to take the $U \to \infty$ limit for ξ (appendix B.2).

We first consider χ at $t' = 0$. The result (Eq. B.7) is

$$\chi_\infty(U, t' = 0) = \frac{8 \ln 2}{U^3} \tag{5.14}$$

in the thermodynamic limit, $L \to \infty$. For large U, χ is finite and the system is insulating, as is already well known [72, 47], but the DMRG gives $\chi(L)$ only for a finite size L. If $\chi(L)$ is analytic in $1/L$, we may consider its Taylor expansion around $1/L = 0$:

$$\chi(L) \; = \; \chi_\infty \; + \; \mathcal{O}\left(\frac{1}{L}\right) \; , \tag{5.15}$$

where χ_∞ is the electric susceptibility in the thermodynamic limit. If we can reach large enough sizes so that higher order corrections in $1/L$ are negligible, a linear fit to the data $\chi(L)$ is possible and an extrapolation at $1/L = 0$ yields χ_∞ directly: this procedure is called *finite-size scaling*[9] [167]; we give one example in Fig. 5.5. For large U, the same procedure can be applied to yield $\chi_\infty(U)$, which may be directly compared to the exact strong-coupling relation (5.14). This is done in Fig. 5.6. As one can see, at $U \approx 100$ and above, the DMRG data match the exact *asymptotic* result, thus confirming the validity of the whole procedure.

For $t' > 0$, $\chi_\infty(U, t')$ still goes like $1/U^3$ for large enough U (see appendix B.1). Since the $J - J'$ model is non-integrable in general, we cannot give the exact proportionality constant, like in the $t' = 0$ case, except at one point: $(J'/J)_{\mathrm{MG}} = t'^2_{\mathrm{MG}} = 1/2$. This is the Majumdar-Ghosh point, where there is an exact solution [168, 169]. For $t' = \frac{1}{\sqrt{2}}$, the electric

[9] This has to be compared to the *finite-temperature scaling* used by experimentalists to get $T = 0$ quantities out of finite-temperature data.

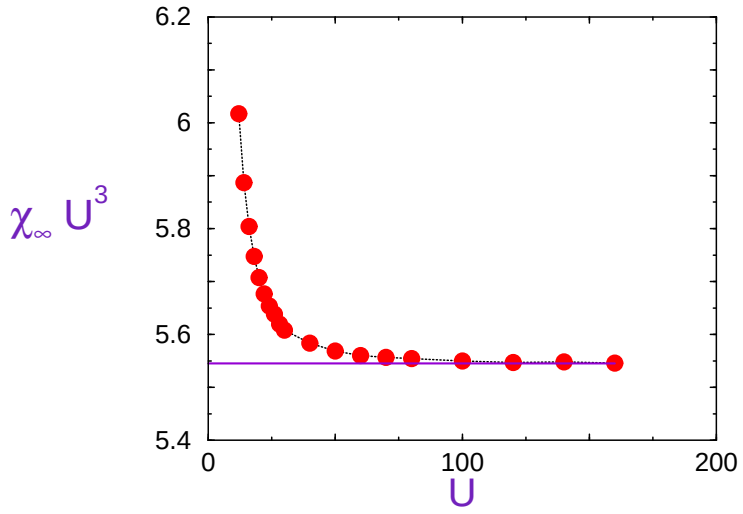

Figure 5.6: Circles: electric susceptibility multiplied by U^3 obtained using the DMRG for $t' = 0$; the dotted line is a guide to the eye. Note that every point comes from a finite-size scaling according to Eq. 5.15. Solid line: strong coupling limit according to Eq. 5.14.

susceptibility becomes

$$\chi_\infty(U, t' = \frac{1}{\sqrt{2}}) \;=\; \frac{9}{U^3} \tag{5.16}$$

for large U (B.15). The comparison with the DMRG results is done in Fig. 5.7. The DMRG data again match the exact *asymptotic* result.

Now we turn our attention to ξ at $t' = 0$. The strong-coupling limit is (B.31)

$$\xi_\infty(t' = 0, U) \;=\; \frac{4 \ln 2}{U^2} \tag{5.17}$$

in the $L \to \infty$ limit. We therefore need to perform a finite-size scaling procedure for the $\xi(L)$ values from DMRG:

$$\xi(L) \;=\; \xi_\infty \;+\; \mathcal{O}\left(\frac{1}{L}\right) . \tag{5.18}$$

At large enough L, only the first order finite-size correction has to be taken into account, and the scaling is similar to that of $\chi(L)$ as shown in Fig. 5.5. We apply this procedure to large U to extract $\xi_\infty(U)$ and compare it to the exact result in Fig. 5.8. For $t' > 0$, we know that

$$\xi_\infty(t', U) \;\propto\; \frac{1}{U^2} , \tag{5.19}$$

but the proportionality constant cannot be determined, and only the $1/U^2$ behavior can be successfully checked with the DMRG (not shown here).

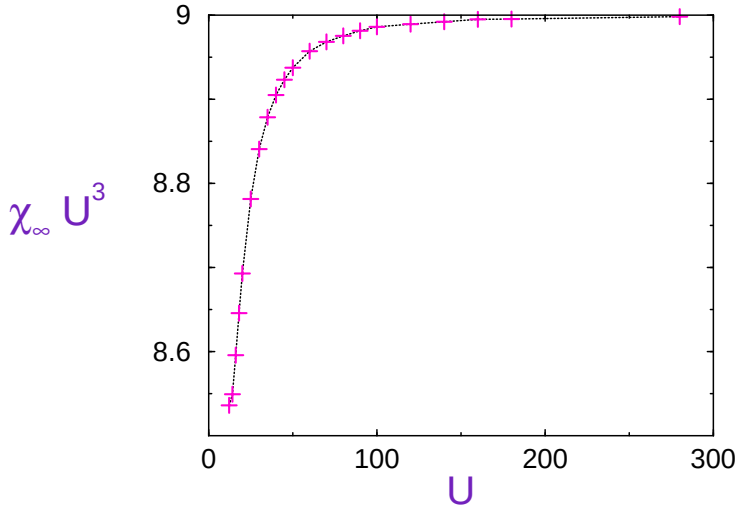

Figure 5.7: Plus signs: electric susceptibility multiplied by U^3, as obtained with DMRG, for $t' = \frac{1}{\sqrt{2}}$; the dotted line is a guide to the eye. Note that every point comes from a finite-size scaling, following Eq. 5.15. Recall that the Majumdar-Ghosh value is 9.

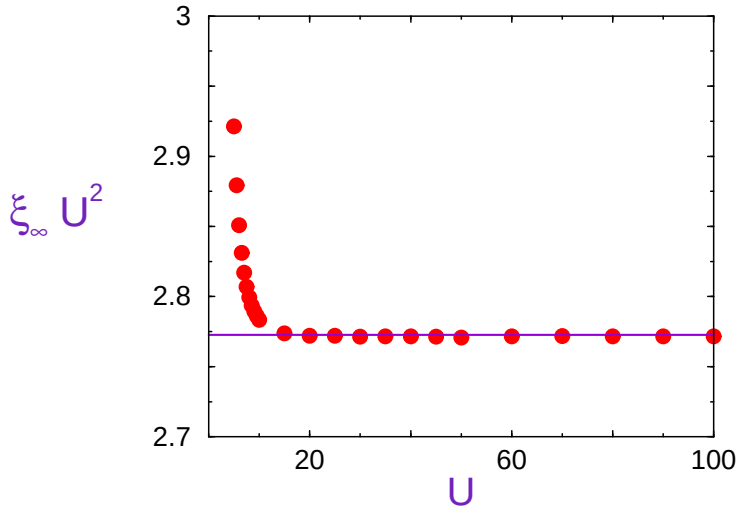

Figure 5.8: Circles: correlation length multiplied by U^2, as obtained with the DMRG, for $t' = 0$. Note that every point comes from a finite-size scaling using Eq. 5.18.

To summarize, the tests we did at $U = 0$ ensure that the DMRG parameters are correctly tuned and that we can obtain results with the desired precision. Since this gapless case in the most difficult one for the DMRG, we can reasonably expect that by keeping the same parameters for the gapped cases, we will also obtain sufficiently accurate results, possibly with an even higher precision. At strong coupling, an analytic solution is also at hand and the DMRG results obtained as described above are a very good match, confirming the validity of the whole procedure.

Chapter 6

The Dielectric Catastrophe

Armed with the implacable DMRG machinery, we can look forward to unraveling the Mott transition's one-dimensional mysteries. Two physical quantities that we expect to behave *critically* are at our disposal: the *electric susceptibility* and the *correlation length*. They are analyzed in detail in the next two sections, respectively, for the $U-t-t'$ model. In the last section we *observe*, by verifying that hyperscaling is satisfied, that the ξ defined by Eq. 3.14 is indeed the true correlation length, therefore resolving the puzzle we posed previously.

6.1 Electric susceptibility

The qualitative phase diagram of the $U-t-t'$ chain at half-filling is already known [142, 145, 144]: for t' between 0 and $\frac{1}{2}$, the system is insulating as soon as $U>0$, while for t' greater than $\frac{1}{2}$, there is a metallic phase up to U_c where the chain becomes insulating. The system is always metallic for $U<0$. We started studying this transition by measuring $\chi(U,t',L)$ for several sizes and interaction strengths, while keeping t' fixed at different values (0, 0.5, 0.6, 0.7, 0.8, 0.9, 1). The results are shown in Fig. 6.1 for $t'=0.7$ and some U values. The situation is similar for any t'. (In order to observe a metallic phase for $t'<\frac{1}{2}$, one has to consider negative U.) There are two characteristically different behaviors. At small U (in blue in Fig. 6.1), the system is metallic and the susceptibility diverges with system size: a fit to a power law in L always yields an exponent very close to 2 (to within 5%), for any values of t' and U in a metallic region.[1] Not only the line $U_c(t')$, but the whole metallic phase in the $U-t-t'$ model is thus *at criticality*. The susceptibility scales like [167]

$$\chi \sim L^{2-\eta}, \tag{6.1}$$

which means that $\eta\equiv 0$ for the whole critical metallic phase. This matches the analytical result for χ (5.4) at $U=0$ and we are led to *conjecture* that such a L^2 divergence is *generic* for a one-dimensional perfect metal.[2] For larger U (in red in Fig. 6.1), χ tends to a finite value as $L\to\infty$, following Eq. 5.15, and a finite-size scaling extrapolation similar to that

[1] for positive or negative U

[2] which is *per force* a Luttinger liquid, as far as the charge degrees of freedom are concerned [113].

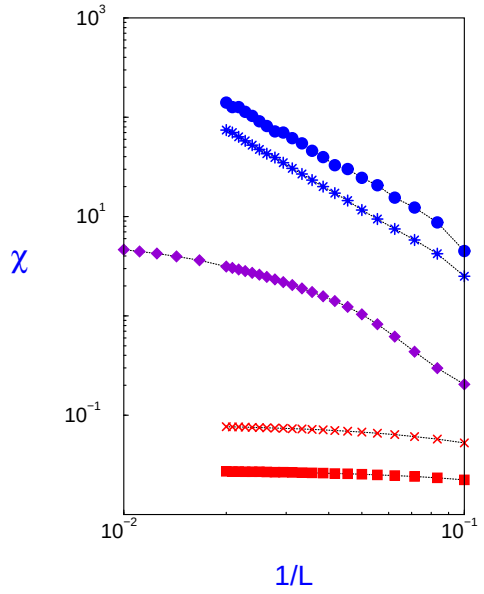

Figure 6.1: Electric susceptibility, χ, as a function of $1/L$ for $t' = 0.7$ and for $U = 1$ (circles), $U = 2.5$ (stars), $U = 4$ (diamonds), $U = 5.5$ (crosses), and $U = 7$ (squares). Dotted lines are guides to the eye. Blue stands for a metallic behavior $\chi \sim L^2$, red for an insulating one $\chi = \chi_\infty + \mathcal{O}(\frac{1}{L})$, and violet for an insulator close to the critical point, where one must consider larger sizes in order to *observe* the insulating character.

shown in Fig. 5.5 for $t' = 0$ will give χ_∞. Away from the transition, a system size of $L \leq 50$ is ample to accurately determine χ_∞. Care must be taken near the transition (U=4, violet, in Fig. 6.1): up to a length scale of the order of the correlation length, which diverges while approaching the transition, the system will *appear* metallic even if it is intrinsically insulating. Such a crossover from metallic to insulating behavior is evident in the $U = 4$ curve, for which lattice sizes of up to $L = 100$ are necessary to extract χ_∞. Very close to the transition, the correlation length will become very large, requiring an L that is larger than can be reached numerically — smaller systems will appear metallic.[3] Thus there will be an insulating region very close to U_c where getting χ_∞ will be impossible. We may just hope that the critical region, i. e. the region where one can actually observe the asymptotic form of the divergences, is *larger than* the fuzzy zone in which the thermodynamic limit cannot be attained.

In Fig. 6.2 we summarize the results for χ_∞ for several values of t'. What is seen is the *dielectric catastrophe* itself (see for instance Figs. 2.2 and 2.3): the electric susceptibility χ diverges when one approaches the critical interaction strength coming from the insulating side. Of course, we would like to discover *how* it diverges and *where* exactly it begins to diverge, i. e. what is $U_c(t')$. Consider first the simple, integrable Hubbard model ($t' = 0$). As discussed previously, the transition takes place at $U_c = 0$. Notice that the width of the

[3] This length is about $L = 1000$, but it depends on how long one is willing to wait; $L = 1000$ takes about one week on a 1Ghz Pentium III processor.

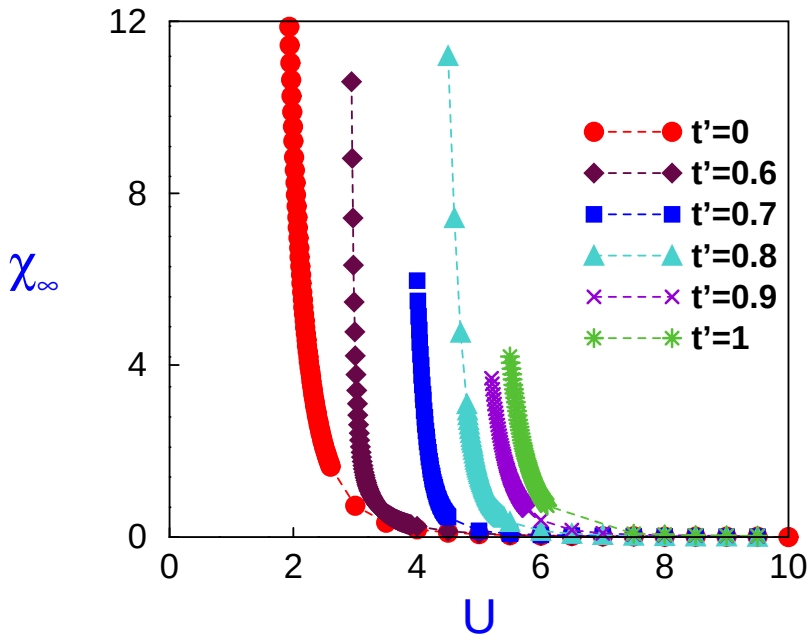

Figure 6.2: Electric susceptibility $\chi_\infty(U, t')$ of the infinite-size system for $t' = 0$, 0.6, 0.7, 0.8, 0.9, 1 as a function of U; the dashed lines are guides to the eye. Each point results from a finite-size scaling according to Eq.5.15.

zone where it is impossible to reach the thermodynamic limit is about 2 (measured in units of t). We expect χ to be a function of the gap for sufficiently small U, as Δ is the unique relevant energy scale close to the transition [6]. Using the formulae for the critical behavior of the gap (2.11) and for the electric susceptibility (2.15) we can write down the following relation:

$$\chi_\infty \sim \Delta^{-\frac{\gamma}{z\nu}} . \tag{6.2}$$

The dynamical critical exponent is $z = 1$, owing to the relativistic invariance of the Hubbard model [38]. We are fortunate enough to know the gap exactly [102] and we can use the analytic formula (4.4) to plot $\chi(U)$ against $\Delta(U)$ in Fig. 6.3. Surprisingly at first, we find a power-law relation satisfying Eq. 6.2 over a wide range of U values, from $U = 1.9$ up to intermediate coupling, $U = 10$. The fit yields

$$\frac{\gamma}{z\nu} \simeq 2.0098(72) \tag{6.3}$$

where the error comes only from the fitting procedure. In other words

$$\chi_\infty \sim \Delta^2 . \tag{6.4}$$

This result should not puzzle us too much however. It could actually have been predicted.

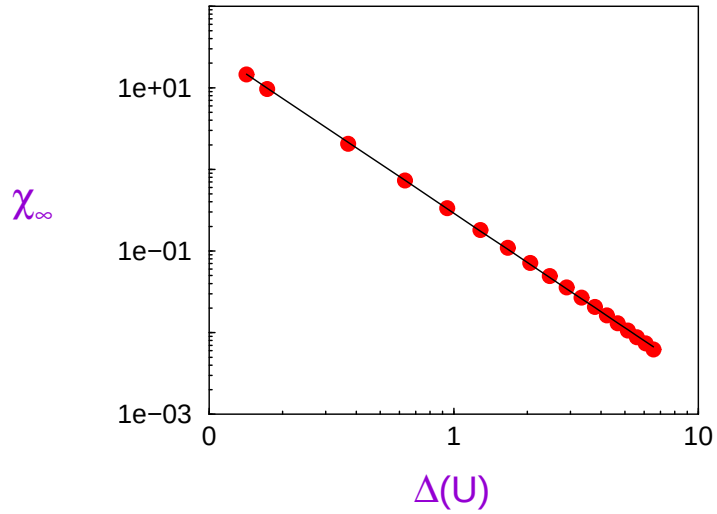

Figure 6.3: Circles: electric susceptibility as a function of the gap on a log-log scale for $t' = 0$. The straight line represents a power-law fit. Each point results from a finite-size scaling according to Eq. 5.15.

The first hint is the inequality (3.17), relating[4] χ, Δ and ξ. A more serious argument comes from continuum field theory [6]: at small U, the *scaling limit* of the Hubbard model is nothing but a *sine-Gordon* model [38], which is *relativisticly invariant* and has *solitons* (quasi-particles) as elementary excitations with the following dispersion relation [38]

$$E_k \;=\; \sqrt{c^2k^2 + \Delta^2}\;. \tag{6.5}$$

Here the "speed of light" c is the soliton speed; it is given to first order in U at $n = 1$ by [111, 38]

$$c \;=\; 2 + \frac{U}{2\pi} + \ldots \quad . \tag{6.6}$$

It is reasonable to expect that the leading term in the large-x decay is determined by the contribution of a simple quasi-particle pole. The dynamic electric susceptibility has the form

$$\chi(k,\omega) \;=\; \frac{\mathcal{A}}{c^2k^2 + \Delta^2 - (\omega + i\delta)^2} + \cdots \tag{6.7}$$

at small k and $T = 0$, where δ is a positive infinitesimal and $\mathcal{A}$ the quasi-particle residue or quasi-particle weight. Close to the transition, $\mathcal{A}$ scales as [6]

$$\mathcal{A} \;\sim\; \Delta^{\frac{\eta}{z}}\;. \tag{6.8}$$

Since $\eta = 0$ (see Eq. 6.1), the quasi-particle residue remains constant and does *not* vanish as $U \to 0$. For the static, homogeneous electric susceptibility, $\omega = 0$, $k = 0$ so that Eq. 6.7 reduces to $\chi_\infty \sim \Delta^2$ (6.4). The same behavior has been observed for the spin susceptibility in Heisenberg chains [170].

[4] The reader's patience will be rewarded in the next section by a full explanation.

The extrapolation to $\Delta \to 0$ confirms that $U_c = 0$, though this should not satisfy us: as soon as we take $t' \neq 0$, the model loses its integrability and there is no longer an analytic formula for the gap. Let us take a closer look at the weak-coupling formula for the gap (4.6)

$$\Delta \;=\; \frac{8}{\pi}\,\sqrt{U}\; e^{-\frac{2\pi}{U}}\;, \tag{6.9}$$

which gives a susceptibility

$$\chi_\infty \;\sim\; \frac{1}{U}\, e^{\frac{4\pi}{U}}\;. \tag{6.10}$$

As noted earlier in Chapter 4, we face an *exponential divergence* of the critical quantities as a function of the coupling constant U, which means the transition is *infinite order*, i.e. the divergence is stronger than any power-law. In such a case, $\nu \to \infty$, as well as $\gamma \to \infty$. Their *ratio* however is well defined, as may be seen from Eq. 6.2. Following [106] we write

$$\tilde{\gamma} \;\equiv\; \frac{\gamma}{\nu} \tag{6.11}$$

where $\tilde{\gamma} = 2$, as $z = 1$. Let us now be naive and pretend we do not believe Eq. 6.10 to be true. We cautiously write the most general exponential divergence

$$\chi_\infty \;=\; \frac{A}{U - U_c}\, e^{\frac{B}{(U-U_c)^\sigma}}\;. \tag{6.12}$$

where A and B are constants, U_c is the "unknown" critical coupling and σ is the exponent classifying infinite-order transitions [134, 135, 136, 137]. A non-linear *fit* of the $t' = 0$ data according to Eq. 6.12 for the smallest U values at our disposal yields $A \simeq 0.011$, $B \simeq 13.47$, $U_c \simeq -0.03$ and $\sigma = 0.848$. We see that we obtain a rather good, although *underestimated*, U_c. A tendency to underestimate χ and thus U_c is in fact quite general for a variational algorithm such as the DMRG and has been reported for other models [127]. On the other hand, the values obtained for B, which should be $4\pi = 12.56637\ldots$, and σ, which should be 1 are pretty imprecise; this can be attributed to the presence of *logarithmic corrections* [137, 171, 151] in the Hubbard model(like $1/U$ in Eq. 6.10). Even including the leading order term explicitly in Eq. 6.12 is not sufficient. Recall that Eq. 6.12 is valid only asymptotically; the mismatch for B and σ, as well as for U_c, would be lifted if we could gain access to χ_∞ for smaller U's.

Logarithmic corrections are, in general, *non-universal*; thus we were wrong when we claimed that we were considering the most general divergence in Eq. 6.12. For small enough U, the logarithmic correction $1/(U - U_c)$ can be simply discarded to yield

$$\chi_\infty \;=\; A\; e^{\frac{B}{(U-U_c)^\sigma}}\;. \tag{6.13}$$

We have gained in universality, but have worsened the conditions for the fitting! The same procedure as before, but with Eq. 6.12 replaced by Eq. 6.13, now gives $A \simeq 0.00097$, $B = 17.42$, $U_c = -0.15$ and $\sigma = 0.84$. The corresponding fit is shown in Fig. 6.4 (left). The result for σ is quite good compared to the previous one, but B is fairly far from the exact

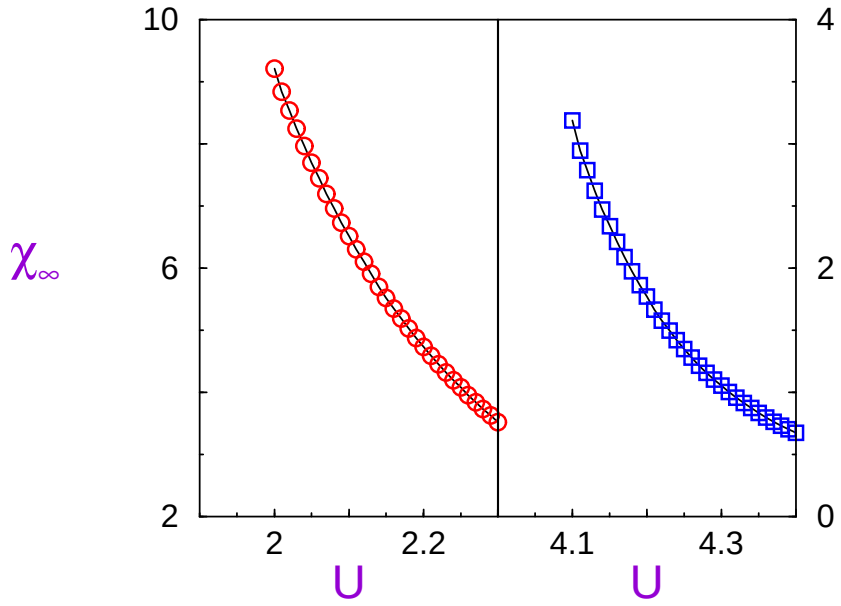

Figure 6.4: Electric susceptibility χ_∞ for $t' = 0$ (left: circles) and for $t' = 0.7$ (right: squares). The lines are non-linear fits according to Eq. 6.13. Each point results from a finite-size scaling (5.15).

value and U_c is underestimated even more: these values are nevertheless consistent with the exact ones, to within quite large error bars, which become smaller if one includes logarithmic corrections.

I am sorry to announce that the fun part is over. We now have to switch t' on. For $t' = 0$ up to $\frac{1}{2}$, there are no significant changes, either qualitative or quantitative, in χ_∞. We do not show these t' on Fig. 6.2, because they would simply overlap the $t' = 0$ data. However for $t' > \frac{1}{2}$, it is clear from Fig. 6.2 that the bigger t', the larger the $U \equiv U_c$ at which χ diverges. Having no analytic formula for the gap any more, we might be stuck. Are we really? No, we just need to fit the DMRG data directly, since we have only two choices at hand. The first one to be tested is a power-law

$$\chi_\infty = \frac{C}{(U - U_c)^\gamma} \tag{6.14}$$

corresponding to a finite value of γ. This is a total failure because it systematically gives a U_c in the insulating phase: more precisely this U_c is in the phase where the system is obviously insulating[5], not yet metallic, but where no reliable finite-size scaling procedure can be done to determine χ_∞ with a sufficient accuracy. Such a power-law divergence is thus not strong enough, and one has to consider $\gamma \to \infty$, i. e. an infinite-order divergence, our second choice. We fit the DMRG data for $t' = 0.6, 0.7, 0.8, 0.9$ and 1 with Eq. 6.13. The result is shown in

[5] i.e. where $\chi(L)$ is not diverging like L^2

Fig. 6.4 for $t' = 0.7$, where we get $B \simeq 12.45$, $\sigma \simeq 1.049$ and $U_c = 2.68$. This time U_c is very reasonable, as may be seen from Fig. 6.1. The nice surprise is that $B \simeq 4\pi$ and $\sigma \simeq 1$, the exact $t' = 0$ values; the fit is even better than for $t' = 0$! This is probably due to the "pathological" character of the simple Hubbard model, where logarithmic corrections are possibly at their strongest. Furthermore, we invariably get, for all the other $t' > \frac{1}{2}$, $B \simeq 4\pi$ and $\sigma \simeq 1$, just as good results as for $t' = 0.7$. Below we list the critical interaction strengths obtained this way, as well as the constant A in Eq. 6.13

$$\begin{aligned} t' = 0.6 \ : \quad & U_c = 2.12 \ , \quad A = 2.1 \ 10^{-6} \\ t' = 0.7 \ : \quad & U_c = 2.68 \ , \quad A = 4.4 \ 10^{-4} \\ t' = 0.8 \ : \quad & U_c = 3.11 \ , \quad A = 1.8 \ 10^{-3} \\ t' = 0.9 \ : \quad & U_c = 3.46 \ , \quad A = 2.8 \ 10^{-3} \\ t' = 1 \ : \quad & U_c = 3.76 \ , \quad A = 3.3 \ 10^{-3} \ . \end{aligned} \tag{6.15}$$

Previous work has underestimated U_c quite severely: $U_c = 3.2$ for $t' = 1$ [145] and $2 < U_c < 3$ for $t' = 0.8$ [143]. Therefore, the exponential form Eq. 6.13 with $B = 4\pi$ and $\sigma = 1$

$$\chi_\infty \ = \ A \, e^{\frac{4\pi}{(U - U_c)}} \tag{6.16}$$

characterizes the transition at all t', irrespective of whether a spin gap exists ($t' > \frac{1}{2}$ [142]) or whether U_c is finite or zero. Presumably, the *universality class* is the same for every t'.

6.2 Correlation length

To confirm this picture, we need to determine the critical exponents z and $\tilde{\gamma}$. This is most easily done by measuring the *correlation length*[6] $\xi(U, t', L)$. This was done for several sizes and interaction strengths while keeping t' fixed at $0, 0.5, 0.7, 0.8$. Because of the large computational effort involved, we have restricted ourselves to the most representative values of t'. The phase diagram of the half-filled $U-t-t'$ chain is again confirmed and the situation depicted in Fig. 6.1 for χ remains unchanged for any t', as may be seen in Fig. 6.5 for $t' = 0.7$, except that in the entire metallic phase, ξ is proportional to the system size:

$$\xi \ \sim \ L \ . \tag{6.17}$$

A power-law fit to the DMRG data invariably gives an exponent equal to 1 to within 5%. Eq. 6.17 being *generic* for a system at criticality, we stress again that the whole metallic phase is indeed *critical* [6]. On the other hand, ξ tends to a finite value at $L \to \infty$ for the insulating state, according to Eq. 5.18. We also find a region in which the system appears metallic up to the largest size we have been able to reach. It is a little wider here than for χ_∞, since we have only treated system sizes up to $L = 160$. We summarize the measurements in Fig. 6.6, the analogue of Fig. 6.2. This time we observe just a *catastrophe*, i. e. a divergence

[6] instead of the charge gap itself

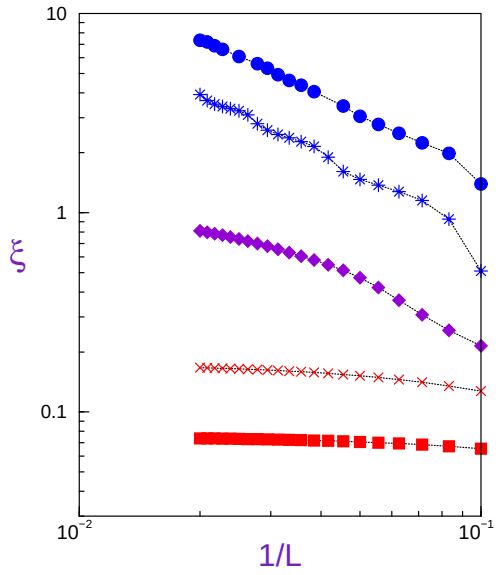

Figure 6.5: Correlation length, ξ, as a function of $1/L$ for $t' = 0.7$ and for $U = 1$ (circles), $U = 3$ (stars), $U = 4$ (diamonds), $U = 5$ (crosses), and $U = 7$ (squares). L goes from 10 to 50. Dotted lines are guides to the eye. Blue stands for a metallic behavior $\xi \sim L$, red for an insulating one $\xi = \xi_\infty + \mathcal{O}(\frac{1}{L})$, and violet for an insulator close to the critical point, where one should consider larger sizes in order to definitely *observe* the insulating character.

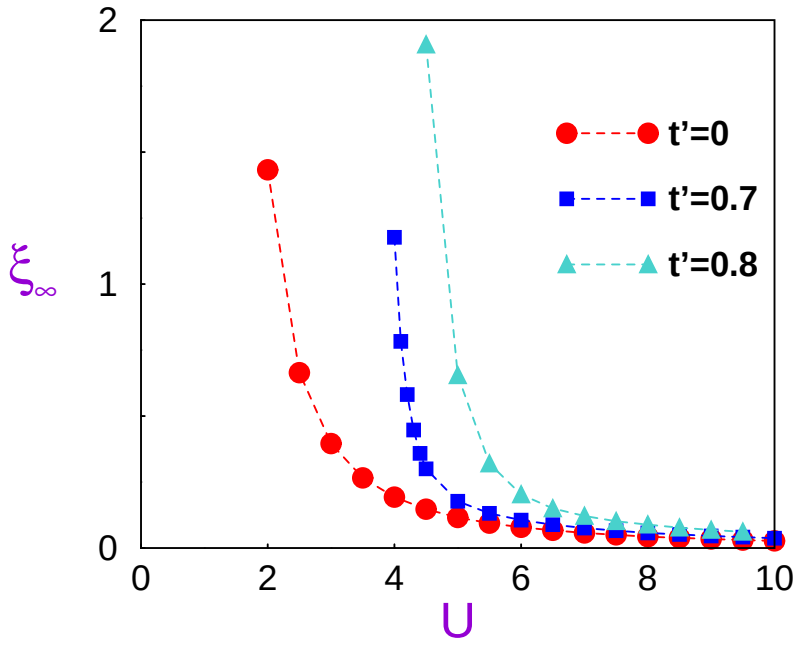

Figure 6.6: Correlation length $\xi_\infty(U, t')$ of the infinite-size system for $t' = 0$, 0.7, 0.8 as a function of U; the dashed lines are guides to the eye. Each point results from a finite-size scaling according to Eq. 5.15.

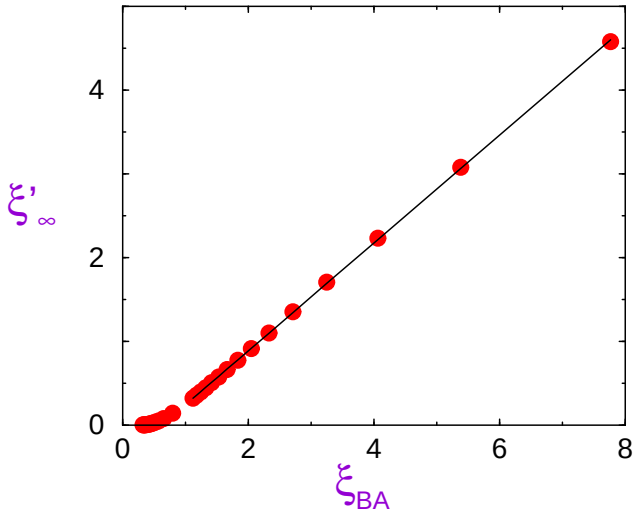

Figure 6.7: Circles: correlation length ξ'_∞ as a function of $\xi_{\rm BA}$ (6.18) from DMRG calculations; every point comes from finite-size scaling using Eq. (5.18); $t' = 0$. The solid line is a linear fit for weak and intermediate coupling.

of the correlation length. This is reassuring, since it is necessary for a phase transition with fully developed critical behavior.[7] Consider first the simple Hubbard model, $t' = 0$, where ξ can be calculated with the Bethe Ansatz [38]

$$\xi_{\rm BA}(U) \;=\; U/\left(4\int_1^\infty dy \frac{\ln(y+\sqrt{y^2-1})}{\cosh(2\pi y/U)}\right) \;. \tag{6.18}$$

With the rescaling

$$\xi'_\infty \;\equiv\; \frac{\pi^4}{7\zeta(3)}\xi_\infty \;, \tag{6.19}$$

ξ_∞ is exactly equal to the system size for $U = 0$, according to Eq. 5.3, which means that it is now expressed in units of the lattice constant and may be compared to $\xi_{\rm BA}$ in Fig. 6.7. In the weak- and intermediate-coupling regimes, both quantities are proportional to each other. A linear fit gives

$$\xi'_\infty \;\simeq\; 0.64\,\xi_{\rm BA} \;. \tag{6.20}$$

Therefore ξ_∞ is the true correlation length for the system for $t' = 0$, at least in the critical region, which is exactly where we want to focus our attention. In the large-U limit, however, they no longer match: $\xi_{\rm BA}$ goes like $1/\ln(U)$ [38] rather than $1/U^2$ like "our" ξ (B.31). This is of no serious concern, however, since in this region, ξ'_∞ and $\xi_{\rm BA} < 1$, i.e. the correlation length becomes smaller than one lattice spacing[8] and its proper definition is then awkward anyway. The weak coupling limit of Eq. 6.18 is what we expect if $z = 1$ (see Eqs. 2.11 and 2.13) [38]:

[7] And not just "mean-field" like, or above the upper critical dimension.

[8] recall that $a \equiv 1$

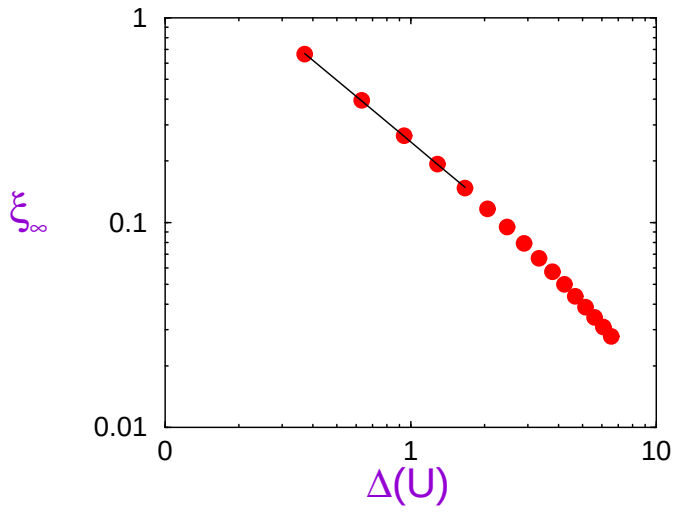

Figure 6.8: Circles: correlation length as a function of the gap $\Delta(U)$ on a log-log scale. Every point comes from a finite-size scaling, according to Eq. (5.18). The straight line is a power-law fit for $U = 2.5, 3, 3.5, 4, 4.5$.

$$\xi_{\mathrm{BA}} = \frac{2}{\Delta} . \tag{6.21}$$

This behavior is again confirmed for ξ_∞ in Fig. 6.8, the analog of Fig. 6.3: the DMRG data for ξ_∞ are plotted against the gap $\Delta(U)$ determined with the analytical formula (4.4). A power-law fit for $U < 5$ yields a numerical estimate of the exponent z

$$\frac{1}{z} = 1.002(9) \tag{6.22}$$

fully consistent with the exact value. One can and *should* try to fit ξ_∞ to an exponential divergence like Eqs. 6.13 or 6.12 with a logarithmic correction. Unfortunately the precision in ξ_∞ is not high enough and one obtains rather inaccurate — but still consistent — results, that we will not even quote here.

Let us switch on t' again: for $t' = 0.5$, the correlation length changes very little: ξ_∞ is not even shown in Fig. 6.6 since it would nearly overlap the $t' = 0$ data. However for $t' > \frac{1}{2}$ the behavior of ξ_∞ supports the same conclusions as with χ_∞: the bigger the t' the greater the U_c at which ξ_∞ diverges. Fits according to Eq. 6.13 may also be made and, as previously noticed for χ, they give results which are slightly better than at $t' = 0$, but which are still not entirely satisfactory. We now encourage the reader to slide to the next section for a deeper understanding of ξ_∞ and its relation to χ.

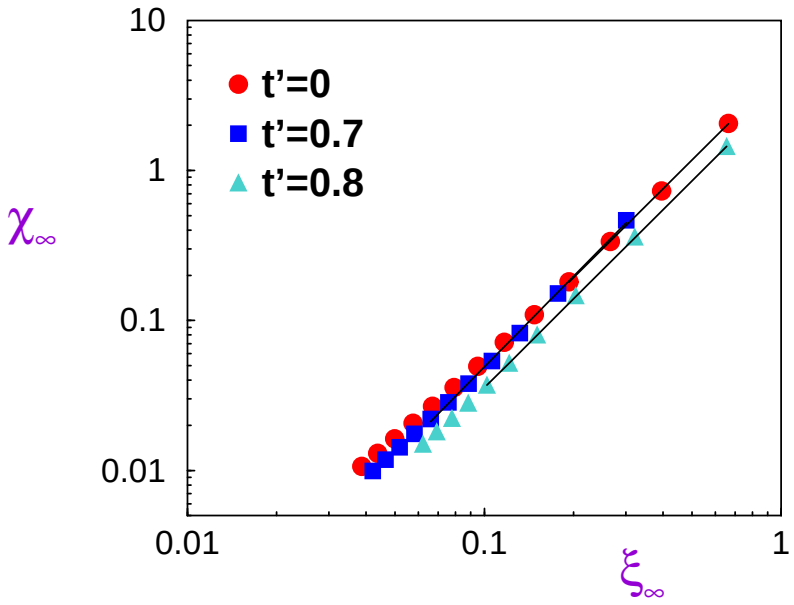

Figure 6.9: Electric susceptibility χ_∞, versus correlation length ξ_∞ for different values of t'. Lines are power–law fits.

6.3 Hyperscaling

A little puzzle has not been solved yet: what are the values of $\tilde{\gamma}$ and z for $t' > 0$? From Eqs. 2.15 and 2.13, we readily get

$$\chi_\infty \sim \xi_\infty^{\tilde{\gamma}} . \tag{6.23}$$

Since both quantities were determined for the same U values at $t' = 0, 0.7, 0.8$, checking Eq. 6.23 is straightforward to do and is shown in Fig. 6.9. Close to the transition, we find power–law behavior with the following exponents (the error comes only from the fitting procedure): $\tilde{\gamma}(t' = 0) \simeq 1.97(1)$, $\tilde{\gamma}(t' = 0.7) \simeq 2.01(2)$, $\tilde{\gamma}(t' = 0.8) \simeq 1.976(5)$. All of these results are consistent with

$$\tilde{\gamma} = 2 \tag{6.24}$$

for *any* t'; this value for $\tilde{\gamma}$ matches the one obtained by comparing χ_∞ with the gap at $t' = 0$ (see Eq. 6.3).

In order to confirm that ξ_∞ is indeed the correlation length characterizing the transition, we would like to prove that hyperscaling is satisfied with exactly this ξ_∞ as the correlation length. Let us first state the *hyperscaling hypothesis* [172]: the ground state energy may be split in two parts

$$E_o(u, E, L) = E_o^{\rm sing}(u, E, L) + E_o^{\rm reg}(u, L) , \tag{6.25}$$

where $u = U - U_c$ is the reduced interaction.[9] The *regular* part $E_o^{\rm reg}$ does *not* change when one crosses the transition and does not depend on the external electric field E. The *singular*

[9] You are maybe more familiar with the following definition of the reduced temperature $t = (T - T_c)/T_c$

part $E_o^{\rm sing}$ *does* change at criticality and behaves in a, well, singular way. The hyperscaling hypothesis further states that close to the transition, this latter part satisfies the homogeneity relation [172, 173]

$$\frac{E_o^{\rm sing}(u,E,L)}{L^d} \;=\; L^{-(d+z)}\; Y(C_1 u^\nu L, C_2 E L^{1+z}) \tag{6.26}$$

where Y is a *universal* function. (Although it depends on the geometry of the lattice and on the boundary conditions.) The microscopic system-dependent details manifest themselves only in the non-universal *metric* factors C_1 and C_2. The quantities u and E are called *scaling fields*; they *vanish* only at criticality. In a classical ferromagnetic-paramagnetic transition,[10] the reduced temperature t would replace u and the magnetic field B would replace E. The inverse length $1/L$ is also a scaling field because true critical behavior can only be realized in an infinite size system. Since time and space are "entangled" in a quantum phase transition, the effective dimension is increased and one must replace the L^d one would have on the right-hand side[11] of Eq. 6.26 for a classical phase transition by L^{d+z} [173, 6]. Here ν is still the exponent of the correlation length and is allowed to take on an infinite value. The exponent of L is $1+z$, since EL is an energy [10]. Let us now derive a corresponding homogeneity relation for the electric susceptibility from the hyperscaling hypothesis (6.26). Applying the definition of χ (3.11) we differentiate Eq. 6.26 twice with respect to E to obtain

$$\chi(L) \;=\; L^{2+z-d}\; C_2^2\; \tilde{\Phi}(C_1 u^\nu L)\;, \tag{6.27}$$

where $\tilde{\Phi}$ is another *universal* function. We take $\xi_\infty = u^{-\nu}/C_1$, absorbing the metric factor into the correlation length at the same time as the coupling constant itself [174]. Defining $C := C_2^2$, we can write down the scaling behavior of the electric susceptibility [174]

$$\chi(L) \;=\; L^{2+z-d}\; C\; \Phi(L/\xi_\infty)\;. \tag{6.28}$$

Here Φ is a *universal* function; the only remaining non-universality is contained in the metric factor C. The entire physics is now governed by the ratio L/ξ_∞. This is a direct implication of the hyperscaling hypothesis: a *unique* relevant length scale governs the physics in the vicinity of the phase transition, and this length scale *diverges* as one approaches the quantum critical point [174, 173]. This is indeed what we have observed before: for $L \gg \xi_\infty$, the system behaves as an insulator — it "feels" the finiteness of its correlation length — whereas for $L \ll \xi_\infty$, the correlation length exceeds the size of the system which therefore "thinks" it is in the critical, metallic state. The function $\Phi(x)$ tends to a (universal) constant as $x \to 0$ [173]; at $x = 0$, the system is at criticality and χ scales like L^2 (6.1). This means that

$$\eta \;=\; d - z \tag{6.29}$$

in the theory of classical phase transition. Recall however that in our case, U_c may be zero, which requires an alternative definition. Both definitions are in fact equivalent, since T_c is constant and can be absorbed into a metric factor (see below).

[10] in the familiar Ising model for instance

[11] Note that on the left-hand side, we have the energy density, i.e. the energy per volume, which is not affected.

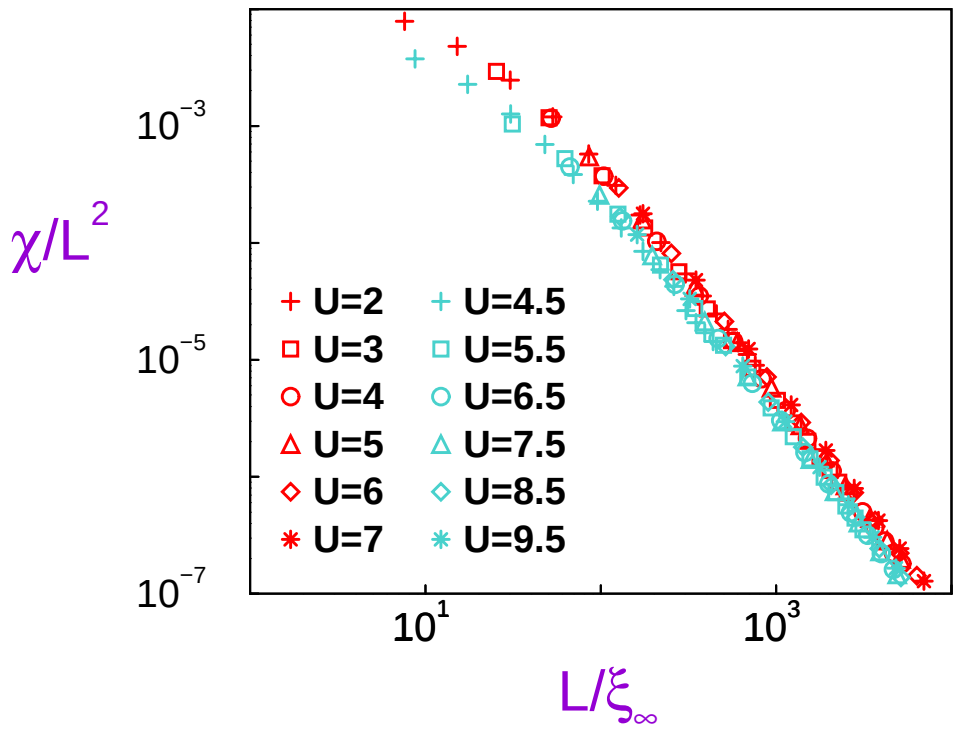

Figure 6.10: Scaling plots of $\chi(L,U,t')/L^2$ versus $L/\xi_\infty(U,t')$ in a log–log scale: $t'=0$ (red), $t'=0.8$ (turquoise).

and that $z=1$. This is the result we have been seeking. It confirms the $t'=0$ value. We can now write the scaling form of the electric susceptibility in one dimension as

$$\chi(L) \;=\; L^2\, C\, \Phi(L/\xi_\infty)\;. \tag{6.30}$$

In Fig. 6.10, $\chi(L)/L^2$ is plotted as a function of L/ξ_∞ for $t'=0$ and $t'=0.8$. For a given t', we observe a collapse of *all* the data for different L and U values onto one single curve, confirming *hyperscaling*: the transition is *below* its upper critical dimension.[12] Therefore, ξ_∞ behaves as the *correlation length*. For different values of t', the curves are proportional to each other. Eq. 6.30 is thus confirmed: we get a universal Φ and a non-universal constant C depending on t'. For instance for $t'=0$ the value $C\Phi(0)=\frac{1}{12\pi}$ (5.2) may be read off from Fig. 6.10. Results in the $x\to 0$ region are quite scarce, since we can calculate ξ_∞ only down to $U\simeq 2$. Exactly the same kind of scaling in the spin glass susceptibility has been observed in the classical 2D XY spin glass [176], while very similar scaling behaviors have been observed for the Anderson model [177, 178, 179, 180], various quantum [181, 182, 183] and classical [184, 185] models. In the opposite limit, $L/\xi_\infty\to\infty$, the system behaves as

[12] An example of an infinite-order transition where hyperscaling does *not* hold can be found in [175].

an insulator for all sizes and $\chi(L)$ tends to a finite value χ_∞. The scaling form (6.30) thus implies $\lim_{x\to\infty}\Phi(x) = A/x^2$ and

$$\chi_\infty \;=\; C\,A\,\xi_\infty^2 \tag{6.31}$$

where A is a universal constant. This is nothing but Eq. 6.23, confirming $\tilde{\gamma} \equiv 2$ and the results of Fig. 6.9.

6.4 The hyperscaling strikes back

The scaling behavior of the electric susceptibility (6.30) is plagued by the non-universal constant C in front of the universal scaling function Φ. How can we get rid of this thorn in the flesh? Combining χ with the non-linear susceptibility would make it disappear.[13] But we already have at our disposal a fundamental quantity which will have a *fully universal* scaling: the correlation length [172, 174, 173]

$$\xi(L) \;=\; L\,S(C_1 u^\nu L)\;. \tag{6.32}$$

Here we have set the electric field to zero, and S is a universal scaling function, just like Φ. It has no non-universal prefactor, though, because no derivation from a more fundamental scaling relation was necessary to get Eq. 6.32, unlike Eq. 6.30 in which the metric constant C comes from differentiating twice with respect to E. The hyperscaling hypothesis, $\xi_\infty^{-1} = C_1 u^\nu$, would now give

$$\xi(L) \;=\; L\,S(L/\xi_\infty)\;. \tag{6.33}$$

This relation is satisfied by the DMRG data, as shown in Fig. 6.11. Note that the $t' = 0$ curve and the $t' = 0.8$ curve overlap this time, in contrast to the electric susceptibility depicted in Fig. 6.10. The hyperscaling hypothesis is again confirmed: all data points for different U, L (and t' this time) collapse onto a single curve, which is nothing but the universal scaling function of Eq. 6.33. Exactly the same kind of correlation length scaling has been observed in many systems, including the Anderson model [186, 187, 188, 189], the quantum Hall liquid [190, 191], and other models [192, 193, 194]. In the $L/\xi_\infty \to \infty$ limit, the system behaves as an insulator for all sizes and $\xi(L)$ tends to ξ_∞, the value in the thermodynamic limit. We obtain the simple result $\lim_{x\to\infty} S(x) = 1/x$.

In the opposite limit, $L/\xi_\infty \to 0$, the system behaves as a metal,[14] although it is still an insulator for a large enough size: ξ scales linearly with L and S tends to a *universal constant* $S(0)$. At criticality, i.e. at $U = U_c$ exactly,

$$\xi(L) \;=\; S(0)\,L\;. \tag{6.34}$$

[13] giving a sort of *Binder cumulant*, see [174]

[14] Actually, a system of finite–size L will always have a charge gap. It can be neglected at a large (say $L \geq 10$ here), but still finite, size. At a smaller size though, this charge gap is substantial and the system is *insulating* even if $L/\xi_\infty \to 0$. This possibly accounts for the breakdown of the hyperscaling at $L < 10$. One could also state it that way: there are finite–size corrections to the hyperscaling at small enough sizes.

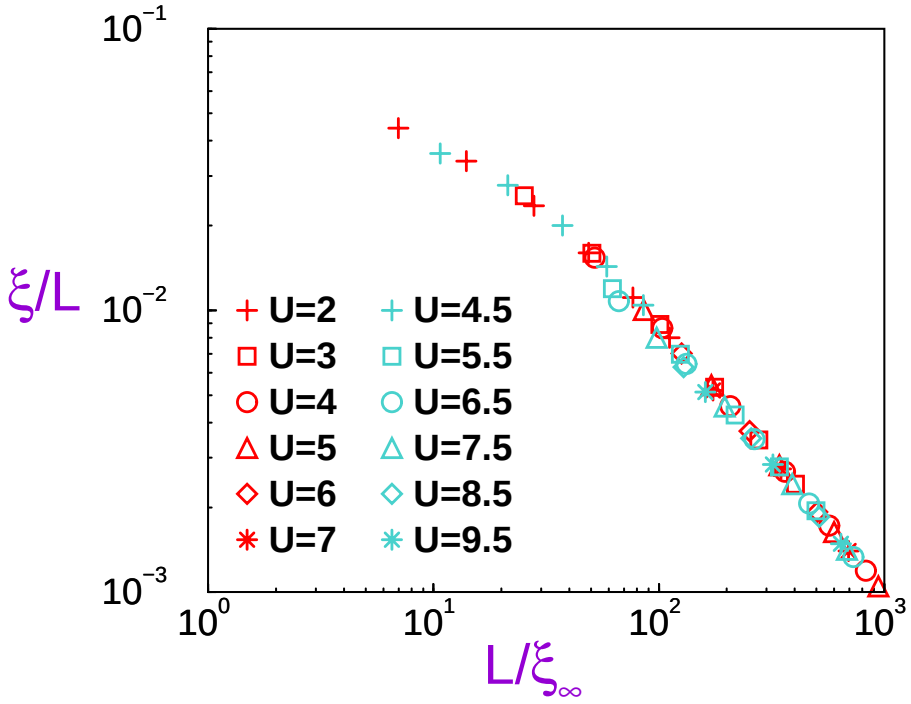

Figure 6.11: Scaling plot of $\xi(L,U,t')/L$ versus $L/\xi_\infty(U,t')$ in a log–log scale: $t'=0$ (red), $t'=0.8$ (turquoise).

Since $S(x)$ is a universal function, the proportionality constant between the finite-size correlation length and the size of the system at a critical point is a *universal amplitude*. Alternatively stated, the *ratio* $\xi(L)/L$ *is universal for a critical system*. This was predicted by Privman and Fisher in their milestone paper of 1984, albeit for *classical phase transitions* [174, 172]. We have already determined $S(0)$ for open boundary conditions (OBC) in a $t'=0$ calculation at $U_c=0$ (see Eq. A.34):

$$S(0) \;=\; \frac{4\zeta(3)}{\pi^4}\,. \tag{6.35}$$

However, this point cannot be seen explicitly in Fig. 6.11, since the scaling function $S(x)$ is shown only down to $x\simeq 8$, corresponding to $L=10$ and $U=2$. For smaller sizes, one will get finite-size corrections to the scaling while for $U<2$ it is impossible to extract ξ_∞ from finite-size scaling. Fortunately, however, the correlation length is exactly known for $t'=0$ (6.18). Using the relation (6.20) between ξ_{BA} and ξ_∞, we determine ξ_∞ for $U<2$ and exhibit the $x\to 0$ limit of $S(x)$ in Fig. 6.12. Only the insulating phase, which has a finite ξ_∞, and the critical point $U=U_c$ itself, which is the first point to have $\xi_\infty=\infty$, appear on Figs. 6.12 and 6.11. What happens to the remaining metallic phase[15] at $U<U_c$? Remember that it is *critical* and therefore $\xi(U,t',L)=\Theta(U,t')\,L$. According to Privman and Fisher [174], the function Θ should also be universal in the whole critical region. A naive guess would be

[15]Recall that a negative U makes sense and that it characterizes the metallic state at $t'<1/2$.

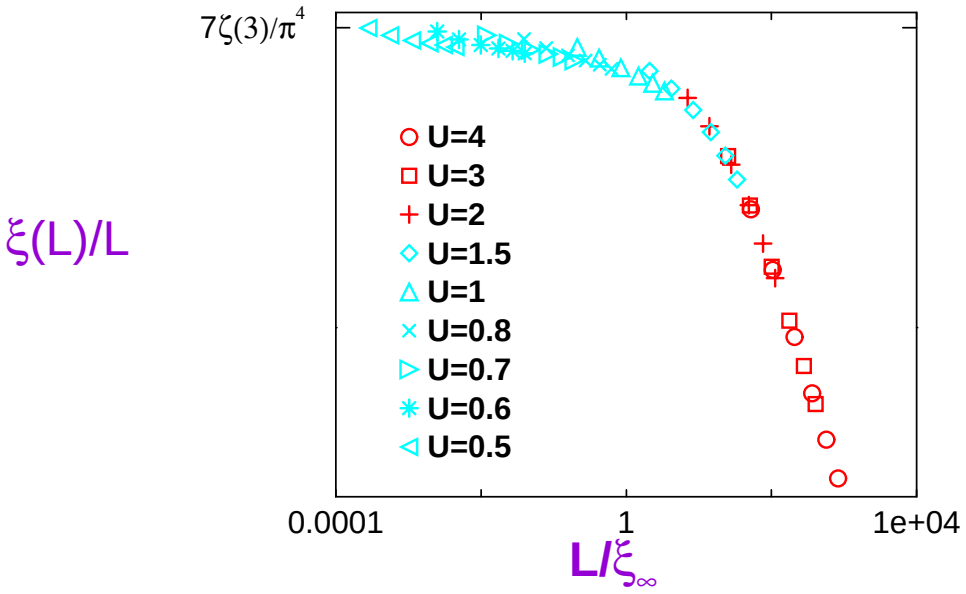

Figure 6.12: Scaling plot of $\xi(L, U, t' = 0)/L$ versus $L/\xi_\infty(U, t' = 0)$ on a log–log scale for $t' = 0$. For $U = 1.5$ and below, ξ_∞ is determined using Eqs. 6.18 and 6.20. Note that $\lim_{x\to 0} S(x) = 7\zeta(3)/\pi^4 = 0.0863821\ldots$ from Eq. 6.35 is confirmed.

that $\Theta \equiv S(0)$. This is not the case, however: for fixed t', the coefficient of proportionality $\Theta(U, t')$ is a decreasing function of U (see Fig 6.1 for χ: the situation is analogous for ξ) that reaches $S(0)$ only at U_c:

$$\Theta(U_c(t'), t') \;=\; S(0)\;. \tag{6.36}$$

The function $\Theta(U, t')$ can be obtained from a finite-size scaling procedure analogous to the one depicted in Fig. 5.4. In Fig. 6.13, we plot the results as a function of $U/U_c(t')$ for several values of $t' > 1/2$ for which $U_c(t') > 0$. The U_c are taken from (6.15) and are thus fully independent of calculation of ξ. At $U = 0$, the exact solution (see Eqs. A.35 and A.37) gives $\Theta(0, t' > 1/2) = 14\zeta(3)/\pi^4 = 2S(0)$, which is confirmed by the DMRG data. All the data points for different U and t' values then continue to overlap to give one single curve, which seems to be *universal*. At $U = U_c(t')$, we have $t'\ \Theta(U_c(t'), t') = S(0)$ for any t', as discussed previously. Note the slight systematic error: recall that DMRG *underestimates* critical coupling constants. For $U > U_c$, $\Theta \equiv 0$, because the system is insulating. The ratio $\xi(L)/L$ makes a *universal jump* at the metal-insulator transition.[16] The scaling function Θ does not vanish smoothly at the critical U_c; instead it goes *discontinuously* from the metallic to the insulating state. This is indeed what we expect since the Drude weight also makes a universal jump at the one-dimensional Mott transition [38, 195]. There are also reports of universal jumps in the conductance [196, 195] and in the resistivity [197, 196] for other transitions. Mott himself conjectured the existence of a *minimum metallic conductivity*, possibly

[16] It is the same at $t' < 1/2$, see Eqs. A.35 and A.34.

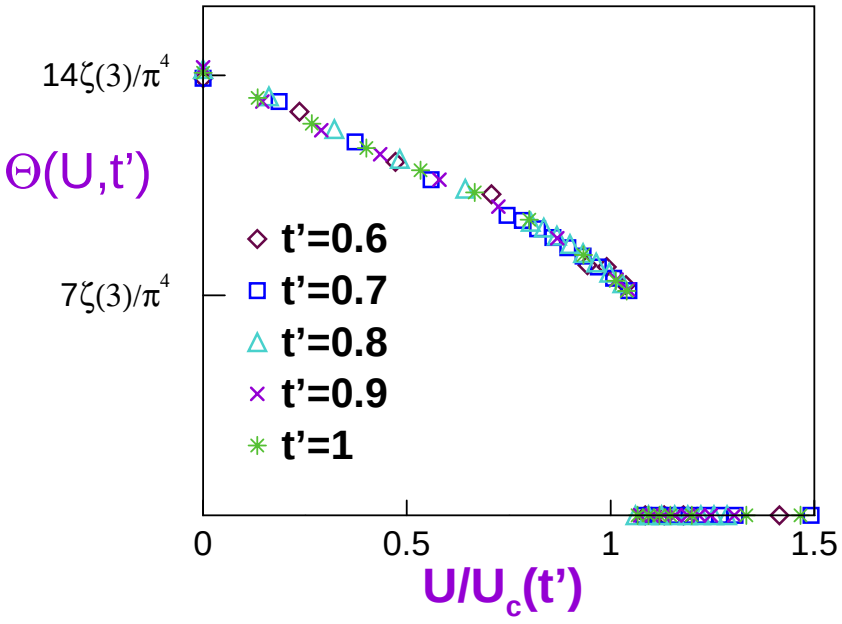

Figure 6.13: $\Theta(U,t') = \lim_{L\to\infty} \xi(U,t',L)/L$ as a function of $U/U_c(t')$. The critical interaction strengths are obtained from the non-linear fits to χ (summarized in (6.15)). At $U > U_c$, $\Theta = 0$, since the system is in the insulating phase.

universal, for metal-insulator transitions in general [8]. Such a minimum conductivity was successfully probed in some systems [198], but was questioned in others [8].

What about Privman and Fisher's argument of the constancy of $\xi(L)/L$ at criticality [174]? It still holds, albeit with a slight modification. Each point (U,t') in the metallic part of the phase diagram is critical in its own right. For each of those points separately, the ratio $\xi(U,t',L)/L$ may be considered universal, although its value changes as a function of U and t'. Only when one looks at Θ as a function of a particular combination of U and t', namely $U/U_c(t')$, does one recover a universal curve: the value of Θ depends on the coupling constants of the model, but in a universal way. Such a breaking or softening of the universality usually reveals the presence of a *persistent marginal* scaling field in the vicinity of an infinite-order transition, such as the temperature in the XY model [105, 106, 137]. This should not be a big surprise, since this kind of field is *necessary* to form a line (XY model) or a surface ($U-t-t'$ model) of critical points [137].

Since the ratio $\xi(U,t',L)/L$ has a universal jump at $U_c(t')$, one may use this fact as a — possibly accurate — criterion to determine the phase boundary between the metallic and the insulating states; an analogous procedure has been used in [199, 200].

Chapter 7

Phase Diagram

It might seem that we have already finished: the universality class does not change with t'. This is shown definitely by the universal scaling of the correlation length. So why bother? We should just set $t' = 0$ and turn back to our good old friend, the sacrosanct Hubbard model? We would rather kindly ask you to let us look beyond the polished façade that we just introduced to you. The nature of the insulating phase has not been clarified, and it may actually change[1] with t'. Herein lies the cornerstone necessary to build a complete phase diagram, possibly the *general* phase diagram of the Mott transition in one dimension. The occurrence of a *universal jump* at the transition is a further hint.

7.1 Dimerization

Up to now, we have ignored all the possible changes in the insulating phase that could be generated by increasing t'. We have concentrated on the electric susceptibility, which is finite and behaves similarly whatever t' is. This is not the entire story, however. At small t', and for $U > U_c$, the system has antiferromagnetic correlations[2] [47]. For t' larger than about $1/2$, and for $U > U_c$, *dimerization* should occur, as Fabrizio predicts [142]. This is a new *phase transition* that is associated with the opening of a spin gap[3] [201, 202] and the breaking of a *discrete* symmetry: "weak" and "strong" bonds alternate with each other. The order parameter is thus the difference in the strength of two adjacent bonds and we call this phase *bond-ordered*. Its local definition is

$$\hat{b}_i \;:=\; \sum_{\sigma} (c^{\dagger}_{\mathrm{i}\sigma} c_{\mathrm{i}+1\sigma} - c^{\dagger}_{\mathrm{i}+1\sigma} c_{\mathrm{i}+2\sigma} \;+\; \mathrm{h.c.}) \tag{7.1}$$

where we write $b_i = \langle \hat{b}_i \rangle$ for the ground state expectation value. With periodic boundary conditions, there are two degenerate ground states, shifted by one site relative to one another. Open boundary conditions, on the other hand, break the translational symmetry so that only

[1] This is already understood and presented in Refs. [142, 145].

[2] There is no no true antiferromagnetic order: we are in *one* dimension and no continuous symmetry may be broken.

[3] present as well in the metallic phase

one of the two ground states cited above survives: the one with an odd number of strong links for an even number of sites.[4] Because of this the order parameter for a finite system of size L can be calculated directly with the DMRG as

$$b(L) \;:=\; \frac{2}{L-2} \sum_{i=1}^{L-3} b_i \;. \tag{7.2}$$

The measurements are easy, just as for the local densities n_i. We follow the same procedure as for χ to tune the DMRG parameters: we determine $b(L)$ at $U = 0$ and compare the DMRG results to the exact solution.[5] The results for $U > 0$ can be then regarded with confidence. We find the following behavior: for $t' < 1/2$, $b(L)$ always scales to zero with L. For $t' > 1/2$, $b(L)$ scales to zero with L in the metallic phase: a bond order is obviously incompatible with a perfect metal. Then, exactly at $U_c(t')$, $b(L)$ starts to scale smoothly to a finite value. Finite-size scaling may be performed to extract the thermodynamic limit $b_\infty = \lim_{L\to\infty} b(L)$ in the same way as for χ (5.15) and ξ (5.18). An analytic strong-coupling calculation is also presented in Appendix B.3. This calculation states that at large enough U,

$$b_\infty(t') \;=\; \frac{4}{U}\, d_\infty(t') \tag{7.3}$$

where $d \;:=\; \frac{2}{L-2} \sum_{i=1}^{L-3} d_i$, with

$$d_i \;\equiv\; \langle \mathbf{S}_\mathrm{i} \cdot \mathbf{S}_{\mathrm{i}+1} \rangle \;-\; \langle \mathbf{S}_{\mathrm{i}+1} \cdot \mathbf{S}_{\mathrm{i}+2} \rangle \tag{7.4}$$

which is nothing but the corresponding order parameter for the spin dimerization present in the $J - J'$ model at $J' > J'_c = 0.241167(5)J$ [151, 128]. The order parameter is known only at the Majumdar-Ghosh point $d = 3/4$ where it has the value (B.42)

$$b_\infty(t' = \frac{1}{\sqrt{2}}) \;=\; \frac{3}{U} \;. \tag{7.5}$$

This is compared to the DMRG data at large U in Fig. 7.1. Although d is not known exactly for other values of t', it can nonetheless be extracted from the DMRG data at large U by a power-law fit according to Eq. 7.3. The result is depicted in Fig. 7.2 for several t' values. This matches exactly the order parameter obtained by White and Affleck [128] who performed a careful DMRG calculation on the $J - J'$ model itself to determine $d(J'/J = t'^2)$.

We have determined the bond order parameter in the intermediate-coupling regime for several values of t' and U. In the metallic phase, $b(L)$ scales to zero,[6] while it reaches a finite value in the insulating phase for $t' \tilde{>} 1/2$. Finite–size scaling can be done as shown in Fig. 7.3 for $t' = 0.7$, where we plot $1/b(L)$, which goes to infinity at the transition, rather than $b(L)$, in order to enable an easy comparison with the corresponding figures for χ (Fig. 6.1) and for ξ (Fig. 6.5). In the insulating phase, we have determined b_∞ by the standard finite-size

[4] We treat only systems of even size.

[5] found with Mathematica

[6] We pretty much have $b(L) \sim \mathrm{L}^{-\tau}$ with an exponent $\tau \simeq 1$, but finite-size corrections are here so important that it is impossible to get a reliable value for τ. This has to be contrasted to the analytic form found in the insulating phase.

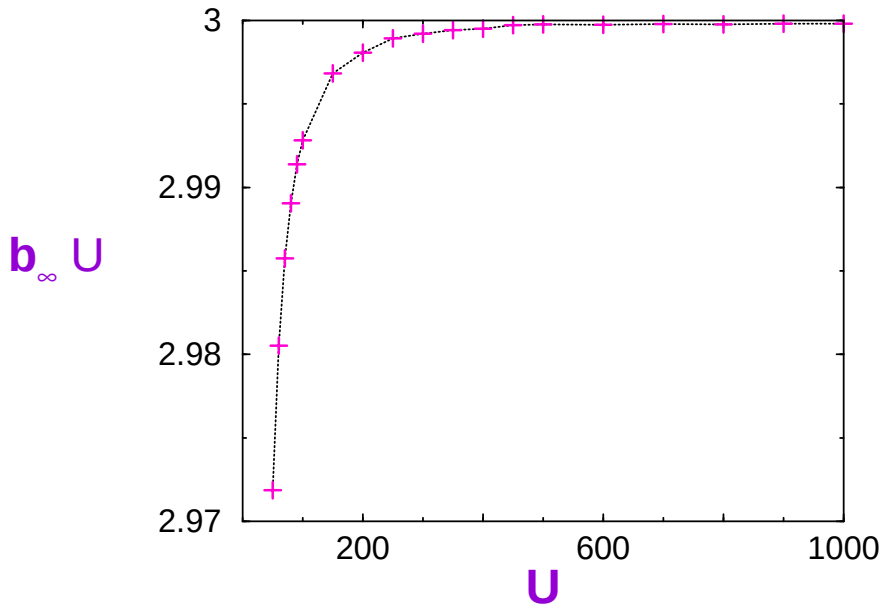

Figure 7.1: Plus signs: bond order parameter b_∞ multiplied by U as a function of U. The dotted line is a guide to the eye. Note that $b_\infty U = 3$ is the large-U limit.

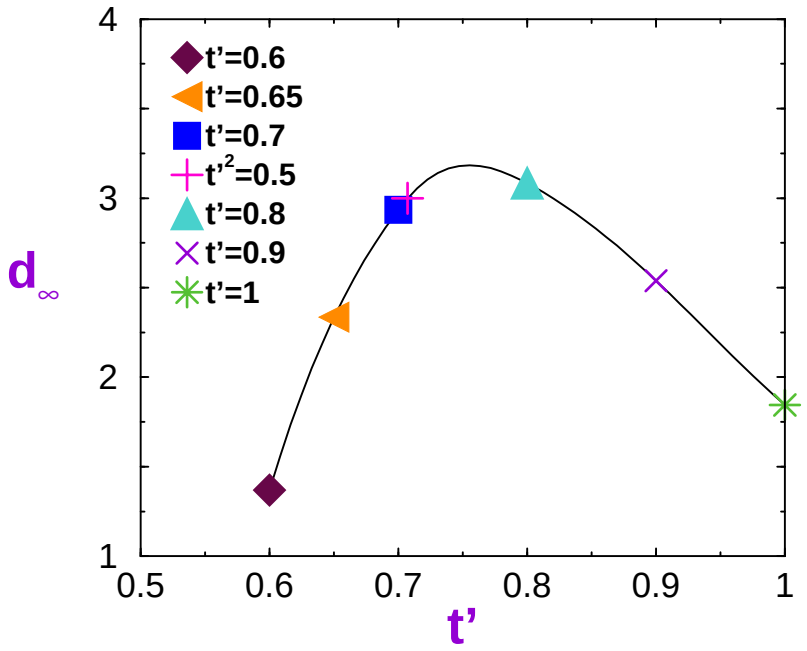

Figure 7.2: Symbols: spin dimerization order parameter d_∞ as a function of t'. The order parameter d_∞ is determined by a power-law fit to the DMRG data for $b_\infty = 4d_\infty/U$. The solid line is a spline through the data points.

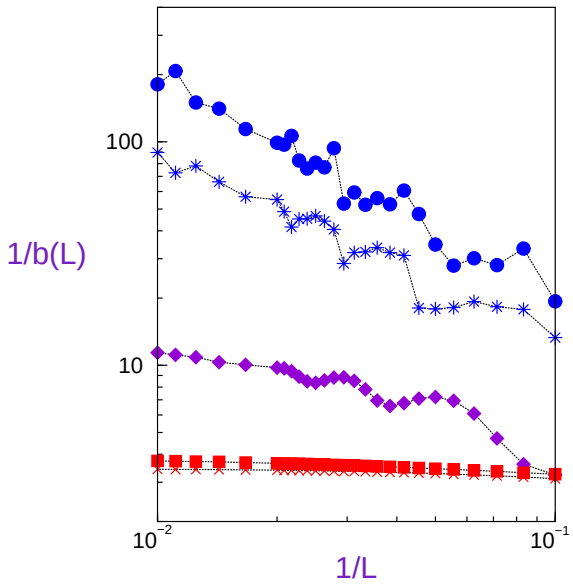

Figure 7.3: Inverse of the bond order parameter, b, as a function of $1/L$ for $t' = 0.7$ and for $U = 1$ (circles), $U = 2$ (stars), $U = 3.5$ (diamonds), $U = 4.5$ (crosses), and $U = 6$ (squares). Dotted lines are guides to the eye. Blue stands for a metallic behavior $\lim_{L\to\infty} b(L) = 0$, red for an insulating one $b(L) = b_\infty + \mathcal{O}(\frac{1}{L})$, and violet for an insulator close to the critical point, where one should consider larger sizes in order to obtain b_∞.

scaling procedure, $b(L)$ being analytic in $1/L$. The extrapolated values of b_∞ are plotted in Fig. 7.4 as a function of U. Note that for $0.5 < t' \leq 0.65$ there is a region in which the bond order parameter b_∞ drops to zero as a function of U (at fixed t'), but then becomes nonzero again, going like $4d_\infty/U$ at large U. This implies that the phase boundary between the two insulating states as a function of U is not a straight line! One should notice that the critical $(J'/J)_c \simeq 0.241\ldots < 0.25 = t'^2$ for the $J - J'$ model [151]. This means that for $t' = 0.5$, one should obtain a finite b_∞ for very large but finite U. Even for $t' = 0.55$, the bond-ordered phase reappears only at extremely large U. This critical region is thus out of reach, because the DMRG[7] becomes unstable and gives erratic results.

7.2 Universality Class

Now that we have determined the bond order parameter, we can draw the *phase diagram* of the $U - t - t'$ model. This is done in Fig. 7.5, where we collected the critical values from Eq. (6.15) and from Fig. 7.4. There are two distinct insulating phases, which we call "Mott Insulator I" ($t' \lesssim \frac{1}{2}$) and "Mott Insulator II" (large U $t' \gtrsim \frac{1}{2}$). The Mott Insulator I phase possesses antiferromagnetic correlations and quasi-long range order, with a power-law decay

[7] as would any numerical method

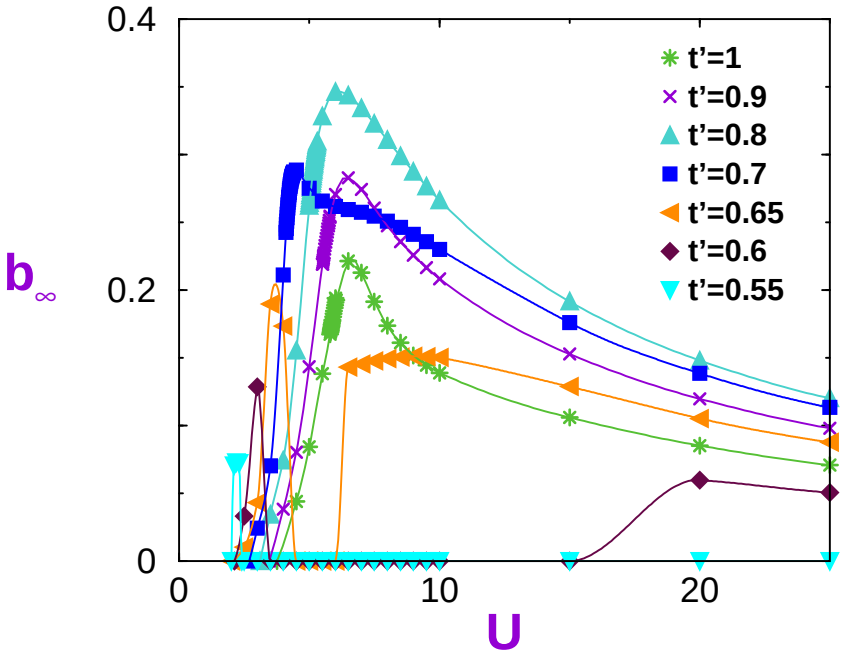

Figure 7.4: Symbols: bond order parameter b_∞ as a function of U for several values of t'. The solid lines are spline through the data.

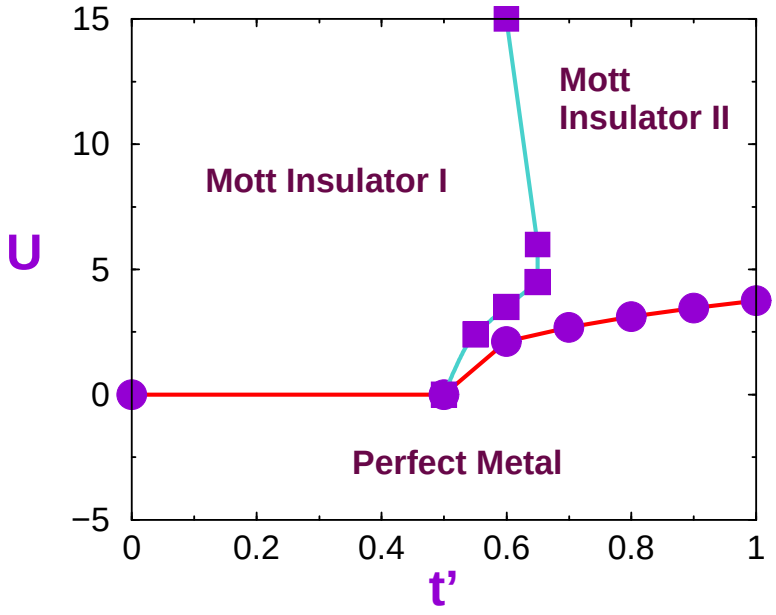

Figure 7.5: Phase diagram of the $U - t - t'$ model at half-filling; recall that the sign of t' is irrelevant. Circles: critical U_c taken from (6.15). Squares: critical points where the bond-order parameter drops to zero; taken from Fig. 7.4.

of the correlation functions[8] which means that there is a charge gap, but no spin gap.

The bond order parameter b_∞ certainly vanishes along the line dividing the two insulating phase and remains finite in the Mott II phase. This bond-ordering for the charge degrees of freedom turns into bond-ordering for the spin exchange at large U, where the $U-t-t'$ model gets metamorphosed into the $J-J'$ model. In this phase, a *spin gap* Δ_σ is present [142]: it should open simultaneously with b_∞ when one varies t' at any fixed $U>0$. We have not calculated Δ_σ, but we nevertheless risk the conjecture that

$$b_\infty \sim \sqrt{\Delta_\sigma} \tag{7.6}$$

based on the $J-J'$ model results [128]. Both Mott phases are also present in the two-dimensional Mott insulating state [203, 204, 205, 206]. We still have a spin gap in the metallic phase at positive U [142]. On the $U=0$ line, Δ_σ is zero, because the system is completely gapless, while for negative U, it comes back to life.

This phase diagram is very close to that of models in the *sine-Gordon* (sG) universality class, which is shown in Fig. 7.6. The sine-Gordon model is a continuous model that emerges from the scaling limit of underlying lattice Hamiltonians; its action[9] reads [6]

$$\mathcal{S}_{\rm sG} = \int dx d\tau \left[\frac{1}{2\pi K v_F}((\partial_\tau\phi)^2 + v_F^2(\nabla\phi)^2) - v\cos(4\phi)\right] , \tag{7.7}$$

where K and v are coupling constants and v_F is a velocity that sets the relative scales of time and space. This model is $(1+1)$ dimensional, which matches our case, since $d=z=1$, and ϕ is a *bosonic* field. A possible, but not unique, Hamiltonian that leads to (7.7) is the J_1-J_2 model which we mentioned before as the $J-J'$ model, but here we add an anisotropy parameter λ:

$$\mathcal{H} = J_1\sum_{\langle ij\rangle}(S_i^xS_j^x + S_i^yS_j^y + \lambda S_i^zS_j^z) + J_2\sum_{\langle\langle ij\rangle\rangle}\mathbf{S}_i\cdot\mathbf{S}_j . \tag{7.8}$$

We emphasize that this $J_1-J_2-\lambda$ spin model is taken here only as a realization of the sine-Gordon model, shown in Fig. 7.6 and has nothing to do with the strong-coupling limit of the $U-t-t'$ model[10].

Let us now forget about the spin degrees of freedom in the $U-t-t'$ model, which is likely to be legitimate due to the *spin-charge* separation reigning in one dimension [207, 208], and let us consider its phase diagram only for the charge degrees of freedom. We will now try to compare the latter phase diagram to the one of the sine-Gordon model, or, more precisely, to the one of the $J_1-J_2-\lambda$ model. Since both the charge sector of the $U-t-t'$ model and the sine-Gordon model have a general $U(1)$ symmetry, such a comparison is possible. The perfect metallic phase in Fig. 7.5 is nothing but a *Luttinger liquid* [209, 113, 210], which matches the *massless* phase of Fig. 7.6. The Mott II phase has bond order, the equivalent of

[8] At $t'=0$, and possibly in the whole Mott I phase, there may exist a breaking of a *discrete* symmetry, and one could define a corresponding non-local order parameter, see Ref. [140]. We expect this order parameter to vanish on the transition line between the two insulators, but this is *science-fiction*.

[9] There is a whole jungle of conventions, notations and flavours for the sine-Gordon model; we use here and in the following the formalism of [6].

[10] The different notation is meant to reinforce this.

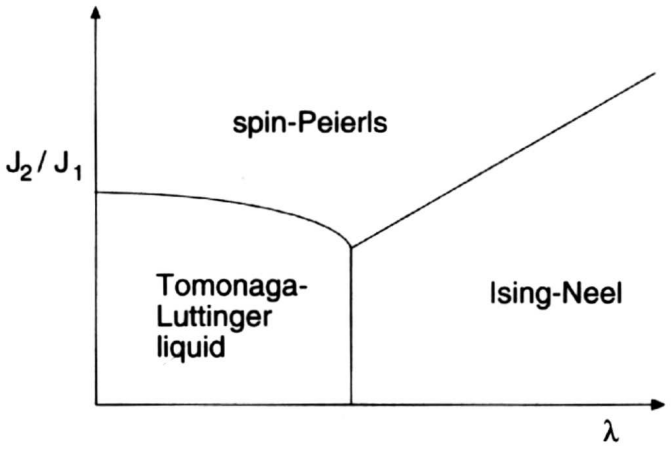

Figure 7.6: Phase diagram of the $J_1 - J_2$ model with anisotropy λ (Eq. 7.8) lying in the sine-Gordon universality class. The multi-critical point, where all three phases meet, has $v = 0$ and $K = 1/2$ [6].

spin dimerized order for the charge degrees of freedom: this is nothing but the spin-Peierls phase in Fig. 7.6. Last but not least, the Mott I phase has antiferromagnetic correlations albeit no breaking of symmetry (Ising-Néel) as in Fig. 7.6.

The intricate relation between the Mott transition and the sine-Gordon model is even deeper than is indicated by this superficial resemblance: at $t' = 0$ the simple Hubbard model, which may be mirrored to $J_2 = 0$ in Fig. 7.6, has as its scaling limit as $U \to U_c = 0$ [211, 212, 213, 214, 215, 195] the sine-Gordon model. In this limiting case, the $U(1)$ symmetry turns into a $SU(2)$ symmetry.[11] The "free" part of the action (7.7) is the *Gaussian model*[12] which corresponds to the gapless charge degrees of freedom of the negative–U metallic phase [216], while the cosine term arises from the Umklapp processes [111]. The mapping to the sG model reveals that at $U_c = 0$ there is an infinite-order transition of the *Kosterlitz-Thouless* universality class [6]. We have just demonstrated that this does not change when one triggers t', regardless of the symmetry of the insulating phase. The same happens for the sG model [6]: the transition from the Luttinger liquid to both massive phases in Fig. 7.6 bears the same infinite-order divergence.

This may well resolve the issue of the *order parameter* on the metallic side of the one-dimensional Mott transition: there may be an order parameter, but it will be zero in the whole critical phase anyway! There is no transition to a phase with long-ranged order but rather to a whole phase of critical points with only quasi long-range order, just like in the Kosterlitz-Thouless universality class. In the latter case, the *magnetization* is the order parameter, which reaches a non-zero value only at $T = 0$. The *Drude weight* D, often cited as

[11] The latter symmetry is lost when one triggers t' (for the charges), respectively J_2.
[12] conformallly invariant

a candidate of choice for an order parameter even though it lacks a *local* definition is related rather to the *helicity modulus* Y [217]. Y also makes a finite *universal jump* at the Kosterlitz-Thouless transition [218, 219, 220, 221]: in that sense, one also goes discontinuously from the massless to the massive phase. The same occurs in the $U-t-t'$ model, as we have seen in the first section of this chapter, with a *universal jump* in $\lim_{L\to\infty}\xi(L)/L$ at the Mott transition. Finally, let us mention that there is a further analogy: the vortices present in the XY model may also have been identified in the sine-Gordon [222] and in diverse strongly correlated electron [223] models.

Chapter 8

Certain Avatars

Last summer, Amir Caldeira[1] came into the office I was sharing with Alvaro Ferraz[2], and asked us frankly: "Do you believe in electrons? Because *I* do not". Neither do I, if I might add. This question definitely opened my mind. I do not believe in a particular model either, or in an intricate combination of facts that gives me back exactly what I put in first. Of course, theoretical physics is about phenomenology, about tuning parameters and finding the correct Hamiltonian to describe a given system; it is about peculiar details behind which a realm of new perspectives might open. However, theoretical physics is also about finding the *essence*, which one may call *universality*. Electrons and spins are here and there; you do not have to "believe" in them, as if they were sacrosanct, even though the traces of their presence may be measured, therefore bringing them to "reality". They instead need to be transcended in order to let the phenomenon express itself through them: the metal-insulator transition in all its varieties, for instance.

Isolated strongly correlated electrons is a *theoretical dream* that one should *never* believe in. Disorder, complicated lattice structures and so on always perturb the nice landscape we now have in mind after the past few chapters. That is why we would like to try to go beyond the Mott transition and possibly to unravel universal features that hold for other metal-insulator transitions. We will not be exhaustive however, since this would bring us too far afield. The first *avatar* is the good old *band insulator* while the second is the so-called *ionic Hubbard model*, a coalescence of the Hubbard model and the band insulator.

8.1 Band Insulator

We have some good news: let us forget about correlations for the time being and consider the $\delta - t - t'$ model:

$$\mathcal{H}_{\rm BI} \;=\; -\sum_{i\sigma}\Big[t\; c^{\dagger}_{i\sigma}c_{i+1\sigma} + t'\; c^{\dagger}_{i\sigma}c_{i+2\sigma} \;+ \text{h.c.}\Big] + \delta\sum_{j\sigma}(1+(-1)^{j})n_{j\sigma}\;. \tag{8.1}$$

[1] visiting professor from the University of Campinhas
[2] visiting professor from the University of Brazilia

As usual we set $t = 1$ and restrict ourselves to $\delta \geq 0$ without loss of generality. We again study the half-filled case exclusively: the sign of t' is then irrelevant[3] as before and we consider $t' \geq 0$ only. At $\delta = 0$, the system is obviously metallic, and, of course, the same state as the non-interacting limit $U = 0$ of the $U - t - t'$ model.

The $\delta - t - t'$ model contains only one-body operators and is therefore easily diagonalized; this is done in the Appendix C.1. For $\delta > 0$, there are two separate bands whose dispersion relation is

$$\begin{aligned} \varepsilon_{\pm}(k) &= \delta - 2t' \cos\ k \pm \sqrt{\delta^2 + 2(1 + \cos\ k)} \\ k &= \frac{4n\pi}{L},\ n = -\frac{L}{4}, \ldots, \frac{L}{4} - 1\ . \end{aligned} \tag{8.2}$$

We consider only sizes L divisible by 4. For $\delta > 0$ and $0 \leq t' \leq 1/2$, the two bands are separated by a direct gap $\Delta = 2\delta$ and (8.1) describes an *insulator* at half-filling. There is a *metal-insulator transition* at $\delta_c = 0$. This is a *quantum critical point* since the ground state energy density

$$\frac{E_0(\delta)}{L} = \sum_k \varepsilon_-(k) = -\frac{2}{\pi}\sqrt{\delta^2 + 4}\ E(\frac{2}{\sqrt{\delta^2 + 4}}) \tag{8.3}$$

is non-analytic at $\delta_c = 0$ [6]. The complete elliptic integral of the second kind $E(x)$ is discontinuous at $x = 1$. For $t' > 1/2$, the two bands overlap and the system is metallic. This reminds us strongly of the $U - t - t'$ model. The metallic phase is not critical, however, since it possesses a finite relevant energy scale, the width of the overlap between the bands. At a $\delta_c(t') > 0$, the two bands just touch each other and for $\delta > \delta_c(t')$ an indirect gap Δ opens between the two:

$$\Delta(t', \delta) = \varepsilon_+(0) - \varepsilon_-(\pm\pi) = \delta + \sqrt{\delta^2 + 4} - 4t'\ , \tag{8.4}$$

turning the system into an insulator. The phase boundary between the metal and the insulator is given by

$$\delta_c(t') = \begin{cases} 0\ , & 0 \leq t' \leq \frac{1}{2} \\ \frac{4t'^2 - 1}{2t'}\ , & t' > \frac{1}{2} \end{cases}\ . \tag{8.5}$$

The phase diagram, depicted in Fig. 8.1, has interesting similarities with the one of the half-filled $U - t - t'$ chain (Fig. 7.5). The universality class does not change with t', so we just concentrate on the $t' = 0$ case where analytic calculations are less tedious. Since the gap closes like $\Delta \sim |\delta - \delta_c|$, we have $z\nu = 1$ according to Eq. 2.11: this is a *second order phase transition*. The electric susceptibility (calculated in Appendix C.2) is finite for $\delta > 0$:

$$\chi_\infty(\delta) = \frac{1}{12\pi}\frac{1}{\sqrt{\delta^2 + 4}}\left(\frac{\delta^2 + 8}{\delta^2}E(\frac{2}{\sqrt{\delta^2 + 4}}) - K(\frac{2}{\sqrt{\delta^2 + 4}})\right)\ . \tag{8.6}$$

As $\delta \to 0$, (8.6) reduces to the form ($\Delta = 2\delta$):

$$\chi_\infty(\Delta \to 0) = \frac{4}{3\pi}\frac{1}{\Delta^2}\ , \tag{8.7}$$

[3]The argument is the same for the $U - t - t'$ model, see (4.5).

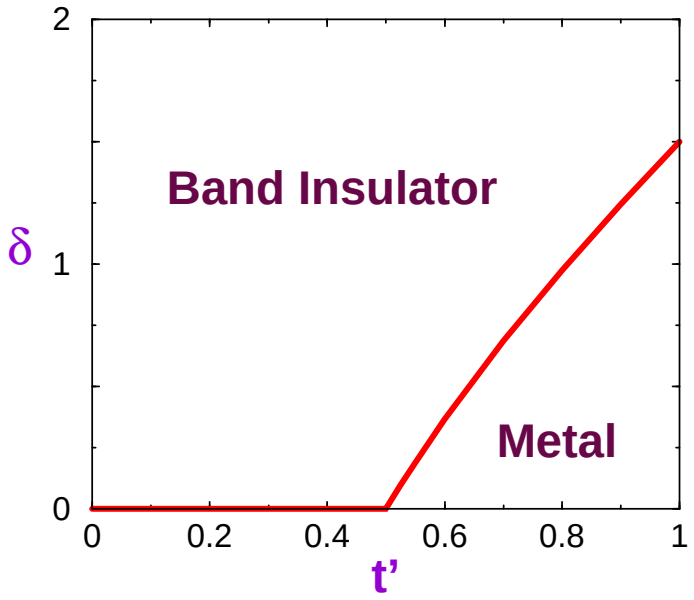

Figure 8.1: Phase diagram of the $\delta - t - t'$ model at half-filling; recall that the sign of t' is irrelevant. Only the line delimiting the phase boundary is critical here — the metallic phase has a relevant energy scale, namely the width of the band overlap.

which gives $\gamma = 2$. Eq. 8.7 is analogous to what we obtained for the simple Hubbard model, see Eq. 6.4! The same weak-coupling behavior $\chi \sim 1/\Delta^2$ is thus found in two totally different models: the Hubbard model, where the metal-insulator transition is driven by repulsive local correlations of strength U, opening a gap $\Delta(U)$, and a "simple" band insulator with independent electrons, where the gap itself $\Delta = 2\delta$ is the coupling constant. Thus we are led to conjecture that

$$\chi_\infty(\Delta \to 0) \sim \frac{1}{\Delta^2} \tag{8.8}$$

is a general relation for a *gapped insulator*. This yields with Eqs. 2.11 and 2.15 the general relation between exponents for a metal-to-gapped-insulator transition

$$\frac{\gamma}{z\nu} = 2 \tag{8.9}$$

which would give $\tilde{\gamma} = 2$ for the $U - t - t'$ model,[4] see Eq. 6.23. This analogy goes even further: in the strong-coupling limit, we have

$$\chi_\infty(\Delta \to \infty) \sim \frac{2}{\Delta^3} \,. \tag{8.10}$$

Again we recover the same result as in the Hubbard model (B.7), where the gap is proportional to U for $U \to \infty$ [47] and therefore $\chi_\infty(U \to \infty) \sim \frac{1}{\Delta^3}$.

[4] Recall that z=1.

The correlation length may be determined as well: the calculations are presented in Appendix C.3. As one would expect, ξ_∞ is finite for $\delta > 0$:

$$\xi_\infty(\delta) \;=\; \frac{1}{4\delta\sqrt{\delta^2+4}}\,. \tag{8.11}$$

In the weak-coupling regime, we get

$$\xi_\infty(\Delta \to 0) \;=\; \frac{1}{2}\,\frac{1}{\Delta} \tag{8.12}$$

which yields $\nu = 1$ with Eq. 2.13 and $z = 1$ together with the relation $z\nu = 1$ derived above. The behavior $\xi \sim 1/\Delta$ in the critical region again matches the Hubbard model result [38] (see Fig. 6.8 as well). This should not be surprising though, since $z = 1$ for both models: time and space are on equal footing, which means that ξ_∞ must diverge as the inverse of the relevant energy scale. Interestingly, in the strong-coupling limit

$$\xi_\infty(\Delta \to \infty) \;=\; \frac{1}{\Delta^2} \tag{8.13}$$

which corresponds to the large–U limit of the Hubbard model, see Eq. B.31.

There has always been some haunting incertitude about the real meaning of the correlation length ξ. Such an issue can be addressed in the framework of this analytically solvable model by determining the Drude weight D in the insulator ($\delta > 0$, $t' = 0$). In the thermodynamic limit, D is of course zero; but we are interested instead in the way it scales to zero when $L \to \infty$. For the simple Hubbard model, a Bethe Ansatz calculation gives

$$D(U, L) \;\sim\; \sqrt{L}e^{-L/\xi_{\rm BA}} \tag{8.14}$$

at a large but finite size L [38], where $\xi_{\rm BA}$ is nothing but the correlation length mentioned earlier in Eq. 6.18. A comparable calculation can be carried out for the band insulator, see the Appendix C.4 and Eq. C.31. For large enough system sizes we obtain pretty much the same L–dependence as in Eq. 8.14,

$$D(\delta, L) \;=\; \frac{1}{\sqrt{2\pi}}\sqrt{\frac{L}{\xi}}\,e^{-L\,\mathrm{arsinh}\left(\frac{1}{8\xi}\right)/2}\quad. \tag{8.15}$$

The correlation length that one would define starting from Eq. 8.15

$$\xi_{\rm Drude}(\delta) \;:=\; \frac{2}{\mathrm{arsinh}\frac{\delta\sqrt{\delta^2+4}}{2}} \tag{8.16}$$

does not match ξ. Recall that $\xi_{\rm BA}$ does not match our definition of $\xi_\infty(U)$ in general either, but only in the vicinity of the critical region. The situation is exactly the same here, since

$$\xi_{\rm Drude}(\delta \to 0) \;=\; 4\xi(\delta)\,. \tag{8.17}$$

Sufficiently close to the critical point, the correlation length $\xi_{\rm Drude}$ defined from the large–L decay of the Drude weight coincides[5] with the length scale ξ determined by the fluctuations of polarization. At strong coupling, they behave in radically different ways. Whereas $\xi(\delta \to \infty) \sim \delta^{-2}$, $\xi_{\rm Drude} \sim 1/\ln \delta$, very much like the large-U limit of $\xi_{\rm BA}$, which is $1/\ln U$ [38].

Let us return to the weak-coupling regime, where hyperscaling *is* satisfied, since Eq. 8.15 maybe recast as

$$D(L,\xi) \;=\; Y(L/\xi)\;, \tag{8.18}$$

where we choose as the correlation length(C.15) rescaled by $\xi \to \xi/4$. The scaling function Y is then

$$Y(x) \;=\; \sqrt{\frac{2x}{\pi}}\, e^{-x}\, \left(1+\frac{3}{2x}\right)\;. \tag{8.19}$$

At large x, which means $L \gg \xi$, we recover the result for the Hubbard model [38],

$$Y(x) \;=\; \sqrt{\frac{2x}{\pi}}\, e^{-x}\;. \tag{8.20}$$

Does the band insulator to metal transition belong to the same universality class as the Mott transition? This anxious query was *too quickly* answered "yes" many times, because of the similarities between the two transitions [224]. However, even a superficial investigation makes this issue clear cut: the Mott transition is *infinite order* whereas the band-insulator-to-metal transition is *second order*: thus they *cannot* belong to the same universality class, period. Resolving this dilemma in terms of the scaling function Y is in fact easy: one simply must examine the higher order terms $1+\frac{3}{2x}+\mathcal{O}(\frac{1}{x^2})$ which do *not* correspond to the ones of the Mott insulator [224].

In order to observe this mismatch explicitely, we compare the complete scaling functions $\Psi(x)$ of some critical quantity for both models: we choose the correlation length, since the corresponding scaling function $S(x)$ is fully universal [174]. Furthermore, $S_{\rm Mott}(x)$ has already been determined for the whole range of $x = L/\xi_\infty$ for the Hubbard model (Fig. 6.12). In order to compare it to $S_{\rm Mott}$, $S_{\rm BI}(x)$ must be calculated for *open boundary conditions*[6] (OBC). This is most conveniently done numerically: $\mathcal{H}_{\rm BI}$ (8.1) may be reduced to a one-electron problem, which yields a tridiagonal matrix for $t' = 0$ and OBC. This matrix is readily diagonalized using standard algorithms [162] and the determination of $\xi(\delta, L)$ is painless. In Fig. 8.2 we present $\xi(\delta,L)/L$ as a function of $L/\xi_\infty(\delta)$ for the band insulator with $t' = 0$, together with the corresponding quantities for the simple Hubbard model, taken from Figs. 6.12 and 6.11. Hyperscaling is once again confirmed for the band insulator, since all the data for different sizes L and coupling constants δ fall on one curve. For $L \gg \xi_\infty$ both scaling functions match, as previously found for the Drude weight (8.20), whereas for $L \sim \xi_\infty$ they are clearly distinguishable due to the higher order terms: the band and the

[5] up to a proportionality constant

[6] Recall that S, although universal, depends precisely on the boundary conditions [174].

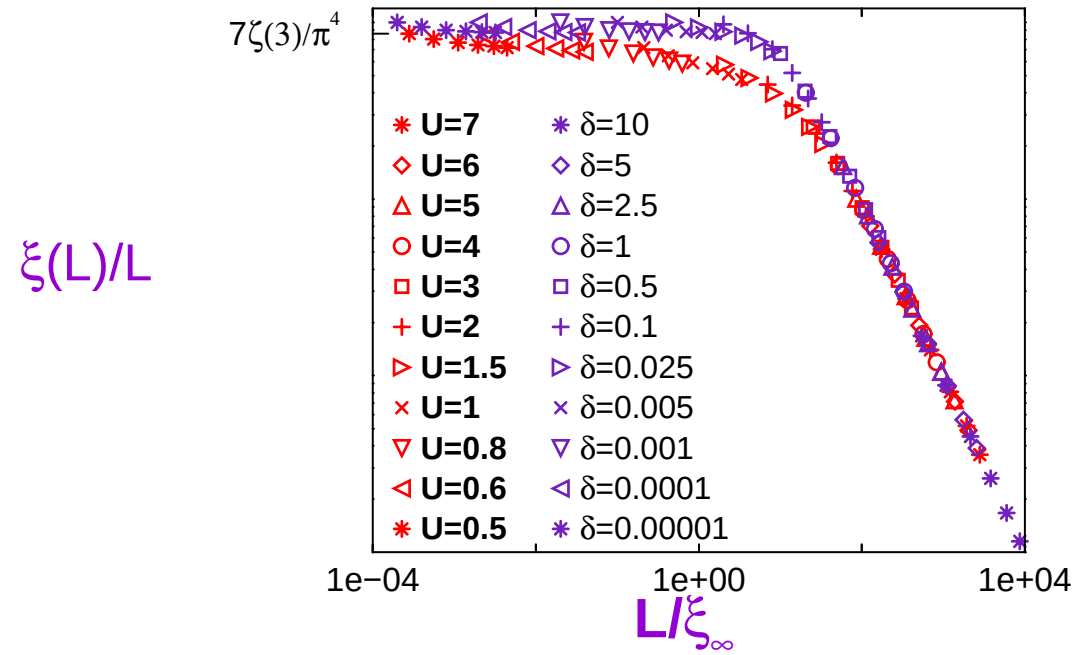

Figure 8.2: Plot of the scaling functions $S_{\mathrm{Mott,BI}} = \xi(L, U, t' = 0)/L$ vs. $L/\xi_\infty(U, t' = 0)$ in a log–log scale for the simple Hubbard model (red) and the band insulator (violet). Note that $\lim_{x\to 0} S(x) = 7\zeta(3)/\pi^4 = 0.0863821\ldots$ in both cases.

Mott insulators do *not* lie in the same universality class [224, 225]. Both scaling functions $S_{\mathrm{Mott}}(L/\xi_\infty)$ and $S_{\mathrm{BI}}(L/\xi_\infty)$ merge again as $L/\xi_\infty \to 0$ because both critical points, $U_c = 0$ or $\delta_c = 0$, and the boundary conditions are the same in both cases: $S_{\mathrm{Mott}}(0) = S_{\mathrm{BI}}(0) = \frac{7\zeta(3)}{\pi^4}$ (A.34). Recall that $\lim_{L\to\infty} \xi(L)/L$ is predicted to be universal at the critical point [174] — in other words it should remain the same on the whole critical line (8.5). This can be checked explicitly for periodic boundary conditions (appendix C.5). For open boundary conditions, we will always have

$$\xi(L) = \frac{7\zeta(3)}{\pi^4}\, L \tag{8.21}$$

at criticality whatever $\delta_c(t')$ is, thus matching the result of Fig. 6.13 for the $U - t - t'$ model. However, since the metallic phase is not critical in the band insulator model, some correlation length ξ will assume a *finite* value for $\delta < \delta_c(t')$ in the thermodynamic limit. In the vicinity of the transition on the metallic side, ξ will be inversely proportional to the energy overlap between the bands because $z = 1$. The scaling function $\xi(L)/L$ makes a universal jump between the critical point and both phases.

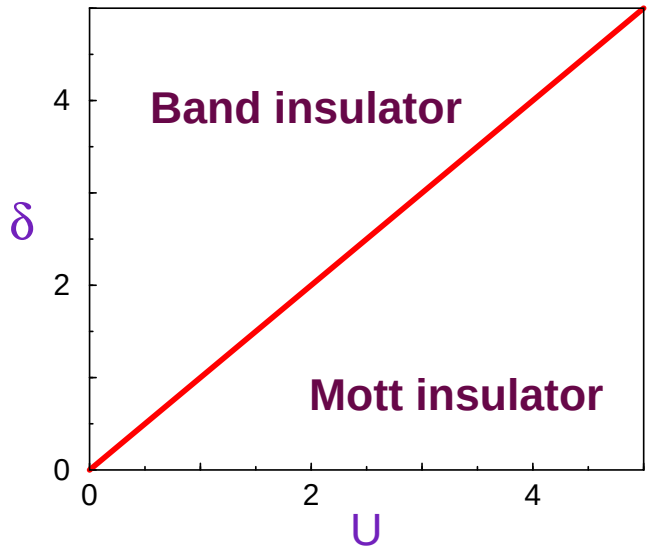

Figure 8.3: Schematic phase diagram of the ionic Hubbard model; the transition line is given by $U \sim \delta$. The Mott insulator has a charge gap but no spin gap, while the band insulator has both gaps.

8.2 Ionic Hubbard Model

Let us now resuscitate the on-site Hubbard repulsive term in the band insulator and formulate what has been named the *ionic Hubbard model*

$$\mathcal{H}_{\rm ionic} \;=\; -t\sum_{i\sigma}\left(c^{\dagger}_{i\sigma}c_{i+1\sigma}\;+\text{h.c.}\right)\;+\;\delta\sum_{j\sigma}(1+(-1)^{j})n_{j\sigma}\;+\;U\;\sum_{i}n_{i\uparrow}n_{i\downarrow}\,. \tag{8.22}$$

For the sake of conciseness, we have not included a t'; we work at half-filling and set $t \equiv 1$. At $U = \delta = 0$, we have our well-known metallic point. As soon as $U > 0$ and/or $\delta > 0$, the system becomes an insulator and $\xi(L)/L$ makes the same universal jump observed in the Mott and the band insulators separately. Say we trigger δ first: the system is in a band insulating state, where charge and spin gaps are exactly the same. If U is subsequently turned on, things will evolve and the system will eventually get metamorphosed into a Mott insulator at large enough U, most probably at a value of the order of δ [226]. The spin gap will vanish at the transition, leaving the charge gap alone[7]. We show a schematic phase diagram in Fig. 8.3 There has been quite a lot of controversy about the way this transition takes place. All authors agree with the fact that the charge gap drops dangerously close to zero in the vicinity of the transition. Does it actually vanish at the transition point? Almost everybody answers "yes": it does drop to zero precisely at the transition, yielding a unique metallic point in the phase diagram [226, 227, 228, 229, 230, 231]. Some claim that the

[7] this picture of the Mott insulating state is only consistent with a small or zero frustration t'.

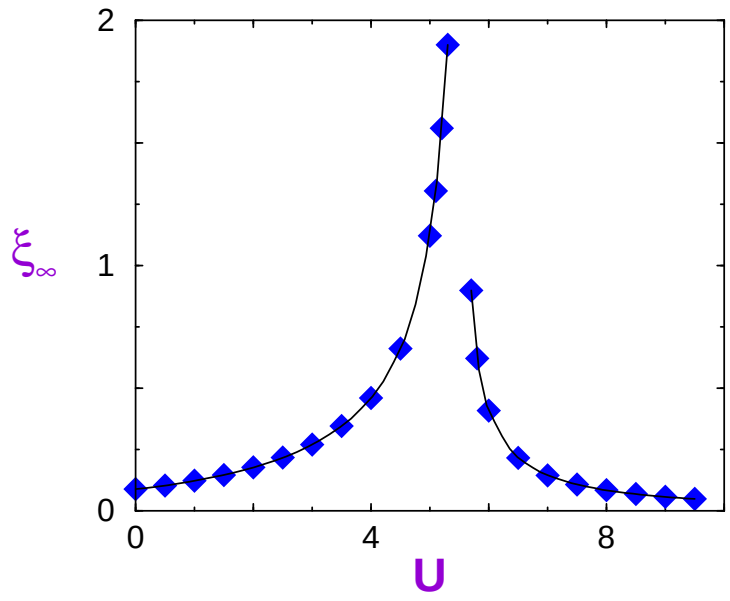

Figure 8.4: Diamonds: correlation length ξ_∞ as a function of U for $\delta = 4$ in the ionic Hubbard model (8.22). Each point comes from a finite-size scaling procedure applied to the DMRG data according to Eq. 5.18. The lines are splines through the data.

metallic region has a finite extent [229]. However, there has been speculation that there is no metallic phase at all [232].

A closer investigation of this model using critical quantities like the electric susceptibility χ or the correlation length ξ instead of the charge gap could possibly resolve the controversial issue of whether there is a *metallic point at finite U and δ* in the ionic Hubbard model. We choose $\delta > 0$ and $U = 0$ first, so that we start with the pure band insulator. In order to measure χ and ξ, we use the same parameters in the DMRG calculation as for the simple Hubbard model: as we have argued in the Chapter 5, the accuracy would definitely be high enough since turning on δ induces a charge gap at $U = 0$. We can then compare the results with the exact solution. The linear response regime is quite hard to reach — i.e. EL must be made quite small — if one couples $\mathcal{H}_{\text{ionic}}(U = 0)$ to an electric field by the usual method, especially for reasonably large values of δ (of the order of 1): such values are needed to investigate a possible metal-insulator transition. Turn U on and you can tell the linear response goodbye.

Therefore we have decided to focus our attention on ξ. Calculations are much more difficult than for the simple Hubbard model, owing to the staggered ("ionic") on-site potential. At $U = 0$ the DMRG calculation reproduces the exact result at large L (C.15). For $U \geq 0$, we display ξ_∞ in Fig. 8.4. The correlation length evidently increases when one approaches the assumed transition point, around $U = 5.5$. Does it really diverge, at least at the transition point? If so, a metallic region will be present, perhaps only at one point. As usual, there is a small window around the presumed critical point where the correlation length

becomes so large a finite-size scaling is impossible. This window is much smaller than in the Mott transition: if ξ_∞ diverges, it should do it less abruptly, i.e. as a power-law rather than exponentially. However, even if we were able to reach the thermodynamic limit very close to the transition point, there would still be uncertainty as to its location. In the Hubbard model we estimated the error in U_c to be about 0.2. Since the calculations are more delicate here, the value should be at least as large. The error might be even larger than the width of the presumed metallic region, which would lie between $U = 5.3$ and $U = 5.7$ and is therefore (much) smaller than 0.4, as it may be seen from Fig. 8.4.

Do we have a clue as to what's going on? Perhaps: at $U = 0$ and $\delta = 0$ there is definitely a metallic point, and it satisfies Eq. 8.21. Since the quantity $\xi(L)/L = 7\zeta(3)/\pi^4$ is predicted to be universal at criticality [174], we just need to see if $\xi(L)/L$ reaches $7\zeta(3)/\pi^4 = 0.0863821\ldots$ at some point in the region $5.3 < U < 5.7$. If it does, it would be metallic. Since this criterion has been used successfully in two *very* different — but related — models, the Mott transition and the band-insulator-to-metal transition, there is reason to believe that it may be applicable here as well. Unfortunately, we have to stress again that calculations for $\xi(L)$ are not as easy as for the simple Hubbard model. Carrying out a finite-size scaling procedure on $\xi(L)/L$ as we did to get Fig. 6.13 is close to impossible here because it requires large system sizes. However, we can consider reasonable sizes, say below 50 sites, where the system still behaves as a metal[8]: we then have $\xi(L) = \Theta L$. In such a situation, no length scale appears and the constant of proportionality Θ remains the same (apart from small finite-size corrections), until the system realizes that it is an insulator, possibly at a huge size $\tilde{L}$. The correlation length $\xi(L)$ would then reach a gigantic but finite value and we could formally take $\Theta \to 0$. If the system is truly metallic, it will never change its behavior and $\xi(L) = \Theta L$ up to $L \to \infty$, where Θ remains unchanged. The message is clear: as long as we are interested only in the effective value of $\Theta(\delta, U)$ up to a finite size L in a region where $\xi_\infty \gg L$, we do not need to go to very large sizes. If the $\Theta(\delta, U)$ obtained is equal to the universal value, we are at a well defined metallic point.[9] If it is below the universal value, the system will always have a *finite* correlation length, even if we cannot probe it directly. On the other hand that same criterion can be *successfully* applied to regions in which the thermodynamic limit is actually reached.

In Fig. 8.5, $\xi(L)/L$ is depicted as a function of $1/L$ for different U values between $U = 5.3$ and $U = 5.7$. As one can see, $\xi(L)/L$ is well below the "minimal" universal value, $0.0863821\ldots$. This should remain unchanged in this region for other values of U. Thus, if there is no violation of this *universality criterion* and if nothing peculiar occurs between the points at which we did the calculations, ξ_infty only reaches a maximum and does *not* diverge. However, this does not mean that the *charge gap* does not vanish, since the "usual" relation $\xi_\infty \sim 1/\Delta_c$ may not hold in this critical region. In fact, Δ_c has to go to zero, at least at some critical point U_c, since both insulating phases of the ionic Hubbard model are of different nature [233]: we have a (renormalized) band insulator between $U = 0$ and the presumed critical point U_c, and a Mott insulator above U_c. How can we reconcile those two

[8] in which case $L \ll \xi_\infty$

[9] If it is above the univeral value, there may be critical region of finite extent, like the metallic phase of the $U - t - t'$ model.

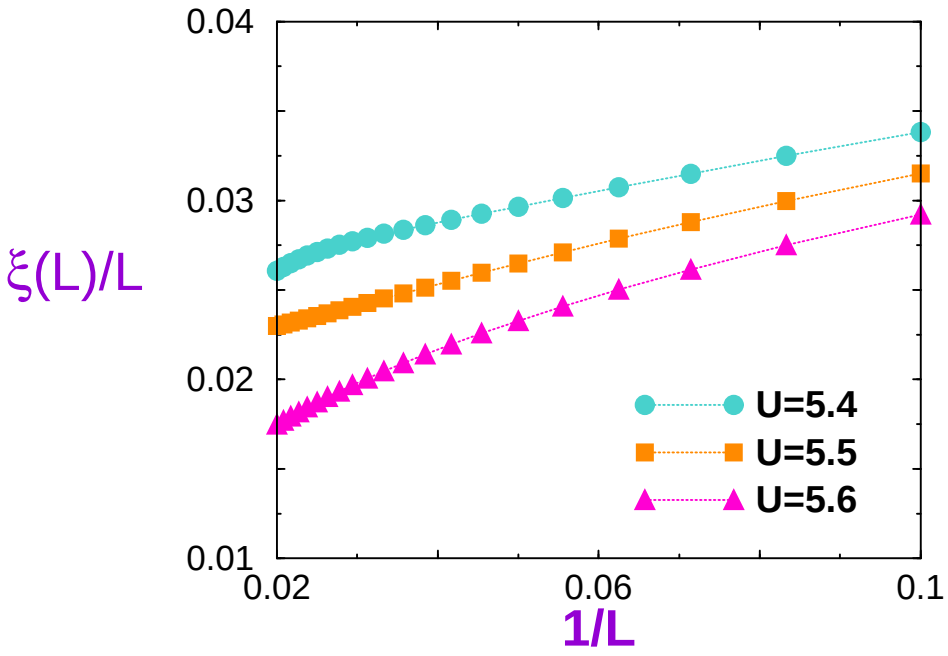

Figure 8.5: Symbols: $\xi(L)/L$ as a function of $1/L$, calculated with the DMRG. The dotted lines are guide to the eye. Note that $\xi(L)/L$ is always well below the universal "minimal" value $7\zeta(3)/\pi^4 = 0.0863821\ldots$.

points of view? This unique metallic point is in fact rather weird [233]: it has a zero charge gap and a zero Drude weight D as well! Astonishing, isn't it? In this case, it is not fully metallic in the common sense, and since $D = 0$, the correlation length ξ_∞ may well remain finite at this point! The quantity $\lim_{L\to\infty} \xi(L)/L$ should thus be related to the Drude weight itself, a relation which might hold for the $U - t - t'$ as well.

Chapter 9

Conclusion

Dear readers, it is now time for me to thank you for your patience and your study of this monograph. Before I let you close this thesis however, I would appreciate sharing a last little while in your company, and summarizing the most relevant streams of facts and ideas that have spanned this thesis.

The starting point and the unaltered cornerstone of this work is the electric susceptibility χ. We have determined it numerically with the DMRG for the Mott transition and analytically for the band-insulator-to-metal transition, obtaining the same result: χ is finite in the insulator and diverges at the transition. This is the *dielectric catastrophe* cherished by Mott. Such a *critical* quantity is thus well suited to study a metal-to-gapped-insulator transition, giving[1]

$$\chi \sim \frac{1}{\Delta^2} . \tag{9.1}$$

As a paradigm of the Mott transition we have studied the $U-t-t'$ model. For all values of t', χ is always found to diverge in the same exponential way and can be used to locate the transition point U_c, i.e.

$$\chi(U) \sim e^{\frac{4\pi}{U-U_c}} . \tag{9.2}$$

For $t' \leq \frac{1}{2}$, relevant Umklapp processes open a charge gap immediately — $U_c = 0$ just like in the simple Hubbard model ($t' = 0$). This insulating phase, which we have named the "Mott I" phase, possesses antiferromagnetic correlations. For $t' > \frac{1}{2}$ on the other hand, the Fermi "surface" jumps from two to four Fermi points and Umklapp processes lose their relevance at small U. At first, no charge gap opens and the system is a perfect metal for a non-zero repulsive interaction. Only later at a $U_c > 0$ does a charge gap open, and does the metal turn into an insulator, named the "Mott II" phase. This phase is a Mott insulator without antiferromagnetic correlations.[2] There is, however, *bond ordering* where the order parameter is the difference in the strength between two adjacent bonds. Where it vanishes determines the transition line between the two types of insulators. These two phases have also been identified in the *two*-dimensional Mott transition [203, 204].

[1] For the Anderson insulator, which is gapless, one would need an alternative definition of χ in order to get relevant results [234].

[2] They are frustrated by the t' term.

The electric susceptibility χ (Eq. 9.2) diverges exponentially, faster than any-power law: the transition is *infinite-order* and $\gamma \to \infty$. This is reminiscent of the Kosterlitz-Thouless transition, which is found in the one-dimensional quantum sine-Gordon model. The phase diagram of the latter is indeed *very* similar to that of the $U-t-t'$ model [6]: such an analogy has already been made for the simple Hubbard model. We *believe* that this is nothing but the *universality class* of the one-dimensional Mott transition.

The fluctuations of the polarization also diverge in general at a metal-insulator transition. In one dimension, they represent the correlation length close to the critical point, a relation which has been confirmed explicitly for the band insulator. For both the Mott and the band insulators, we find

$$\xi \sim \chi^2 \ . \tag{9.3}$$

In other words, $\gamma/\nu = 2$, which is what experimentalists measure in a broad class of $T = 0$ metal-insulator transitions (see Chapter 2). We have possibly touched on a highly universal relation here, transcending various universality classes of such transitions. Close to the transition, we have shown that this length is *unique* and that *hyperscaling* is satisfied for both transitions: the electric susceptibility may be expressed as a *universal* function of L/ξ_∞ albeit multiplied by a non-universal constant:

$$\chi(L) \ = \ L^2 \, C \, \Phi(L/\xi_\infty) \ . \tag{9.4}$$

Note that hyperscaling has been observed in experiments as well (see Chapter 2), even for a "pure" Mott transition (see Fig. 4.1). We have also demonstrated that the scaling function of the correlation is fully universal, confirming earlier work by Privman and Fisher on classical phase transitions [174]:

$$\xi(L) \ = \ L \, S(L/\xi_\infty) \ . \tag{9.5}$$

As $L/\xi_\infty \to 0$ we reach the critical point, where the correlation length diverges proportionally to system size: $\xi(L) = S(0)L$ whereas in the insulating phase $\lim_{L\to\infty} \xi(L) = \xi_\infty$. This means that $\xi(L)/L$ takes on a *universal value* at the critical point.

In the Mott case in particular, the electric susceptibility and the correlation length diverge exponentially, giving $\gamma \to \infty$ and $\nu \to \infty$. In analogy with the Kosterlitz-Thouless case, the whole metallic phase below the Mott insulator is critical. This means that $\xi(L)$ diverges with the system size for $U < U_c$ as well, but not with the same constant of proportionality: $\xi(L) = \Theta(U, t')L$. Here Θ is a *universal* function of $U/U_c(t')$ which makes a *universal jump* from $S(0)$ to zero at the critical interaction strength $U_c(t')$. I cannot resist quoting you again that for open boundary conditions,

$$S(0) \ = \ \frac{7\zeta(3)}{\pi^4} \ . \tag{9.6}$$

The full scaling function $S(x)$ remains the same, whatever t' is, therefore confirming the constancy of the universality class in the $U - t - t'$ model: the simple Hubbard case, $t' = 0$, is not pathological and is definitely representative of the general case. However this is not the same universality class as that of the band insulator — the scaling functions $S(x)$ of both insulators do not match.

Appendix A

Non-Interacting Limit

A.1 Electric susceptibility for $U = 0$

We would like to solve

$$\mathcal{H} = -\sum_{i\sigma} \left(t\ c^\dagger_{i\sigma} c_{i+1\sigma} + t'\ c^\dagger_{i\sigma} c_{i+2\sigma}\right)\ -\ E\ \sum_i x_i n_i\ . \tag{A.1}$$

One can find an exact solution in some limiting cases [163, 235, 236]. It is also important to note that the limits $L \to \infty$ and $E \to 0$ do *not* commute [163]. If we use the definition (3.11) of the electric susceptibility, we must let E go to zero first, at finite size L: in that case, E can be treated as a perturbation whereas the influence of an electric field on an infinite system is singular [163]. Thus we will use Eq. 3.12. For OBC, (3.12) is easily determined for $t' = 0$ only. We take L to be even. Let the Fermi sea be

$$|\Phi_0> = \prod_{n=1,\sigma}^{L/2} c^\dagger_{k_n\sigma}|> , \tag{A.2}$$

where the quantum numbers are given by

$$k_n = \frac{n\pi}{L+1}, \quad n = 1, \ldots, L \tag{A.3}$$

and the (normalized) one-particle wave functions by

$$\varphi_n(j) = < j|n > = < j|c^\dagger_{k_n\sigma}| > = \sqrt{\frac{2}{L+1}} \sin\frac{n\pi j}{L+1}\ . \tag{A.4}$$

The perturbation is just the polarization multiplied by L:

$$\frac{\partial \mathcal{H}_{\text{ext}}}{\partial E} = \sum_{j=1}^{L} j\hat{n}_j \equiv \mathcal{H}_1\ . \tag{A.5}$$

In the second order, only excited states with one hole in the Fermi sea need be taken into account. This readily gives

$$\chi_{\rm obc} = \frac{2}{L}\sum_{n=1}^{L/2}\sum_{m=L/2+1}^{L}\frac{|<n|\mathcal{H}_1|m>|^2}{\cos k_n - \cos k_m} \tag{A.6}$$

$$= \frac{8}{L(L+1)^2}\sum_{n=1}^{L/2}\sum_{\substack{m=L/2+1\\ n+m \text{ odd}}}^{L}\frac{\sin^2 k_n \sin^2 k_m}{(\cos k_m - \cos k_n)^5}\ . \tag{A.7}$$

Since the two set of quantum numbers $\{n\}$ and $\{m\}$ do not overlap, the summand has no divergence and we can, for large L, replace the sum over m by an integral, which yields

$$\chi_{\rm obc} = \frac{1}{2\pi L^2}\sum_{n=1}^{L/2} F(k_n)\ , \tag{A.8}$$

where F is an elementary function of sines, cosines and logarithms that it diverges at $k = \frac{\pi}{2}$:

$$F(k) = \frac{1}{(k-\frac{\pi}{2})^4} - \frac{1}{2(k-\frac{\pi}{2})^2} \tag{A.9}$$

$$+ \text{ logarithmic divergences} + \text{ regular terms}\ . \tag{A.10}$$

For large L, we need to keep only the most divergent term in the sum (A.8), which yields:

$$\chi_{\rm obc} = \frac{1}{2\pi L^2} 16 \left(\frac{L}{\pi}\right)^4 \sum_{n=0}^{\infty}\frac{1}{(2n+1)^4} \tag{A.11}$$

$$= \frac{8L^2}{\pi^5}\frac{2^4-1}{2^4}\zeta(4) \tag{A.12}$$

finally giving

$$\chi_{\rm obc}(t'=0,L) = \frac{1}{12\pi}L^2\ . \tag{A.13}$$

For PBC Eq. 3.12 is still valid, but with X replaced by

$$\tilde{X} = \frac{1}{2qi}\sum_{k\sigma}(c^\dagger_{k+q\sigma}c_{k\sigma} - c^\dagger_{k-q\sigma}c_{k\sigma})\ . \tag{A.14}$$

The calculations starting from Eq. 3.12 are now much easier. At $0 \le t' \le \frac{1}{2}$ the Fermi sea is non degenerate for even L, non divisible by 4, and we immediately obtain:

$$\chi_{\rm pbc}(t' \le \frac{1}{2}, L) = \frac{1}{8\pi^3}L^2 \tag{A.15}$$

for large L. At $t' > \frac{1}{2}$ we have 4 Fermi points $(\pm k_F^{(1)}, \pm k_F^{(2)})$ and we must determine their location in order to use Eq. 3.12. As $k_F^{(2)} - k_F^{(1)} = \frac{\pi}{2}$, we can write the following equation for $k_F^{(1)}$:

$$\varepsilon(k_F^{(1)}) = \varepsilon(k_F^{(1)} + \frac{\pi}{2}) \; . \tag{A.16}$$

This is easily solved and gives

$$k_F^{(1)} = \arccos(\frac{1 + \sqrt{8t'^2 - 1}}{4t'}) \; . \tag{A.17}$$

For the case of L a multiple of four, the Fermi sea is non degenerate, and we find

$$\chi_{\rm pbc}(t' > \frac{1}{2}, L) = \frac{-\sqrt{2} - \sqrt{-2 + 16t'^2} - 2t'(1 + 2\sqrt{-1 + 8t'^2})\sqrt{4 - \frac{\sqrt{-1+8t'^2}}{t'^2}}}{4\pi^3\sqrt{-1 + 8t'^2}(1 + \sqrt{-1 + 8t'^2})\sqrt{4 - \frac{\sqrt{-1+8t'^2}}{t'^2}}(-1 - t'\sqrt{8 - \frac{2\sqrt{-1+8t'^2}}{t'^2}})} L^2 \; . \tag{A.18}$$

Despite its intricate formula (A.18), $\chi_{\rm pbc}$ has a simple behavior: $\chi_{\rm pbc}/L^2$ has a simple pole when $t' \stackrel{>}{\to} \frac{1}{2}$:

$$\chi_{\rm pbc}(t' \stackrel{>}{\longrightarrow} \frac{1}{2}) \sim \frac{1}{16\pi^3} \frac{1}{t' - \frac{1}{2}} \, L^2 \tag{A.19}$$

and it decays monotonically like $1/8\pi^3 t'$ for large t'.

At $t' = 0$ we have the following relation between the results for OBC and PBC:

$$\chi_{\rm obc}(t' = 0, L) = \frac{2\pi^2}{3} \chi_{\rm pbc}(t' = 0, L) \tag{A.20}$$

which can be numerically checked to arbitrary precision for any t' and up to very large L (above 10000 for instance) via exact diagonalization.[1] We therefore can write

$$\chi_{\rm obc}(t', L) = \frac{2\pi^2}{3} \chi_{\rm pbc}(t', L) \; . \tag{A.21}$$

A.2 Correlation length for $U = 0$

The calculation of ξ with OBC (3.15) is analytically tractable only at $t' = 0$. We use the same notation as in the previous section for the wave functions (A.4) and the quantum numbers (A.3). Let the ground state be the Fermi sea (A.2). Using Wick's theorem, we readily get

$$\xi_{\rm obc} = \frac{2}{L} \sum_{n=1}^{L/2} \sum_{m=L/2+1}^{L} \sum_{i,j=1}^{L} ij \varphi_n(i) \varphi_m(i) \varphi_n(j) \varphi_m(j) \tag{A.22}$$

[1] As this is a non-interacting problem, the size of the matrices does not grow exponentially with the system size L.

which gives, see (A.6),

$$\xi_{\rm obc} = \frac{8}{L(L+1)^2} \sum_{n=1}^{L/2} \sum_{\substack{m=L/2+1 \\ n+m \text{ odd}}}^{L} \frac{\sin^2 k_n \sin^2 k_m}{(\cos k_n - \cos k_m)^4} \ . \tag{A.23}$$

Note that this is very much like (A.7). The most important contribution to ξ will come from the most divergent part of the summand, i.e. for k_n close to k_m. This time, we can even directly approximate for large L

$$\frac{\sin^2 k_n \sin^2 k_m}{(\cos k_n - \cos k_m)^4} = \frac{1}{(k_n - k_m)^4} + \mathcal{O}((k_n - k_m)^{-2}) \tag{A.24}$$

which gives

$$\xi_{\rm obc} = \frac{8}{L^3} \sum_{n=1}^{L/2} \sum_{\substack{m=L/2+1 \\ n+m \text{ odd}}}^{L} \frac{1}{(k_n - k_m)^4} \tag{A.25}$$

$$= \frac{8}{\pi^4} L \sum_{n=1}^{L/2} \sum_{\substack{m=L/2+1 \\ n+m \text{ odd}}}^{L} \frac{1}{(n-m)^4} \ . \tag{A.26}$$

Furthermore, for L divisible by 4, we get

$$\xi_{\rm obc} = \frac{L}{12\pi^4} \left(\sum_{m=0}^{L/4-1} \left(\psi^{(3)}\left(\frac{L}{4} + \frac{1}{2} - m\right) - \psi^{(3)}\left(\frac{L}{2} + \frac{1}{2} - m\right)\right) + \sum_{m=1}^{L/4} \left(\psi^{(3)}\left(\frac{L}{4} + \frac{1}{2} - m\right) - \psi^{(3)}\left(\frac{L}{2} + \frac{1}{2} - m\right)\right)\right) \tag{A.27}$$

where $\psi^{(3)}$ is the *pentagamma* function:

$$\psi^{(3)}(x) = \frac{d^3\psi(x)}{dx^3} = \frac{d^4}{dx^4} \ln \Gamma(x) \ . \tag{A.28}$$

ψ is the *digamma* function. A simple rearrangement gives

$$\xi_{\rm obc} = \frac{L}{12\pi^4} \left(\psi^{(3)}\left(\frac{1}{2}\right) - \psi^{(3)}\left(\frac{L+1}{2}\right) + 2 \sum_{m=1}^{L/4-1} \left(\psi^{(3)}\left(\frac{2m+1}{2}\right) - \psi^{(3)}\left(\frac{L/2+2m+1}{2}\right)\right)\right) \ . \tag{A.29}$$

It is known that

$$\psi^{(3)}\left(\frac{1}{2}\right) = \pi^4, \quad \psi^{(3)}(x \to \infty) = 0 \ , \tag{A.30}$$

so that we just need to carry out, for large L, the remaining sum in (A.29). To this end, we represent $\psi^{(3)}$ as the third derivative of the integral representation of the digamma function:

$$\psi^{(3)}(z) = \int_0^\infty \frac{t^3 e^{-zt}}{1 - e^{-t}} dt \ . \tag{A.31}$$

Then we commute sum and integration, which enables us to do the sum exactly:

$$\sum_{m=1}^{L/4-1} e^{-mt} = \frac{e^{-tL/4} - e^{-t}}{e^{-t} - 1} \ . \tag{A.32}$$

By further taking the limit $L \gg 1$, the sum in (A.29) finally becomes

$$\int_0^\infty dt \frac{t^3 e^{-3t/2}}{(1 - e^{-t})^2} = -\frac{\pi^4}{2} + 42\zeta(3) \ , \tag{A.33}$$

which readily gives the result for large L:

$$\xi_{\rm obc}(L) = \frac{7\zeta(3)}{\pi^4} L \ . \tag{A.34}$$

The determination of ξ with PBC (3.27) is very easy and yields

$$\begin{aligned} \xi_{\rm pbc}(t' < \frac{1}{2}, L) &= \frac{L}{4\pi^2} \qquad \text{(2 Fermi points)} \\ \xi_{\rm pbc}(t' > \frac{1}{2}, L) &= \frac{L}{2\pi^2} \qquad \text{(4 Fermi points)} \end{aligned} \tag{A.35}$$

For $t' = 0$, with have the relation between OBC and PBC:

$$\xi_{\rm obc}(t' = 0, L) = \frac{28\zeta(3)}{\pi^2} \xi_{\rm pbc}(t' = 0, L) \ . \tag{A.36}$$

This can be proved numerically with arbitrary accuracy[2] for any t':

$$\xi_{\rm obc}(t', L) = \frac{28\zeta(3)}{\pi^2} \xi_{\rm pbc}(t', L) \ . \tag{A.37}$$

[2] see preceding section

Appendix B

Strong-coupling limit

B.1 Electric susceptibility for $U \to \infty$

We now determine the electric susceptibility of the $U-t-t'$ model (4.16) for $U \to \infty$. To this end, we take the integrable atomic limit of (4.16) coupled with an external electric field with OBC (3.9):

$$\mathcal{H}_0 = U \sum_j n_{j\uparrow} n_{j\downarrow} - E \sum_j j n_j \ . \tag{B.1}$$

We then add the kinetic energy $\mathcal{H}_1 = \mathcal{T}$ of (4.16) as a perturbation, considering:

$$\begin{cases} U & > & LE \\ U & \gg & t, t' \end{cases} \tag{B.2}$$

so that the ground state of (B.1), at half-filling, has no double occupancy and is thus fully degenerate in the spins; its energy is $E_0 = -EL(L+1)/2$. We apply degenerate perturbation theory: let P be the projector onto the subspace with no double occupancy and $P_\perp$ its orthogonal complement so that the total Hilbert space is their orthogonal sum. To first order, we find

$$\mathcal{H}^{(1)} = P\mathcal{T}P \equiv 0 \ , \tag{B.3}$$

whereas in second order

$$\mathcal{H}^{(2)} = P\mathcal{T}\frac{P_\perp}{E_0 - \mathcal{H}_0}\mathcal{T}P \ . \tag{B.4}$$

We first treat the $t' = 0$ limit. The resolvant operator $\frac{1}{E_0 - \mathcal{H}_0}$ will have two distinct eigenvalues $(-\frac{1}{U-E}, -\frac{1}{U+E})$, and $P_\perp \mathcal{T} P \equiv \mathcal{T} P$. Defining the usual spin $-\frac{1}{2}$ operators from the fermionic ones, $\mathcal{H}^{(2)}$ is just the antiferromagnetic Heisenberg model:

$$\mathcal{H}^{(2)} = \frac{4U}{U^2 - E^2}\left(\sum_i \mathbf{S}_i \cdot \mathbf{S}_{i+1} - \frac{1}{4}L\right) \ . \tag{B.5}$$

The ground state energy of $\mathcal{H}_0 + \mathcal{H}^{(1)} + \mathcal{H}^{(2)}$ is then [109]:

$$E_0 + E_0^{(2)} = -E\frac{L(L+1)}{2} - \frac{4\ln 2U}{U^2 - E^2}L \; . \tag{B.6}$$

Using (3.11), we immediately find

$$\chi(U, t' = 0) = \frac{8\ln 2}{U^3} \; . \tag{B.7}$$

We next turn our attention to the general case ($t' \neq 0$). The operator $\frac{1}{E_0 - \mathcal{H}_0}$ will now have four distinct eigenvalues ($-\frac{1}{U-E}, -\frac{1}{U+E}, -\frac{t'}{U-2E}, -\frac{t'}{U+2E}$). Again, $P_\perp \mathcal{T} P \equiv \mathcal{T} P$. Proceeding very much the same way, we obtain the $J - J'$ model:

$$\mathcal{H}^{(2)} = \sum_i (J\mathbf{S}_i \cdot \mathbf{S}_{i+1} + J'\mathbf{S}_i \cdot \mathbf{S}_{i+2}) - \frac{1}{4}(J + J')L \tag{B.8}$$

with

$$J = \frac{4U}{U^2 - E^2} \; , \quad J' = \frac{4Ut'^2}{U^2 - 4E^2} \; . \tag{B.9}$$

The ground state energy of $\mathcal{H}_0 + \mathcal{H}^{(1)} + \mathcal{H}^{(2)}$ can then be written as

$$\begin{aligned} E_0 + E_0^{(2)} \;\; = \;\; & \frac{UL}{U^2 - E^2}\left(4e_0(t'^2\frac{U^2 - E^2}{U^2 - 4E^2}) - 1\right) \\ & - \frac{Ut'^2 L}{U^2 - 4E^2} - E\frac{L(L+1)}{2} \end{aligned} \tag{B.10}$$

where $e_0(y)$ is the ground state energy density of the rescaled $J - J'$ Hamiltonian

$$e_0(y) = \frac{1}{L}\sum_i < \mathbf{S}_i \cdot \mathbf{S}_{i+1} + y\mathbf{S}_i \cdot \mathbf{S}_{i+2} > \; . \tag{B.11}$$

We assume that $e_0(y)$ is at least twice differentiable. Then, using (3.11), we find

$$\chi(U, t') = \frac{2}{U^3}(1 + 4t'^2 - 4e_0(t'^2) - 12e_0'(t'^2)) \; . \tag{B.12}$$

This already proves $\chi(U \to \infty) \sim 1/U^3$ for any t'. From the Hellmann-Feynman theorem, we further see that the first derivative of e_0 is given by

$$e_0'(t'^2) = \frac{1}{L}\sum_i < \mathbf{S}_i \cdot \mathbf{S}_{i+2} > \; . \tag{B.13}$$

The ground state energy density $e_0(y)$ is only known at two finite values of y: $y = 0$ (Bethe Ansatz) and $y = \frac{1}{2}$ which gives in (B.11) the Majumdar-Ghosh model which can be exactly

(and easily) solved [168, 103]. The (degenerate) ground state of (B.11) is then just a product of uncorrelated spin singlets at neighboring sites. We have [103]

$$< \mathbf{S}_i \cdot \mathbf{S}_j >_{\mathrm{MG}} = \begin{cases} \frac{3}{4} & i = j \\ -\frac{3}{4} & i,j \text{ singlet pair} \\ 0 & \text{otherwise} \end{cases} \tag{B.14}$$

This immediately yields $e_0'(\frac{1}{2}) = 0$ and $e_0(\frac{1}{2}) = -\frac{3}{8}$, which finally gives the simple result for large U in the vicinity of the Majumdar-Ghosh point

$$\chi(U, t' = \frac{1}{\sqrt{2}}) = \frac{9}{U^3} \, . \tag{B.15}$$

B.2 Correlation length for $U \to \infty$

We start from the definition (3.15). We consider first $t' = 0$. For OBC, with the usual particle-hole transformation

$$\begin{cases} c_{j\sigma}^\dagger & \to & e^{i\pi j} & c_{j\sigma} \\ c_{j\sigma} & \to & e^{-i\pi j} & c_{j\sigma}^\dagger \end{cases} \tag{B.16}$$

at *half-filling*, the Hubbard model (with $E = 0$) is mapped onto itself with an unchanged number of electrons, while

$$n_i \longrightarrow 2 - n_i \, , \tag{B.17}$$

which gives $n_i \equiv 1$: there are no Friedel oscillations at half-filling in an open Hubbard chain[237]. At sufficiently large U, only short-ranged $\langle \hat{n}_i \hat{n}_j \rangle$'s will be correlated, while

$$\langle \hat{n}_i \hat{n}_j \rangle \stackrel{|i-j| \to \infty}{\longrightarrow} 1 \, . \tag{B.18}$$

Let

$$\hat{d}_i \; := \; \hat{n}_{i\uparrow} \hat{n}_{i\downarrow} \tag{B.19}$$

be the double occupancy operator and d_i its expectation value in the ground state. Using

$$\langle \hat{n}_i^2 \rangle \; = \; 1 + 2 d_i \tag{B.20}$$

and the sum rule

$$\sum_{ij} \langle \hat{n}_i \hat{n}_j \rangle \; = \; L^2 \, , \tag{B.21}$$

we get for large enough U

$$\langle \hat{n}_i \hat{n}_{i\pm 1} \rangle \; = \; 1 - a d_i \tag{B.22}$$

$$\langle \hat{n}_i \hat{n}_{i\pm 2} \rangle \; = \; 1 - b d_i \tag{B.23}$$

while all the longer-ranged correlations are equal to 1, following Eq. B.18. The constants a and b are yet to be determined, using the sum rule (B.21). Introducing Eqs. B.20,B.22 and B.23 in Eq. 3.15, we get

$$\xi(L) = \frac{1}{L}\left[2\sum_{j=1}^{L} j^2 d_j - a\sum_{j=1}^{L-1} j(j+1)d_j - a\sum_{j=2}^{L} j(j-1)d_j - b\sum_{j=1}^{L-2} j(j+2)d_j - b\sum_{j=3}^{L} j(j-2)d_j\right] . \tag{B.24}$$

For large L, $d_j \equiv d$ is independent of j and we write

$$\xi(L) \;=\; \frac{d}{3L}\left[2(1-a-b)L^3 + 3(2b+1)L^2 + (1+2a-b)L - 6b\right] . \tag{B.25}$$

Since $\xi(L)$ must scale to a finite value for $L \to \infty$, we must have

$$1 - a - b \;=\; 0 \tag{B.26}$$

$$2b + 1 \;=\; 0 \tag{B.27}$$

and in order to satisfy the sum rule, the relation

$$2 - 2a - 2b \;=\; 0 \tag{B.28}$$

must also be fulfilled.[1] This set of equations is over-determined, but can be solved, obtaining $b = -\frac{1}{2}$ and $a = \frac{3}{2}$. This gives us

$$\xi(U) \;=\; \frac{3}{4}\, d(U) \tag{B.29}$$

in the thermodynamic limit. The density of doubly occupied sites is given by

$$d \;=\; \frac{1}{L}\langle \hat{D} \rangle \;=\; \frac{\partial (E_o/L)}{\partial U} \tag{B.30}$$

with $\hat{D} = \sum_i \hat{d}_i$ and using the Hellmann-Feynman theorem. The ground state energy E_o of the Hubbard model as a function of U is exactly known [47], and eventually yields

$$\xi(t' = 0, U) \;=\; \frac{4 \ln 2}{U^2} . \tag{B.31}$$

For $t' > 0$, we start from the PBC definition of ξ, (3.27), because $n_i \equiv 1$ no longer holds. The same kind of derivation may be realized, yielding again

$$\xi(t', U) \;\sim\; \frac{\partial (E_o(t', U)/L)}{\partial U} \tag{B.32}$$

but this time $E_o(t', U)$ is unknown. However, certain arguments give the general behavior $E_o \sim 1/U$ [47], which yields

$$\xi(t', U) \;\sim\; \frac{1}{U^2}. \tag{B.33}$$

[1] Satisfying all those constraints would not have been possible by taking $\langle \hat{n}_i \hat{n}_{i\pm 2} \rangle \equiv 1$ at the start.

B.3 Bond order for $U \to \infty$

The local bond order parameter is defined as

$$b_i \;:=\; \sum_\sigma \langle c^\dagger_{\mathrm{i}\sigma} c_{\mathrm{i}+1\sigma} - c^\dagger_{\mathrm{i}+1\sigma} c_{\mathrm{i}+2\sigma} \;+\; \mathrm{h.c.}\rangle \;. \tag{B.34}$$

Let us define local nearest-neighbor kinetic energies (the second-nearest neighbor part remains unchanged):

$$\mathcal{T} \;=\; \sum_{i\sigma} (c^\dagger_{\mathrm{i}\sigma} c_{\mathrm{i}+1\sigma} \;+\; \mathrm{h.c.}) \;. \tag{B.35}$$

This gives with the Hellmann-Feynman theorem

$$b_i \;=\; \frac{\partial E_o}{\partial t_{\mathrm{i}}} \;-\; \frac{\partial E_o}{\partial t_{\mathrm{i}+1}} \;. \tag{B.36}$$

At $U \to \infty$ we have to first order in $\frac{1}{U}$:

$$E_o \;=\; \langle \Phi_o | \sum_{\langle ij \rangle} J_i \mathbf{S}_i \cdot \mathbf{S}_j \;+\; \sum_{\langle\langle ij \rangle\rangle} J' \mathbf{S}_i \cdot \mathbf{S}_j | \Phi_o \rangle \;, \tag{B.37}$$

where $J_i = \frac{2t_i^2}{U}$ and $J' = \frac{2t'^2}{U}$; $\langle\langle \cdots \rangle\rangle$ stands for "second-nearest neighbor". We have then

$$\frac{\partial E_o}{\partial t_{\mathrm{i}}} \;=\; \frac{4t_i}{U} \, \frac{\partial E_o}{\partial J_{\mathrm{i}}} \tag{B.38}$$

which eventually gives for $t_i \equiv 1$

$$b_i \;= \frac{4}{U} \, d_i \;, \tag{B.39}$$

where d_i is the dimerization order parameter for the spins in the $J - J'$ model:

$$d_i \;\equiv\; \langle \mathbf{S}_{\mathrm{i}} \cdot \mathbf{S}_{\mathrm{i}+1} \rangle \;-\; \langle \mathbf{S}_{\mathrm{i}+1} \cdot \mathbf{S}_{\mathrm{i}+2} \rangle \;. \tag{B.40}$$

Taking the mean value over the whole lattice, we can write

$$b \;= \frac{4}{U} \, d \;. \tag{B.41}$$

In particular, at the Majumdar-Ghosh point [168, 169], we have $d = \frac{3}{4}$ [103] and

$$b \;=\; \frac{3}{U} \;. \tag{B.42}$$

Appendix C

Band Insulator

We use *periodic boundary conditions* (PBC) to solve the $\delta - t - t'$ model analytically:

$$\mathcal{H}_{\rm BI} \;=\; -\sum_{i\sigma}\left[t\; c^{\dagger}_{i\sigma}c_{i+1\sigma} + t'\; c^{\dagger}_{i\sigma}c_{i+2\sigma}\right] + \delta\sum_{j\sigma}(1+(-1)^{j})n_{j\sigma}\;. \tag{C.1}$$

We will set t to 1 and take $\delta,\; t' \geq 0$. Throughout this Appendix, we consider only system sizes L that are multiples of four.

C.1 Spectrum

We define new operators: $a^{\dagger}_{i\sigma}$ creates particles on sites of energy 2δ and $b^{\dagger}_{i\sigma}$ creates particles on sites of energy zero. The Hamiltonian (C.1) is then readily diagonalized (Fourier transform and then Bogoliubov transformation):

$$\mathcal{H}_{\rm BI} = \sum_{k\sigma}\left(\varepsilon_{+}(k)\alpha^{\dagger}_{k\sigma}\alpha_{k\sigma} + \varepsilon_{-}(k)\beta^{\dagger}_{k\sigma}\beta_{k\sigma}\right)\;, \tag{C.2}$$

where the energy spectrum is given by

$$\varepsilon_{\pm}(k) \;=\; \delta - 2t'\cos\;k \pm \sqrt{\delta^{2} + 2(1+\cos\;k)} \tag{C.3}$$

and the eigenvectors by

$$\left\{\begin{array}{rcl} \alpha_{k\sigma} & = & v^{\star}_{+1}(k)a_{k\sigma} + v^{\star}_{+2}(k)b_{k\sigma} \\ \beta_{k\sigma} & = & v^{\star}_{-1}(k)a_{k\sigma} + v^{\star}_{-2}(k)b_{k\sigma} \end{array}\right. \tag{C.4}$$

with

$$v_{\pm}(k) = \sqrt{\frac{|\epsilon_{\pm}(k)|}{2\epsilon(k)}}\left(\mp 1, \frac{1+e^{ik}}{|\epsilon_{\pm}(k)|}\right) \tag{C.5}$$

and

$$\epsilon_{\pm}(k) \;=\; \delta \pm \sqrt{\delta^{2} + 2(1+\cos\;k)} \;=\; \varepsilon_{\pm}(k)|_{t'=0} \tag{C.6}$$

$$\epsilon(k) \;=\; \sqrt{\delta^{2} + 2(1+\cos\;k)}\;. \tag{C.7}$$

C.2 Electric susceptibility

We consider only $t' = 0$. At half-filling, the ground state is

$$|\Phi_0\rangle = \prod_{k\sigma} \beta^\dagger_{k\sigma} |\rangle \tag{C.8}$$

where $|\rangle$ stands for the vacuum. The position operator for PBC is given by ($q = \frac{2\pi}{L}$)

$$\tilde{X} \;=\; \frac{L}{4\pi i} \sum_{k\sigma} \left(a^\dagger_{k+2q\sigma} a_{k\sigma} - a^\dagger_{k-2q\sigma} a_{k\sigma} + e^{iq} b^\dagger_{k+2q\sigma} b_{k\sigma} - e^{-iq} b^\dagger_{k-2q\sigma} b_{k\sigma} \right) . \tag{C.9}$$

The only excited states $|\Phi_\nu\rangle$ for which $\langle \Phi_\nu | \tilde{X} | \Phi_0 \rangle \neq 0$ are those where a hole is created in k in the lower filled band and an electron is created in $k \pm 2q$ in the upper empty band. Since χ is finite in the thermodynamic limit, we may immediately replace the sum by an integral for large L and (3.12) becomes:

$$\chi = \frac{1}{2\pi} \sum_{k'=\pm 2q,\sigma} \int_{-\pi}^{\pi} dk \frac{|\langle \Phi_0 | \alpha_{k+k'\sigma} \tilde{X} | \Phi_0 \rangle|^2}{\varepsilon(k+k') + \varepsilon(k)} . \tag{C.10}$$

For large L, the integrand may be developed as a series in powers in q:

$$\frac{|\langle \Phi_0 | \alpha_{k+k'\sigma} \tilde{X} | \Phi_0 \rangle|^2}{\varepsilon(k+k') + \varepsilon(k)} = \frac{\delta^2 \sin^2 \frac{k}{2}}{8(2+\delta^2+2\cos k)^{5/2}} + \mathcal{O}(q) \tag{C.11}$$

which yields for $q = 2\pi/L \to 0$

$$\chi = \frac{\delta^2}{2\pi} \int_0^\pi dk \frac{\sin^2 \frac{k}{2}}{(2+\delta^2+2\cos k)^{5/2}} . \tag{C.12}$$

This is easily integrated to give:

$$\chi(\delta) = \frac{1}{12\pi} \frac{1}{\sqrt{\delta^2+4}} \left(\frac{\delta^2+8}{\delta^2} E(\frac{2}{\sqrt{\delta^2+4}}) - K(\frac{2}{\sqrt{\delta^2+4}}) \right) , \tag{C.13}$$

where K and E are the complete elliptic integrals of the first and second kind, respectively.

C.3 Correlation length

We use (3.27) to determine ξ at $t' = 0$; for $\tilde{X}$, we take (C.9) with (C.4) inverted. As ξ is finite, the remaining sum in (3.27) is converted to an integral at large L and we expand the integrand as a power series in q, see Eq. C.11. For $q = 2\pi/L \to 0$ we have:

$$\xi = \frac{\delta^2}{2\pi} \int_0^\pi dk \frac{\sin^2 \frac{k}{2}}{(2+\delta^2+2\cos k)^2} \tag{C.14}$$

which readily gives

$$\xi(\delta) = \frac{1}{4\delta\sqrt{\delta^2+4}} . \tag{C.15}$$

C.4 Drude weight

We follow closely the method presented in [38]. The Drude weight may be determined through Kohn's formula [47]

$$D \;=\; \frac{1}{2}\,\frac{\partial^2 (E_o/L)}{\partial(\Phi/L)^2}\bigg|_{\Phi=0} \quad , \tag{C.16}$$

where Φ is a magnetic flux piercing the ring. Setting $t' = 0$, and coupling Φ to the Hamiltonian, (C.1) transforms into

$$\mathcal{H}_\Phi \;=\; -\sum_{j\sigma}\left(e^{i\Phi/L}a^\dagger_{j\sigma}b_{j\sigma} \;+\; \text{h.}c.\right) - \sum_{j\sigma}\left(e^{-i\Phi/L}a^\dagger_{\mathrm{j}+1\sigma}b_{j\sigma} \;+\; \text{h.}c.\right) \;+\; 2\delta\,\sum_{j\sigma}\,a^\dagger_{j\sigma}a_{j\sigma} \tag{C.17}$$

where the operator $a^\dagger_{j\sigma}$ creates a particle on a site of energy 2δ, while $b^\dagger_{j\sigma}$ does it on a site of energy zero. $\mathcal{H}_\Phi$ can be diagonalized in very much the same way we did it for (C.1) in section C.1. The spectrum is

$$\varepsilon_\pm(k,\Phi) \;=\; \delta \pm \sqrt{\delta^2 + 2(1+\cos(2\Phi/L + k))}\,. \tag{C.18}$$

The introduction of the magnetic flux just causes a shift $k \to k + 2\Phi/L$ in the first Brillouin zone, and $\varepsilon_\pm(k,\Phi) = \varepsilon_\pm(k + 2\Phi/L)$. At half-filling, the ground state energy is given by

$$E_o(\delta,\Phi,L) \;=\; \sum_k \varepsilon_-(k,\Phi)\,. \tag{C.19}$$

If we naively transform this sum into an integral over k by taking the large L limit, we will lose any Φ-dependence. We instead use the Poisson summation formula to write

$$E_o(\delta,\Phi,L) \;=\; \frac{L}{2\pi}\,\int_{-\pi}^{\pi} dk\;\epsilon_-(k)\sum_{m=-\infty}^{\infty} e^{-im(Lk/2-\Phi)}\,. \tag{C.20}$$

$m = 0$ yields the "zeroth" order, which is exactly the first approximation we were talking about, where we lose the Φ dependence; it will not contribute to the Drude weight. At large enough L we may just keep $m = \pm 1$, which is the first order which gives a non-zero contribution to D. Kohn's formula (C.16) yields

$$D(\delta,L) \;=\; \frac{L^2}{2\pi}\,\int_{-\pi}^{\pi} dk\,\sqrt{\delta^2 + 2 + 2\cos\,k}\;e^{iLk/2}\,. \tag{C.21}$$

The integrand, with the shift $k \to -\pi + ik$ and rewritten as

$$e^{-Lp(k)}\;,\quad p(k) = \frac{i\pi}{2} + \frac{k}{2} - \frac{1}{2L}\ln|\delta^2 + 2 - 2\cos\,k| \tag{C.22}$$

is holomorphic in the complex plane. We have a complex logarithm, with $\ln\,x = \ln|x| \pm i\pi$ if $x \le 0$. The integral (C.21) is dominated by the saddle point

$$k_o \;=\; \text{arsinh}\frac{\delta\sqrt{\delta^2+4}}{2} \;+\; \mathcal{O}(\frac{1}{L})\,. \tag{C.23}$$

Transforming (C.21) into a contour integral in the complex plane, we get for L, large and a multiple of four,

$$D(\delta, L) \;=\; \frac{L^2}{\pi} \int_{k_o}^{\infty} dk \, \sqrt{2\cosh\, k - 2 - \delta^2}\, e^{-Lk/2} \,. \tag{C.24}$$

We make the change of variables $y = k - k_o$ and expand for large L to obtain

$$\cosh(y + k_o) \;=\; \cosh\, k_o \; + y \sinh\, k_o \; + \frac{1}{2} y^2 \cosh\, k_o \,. \tag{C.25}$$

We have

$$\cosh\, k_o \;=\; \frac{\delta^2 + 2}{2} \tag{C.26}$$

$$\sinh\, k_o \;=\; \frac{1}{8\xi(\delta)} \tag{C.27}$$

where $\xi(\delta)$ is the correlation length determined earlier (C.15). This yields

$$D(\delta, L) \;=\; \frac{L^2}{\pi}\, e^{-Lk_o/2} \sqrt{\frac{\delta^2+2}{2}} \int_0^{\infty} dy \, \sqrt{y^2 + \frac{y}{2(\delta^2+2)\xi}}\, e^{-Ly/2} \tag{C.28}$$

which is easily evaluated to give

$$D(\delta, L) \;=\; \frac{L}{2\pi}\, e^{-L \,\mathrm{arsinh}\left(\frac{1}{8\xi}\right)/2} \frac{1}{\sqrt{2(\delta^2+2)\xi}}\, e^{\frac{L}{8(\delta^2+2)\xi}}\, K_1\left(\frac{L}{8(\delta^2+2)\xi}\right) \,. \tag{C.29}$$

The modified Bessel function $K_1(x)$ has the following asymptotic expansion for large x

$$K_1(x) \;\sim\; \sqrt{\frac{\pi}{2}}\, e^z\, \frac{1}{\sqrt{z}} \left(1 + \frac{3}{8}\frac{1}{z}\right) \,, \tag{C.30}$$

which eventually gives for the Drude weight at large L

$$D(\delta, L) \;=\; \frac{1}{\sqrt{2\pi}} \sqrt{\frac{L}{\xi}}\, e^{-L \,\mathrm{arsinh}\left(\frac{1}{8\xi}\right)/2} \left(1 + 3(\delta^2+2)\frac{\xi}{L}\right) \,. \tag{C.31}$$

C.5 $\xi(L)/L$ at criticality

On the critical line (8.5), $\xi(L) \sim L$. The upper band just touches the lower one; they do *not* overlap. At finite L, there is only one electron at $k = 0$ in the upper band and a hole at $k = -\pi$ in the lower band. In $\tilde{X}$, only the two terms $\sim \beta^\dagger_{-\pi\sigma}\beta_{-\pi+2q\sigma}$ and $\sim \alpha^\dagger_{\pm 2q\sigma}\alpha_{0\sigma}$ will contribute to the divergent part of ξ:

$$\xi(L) \;=\; \frac{1}{L}(\langle \tilde{X}^2_{\alpha\alpha}\rangle + \langle \tilde{X}^2_{\beta\beta}\rangle) \,. \tag{C.32}$$

We have

$$\tilde{X}_{\beta\beta} \;=\; -\frac{e^{-iq}}{2qi}\, v_{2-}(-\pi+2q)\, \sum_{\sigma} \;\sim \beta^{\dagger}_{-\pi\sigma}\beta_{-\pi+2q\sigma} \tag{C.33}$$

which gives

$$\langle \tilde{X}^2_{\beta\beta}\rangle \;=\; \frac{|v_{2-}(-\pi+2q)|^2}{2q^2} \;\stackrel{q\to 0}{\longrightarrow}\; \frac{L^2}{8\pi^2}\,. \tag{C.34}$$

We get exactly the same for $\langle \tilde{X}^2_{\alpha\alpha}\rangle$ so that at large L

$$\xi(L) \;=\; \frac{L}{4\pi^2}\,. \tag{C.35}$$

Bibliography

[1] M. E. Fisher. *Rev. Mod. Phys.* , 46(4):597, 1974.

[2] J. A. Hertz. *Phys. Rev. B*, 14(3):1165, 1975.

[3] M. A. Continentino. *Phys. Rep.* , 239(3):179, 1994.

[4] S. L. Sondhi, S. M. Girvin, J. P. Carini, and D. Shahar. *Rev. Mod. Phys.* , 69(1):315, 1997.

[5] D. Belitz and T. R. Kirkpatrick. cond-mat. 9811058.

[6] S. Sachdev. *Quantum Phase Transitions.* Cambridge University Press, 1999.

[7] E. Abrahams and G. Kotliar. *Science*, 274:1853, 1996.

[8] N. F. Mott. *Metal-Insulator Transitions.* Taylor & Francis, 1990.

[9] D. Belitz and T. R. Kirkpatrick. *Rev. Mod. Phys.* , 66(2):261, 1994.

[10] C. Aebischer, D. Baeriswyl, and R. M. Noack. *Phys. Rev. Lett.*, 86(3):468, 2001.

[11] R. M. Noack, C. Aebischer, D. Baeriswyl, and F. Gebhard. In J. Bonča et al., editor, *Open Problems in Strongly Correlated Electron Systems*, pages 347–359. Kluwer Academic Publishers, 2001.

[12] C. Aebischer, D. Baeriswyl, and R. M. Noack. In preparation.

[13] M. Imada, A. Fujimori, and Y. Tokura. *Rev. Mod. Phys.* , 70(4):1039, 1998.

[14] H. F. Hess, K. DeConde, T. F. Rosenbaum, and G. A. Thomas. *Phys. Rev. B*, 25(5):5578, 1982.

[15] J. D. Jackson. *Classical Electrodynamics.* Wiley, 1975.

[16] T. G. Castner, N. K. Lee, G. S. Cieloszyk, and G. L. Salinger. *Phys. Rev. Lett.*, 34(26):1627, 1975.

[17] M. Capizzi, G. A. Thomas, F. DeRosa, R. N. Bhatt, and T. M. Rice. *Phys. Rev. Lett.*, 44(15):1019, 1980.

[18] T. F. Rosenbaum, R. F. Milligan, M. A. Paalanen, G. A. Thomas, R. N. Bhatt, and W. Lin. *Phys. Rev. B*, 27(12):7509, 1983.

[19] F. A. D'Altroy and H. Y. Fan. *Phys. Rev.* , 103(6):1671, 1956.

[20] T. F. Rosenbaum, K. Andres, G. A. Thomas, and R. N. Bhatt. *Phys. Rev. Lett.*, 45(21):1723, 1980.

[21] M. A. Paalanen, T. F. Rosenbaum, G. A. Thomas, and R. N. Bhatt. *Phys. Rev. Lett.*, 48(18):1284, 1982.

[22] G. A. Thomas, Y. Ootuka, S. Kobayashi, and W. Sasaki. *Phys. Rev. B*, 45:1723, 1981.

[23] Y. Imry, Y. Gefen, and D. J. Bergman. *Phys. Rev. B*, 26(6):3436, 1982.

[24] M. Lee, J. G. Massey, V. L. Nguyen, and B. I. Shklovskii. *Phys. Rev. B*, 60(3):1582, 1999.

[25] S. Waffenschmidt, C. Pfleiderer, and H. V. Löhneysen. *Phys. Rev. Lett.*, 83(15):3005, 1999.

[26] S. Bogdanovich, M. P. Sarachik, and R. N. Bhatt. *Phys. Rev. Lett.*, 82(1):137, 1999.

[27] S. Bogdanovich, M. P. Sarachik, and R. N. Bhatt. *Phys. Rev. B*, 60(4):2292, 1999.

[28] S. Bogdanovich, D. Simonian, S. V. Kravchenko, M. P. Sarachik, and R. N. Bhatt. *Phys. Rev. B*, 60(4):2286, 1999.

[29] H.-L. Lee, J. P. Carini, D. V. Baxter, W. Henderson, and G. Grüner. *Science*, 287:633, 2000.

[30] A. N. Ionov, I. S. Shlimak, and M. N. Matveev. *Solid State Comm.*, 47(10):763, 1983.

[31] M. Watanabe, K. M. Itoh, Y. Ootuka, and E. E. Haller. *Phys. Rev. B*, 62(4), 2000.

[32] P. W. Anderson. *Phys. Rev.* , 109:1492, 1958.

[33] P. A. Lee and T. V. Ramakrishnan. *Rev. Mod. Phys.* , 57(2):287, 1985.

[34] E. Abrahams, P. W. Anderson, D. C. Licciardello, and T. V. Ramakrishnan. *Phys. Rev. Lett.*, 42(10):673, 1979.

[35] D. J. Bergman and Y. Imry. *Phys. Rev. Lett.*, 39(19):1222, 1977.

[36] K. M. Itoh, E. E. Haller, J. W. Beeman, W. L. Hansen, J. Emes, L. A. Reichertz, E. Kreysa, T. Shutt, A. Cummings, W. Stockwell, B. Sadoulet, J. Muto, J. W. Farmer, and V. I. Ozhogin. *Phys. Rev. Lett.*, 77(19):4058, 1996.

[37] C. A. Stafford, A. J. Millis, and B. S. Shastry. *Phys. Rev. B*, 43(16):13660, 1991.

[38] C. A. Stafford and A. J. Millis. *Phys. Rev. B*, 48(3):1409, 1993.

[39] E. Jeckelmann, F. Gebhard, and F. H. L. Eßler. *Phys. Rev. Lett.*, 85(18):3910, 2000.

[40] S. Fujimoto and N. Kawakami. cond-mat. 9710313.

[41] N. Kawakami and S.-K. Yang. *Phys. Rev. B*, 44(15):7844, 1991.

[42] R. M. Fye, M. J. Martins, D. J. Scalapino, J. Wagner, and W. Hanke. *Phys. Rev. B*, 45(13):7311, 1992.

[43] H. Castella, X. Zotos, and P. Prelovšek. *Phys. Rev. Lett.*, 74(6):972, 1995.

[44] X. Zotos and P. Prelovšek. *Phys. Rev. B*, 53(3):983, 1996.

[45] J. M. P. Carmelo, N. M. R. Peres, and P. D. Sacramento. *Phys. Rev. Lett.*, 84(20):4673, 2000.

[46] W. Kohn. *Phys. Rev.* , 133:171, 1964.

[47] F. Gebhard. *The Mott Metal-Insulator Transition*. Springer, 1997.

[48] W. L. McMillan. *Phys. Rev. B*, 24(5):2739, 1980.

[49] R. Kupferman and A. Chorin. *SIAM J. Appl. Math.*, 59(5):1843, 1999.

[50] A. Díaz-Sánchez, M. Ortu no, M. Pollak, A. Pérez-Garrido, and A. Möbius. *Phys. Rev. B*, 59(2):910, 1999.

[51] J. H. Davies, P. A. Lee, and T. M. Rice. *Phys. Rev. B*, 29(8):4260, 1984.

[52] R. Resta. cond-mat. 9802004.

[53] E. K. Kudinov. *Sov. Phys. Solid State*, 33:1299, 1991.

[54] I. Souza, T. Wilkens, and R. M. Martin. *Phys. Rev. B*, 62(3):1666, 2000.

[55] N. Marzari and D. Vanderbilt. *Phys. Rev. B*, 56(20):12847, 1997.

[56] K. Huang. *Statistical Mechanics*. Wiley, 1987.

[57] T. R. Kirkpatrick and D. Belitz. *Phys. Rev. Lett.*, 74(7):1178, 1995.

[58] S. N. Dixit, D. Guo, and S. Mazumdar. *Phys. Rev. B*, 43(8):6781, 1991.

[59] A. Takahashi. *Phys. Rev. B*, 51(22):16479, 1995.

[60] A. Takahashi. *Phys. Rev. B*, 56(7):3792, 1997.

[61] R. Resta. *Phys. Rev. Lett.*, 80(9):1800, 1998.

[62] R. Resta and S. Sorella. *Phys. Rev. Lett.*, 82(2):370, 1999.

[63] A. A. Aligia and G. Ortiz. *Phys. Rev. Lett.*, 82(12):2560, 1999.

[64] J. Zak. *Phys. Rev. Lett.*, 85(5):1138, 2000.

[65] J. L. Cardy. Conformal invariance. In C. Domb and J. L. Lebowitz, editors, *Phase Transitions and Critical Phenomena*, volume 11. Academic Press, 1987.

[66] R. A. Römer and B. Sutherland. cond-mat. 9303004.

[67] A. H. Wilson. *Proc. Roy. Soc.*, page 458, 1931.

[68] J. H. de Boer and E. J. W. Verwey. *Proc. Phys. Soc.*, 49:59, 1937.

[69] N. F. Mott. *Proc. Phys. Soc.*, page 416, 1949.

[70] N. F. Mott. *Rev. Mod. Phys.* , 40(4):677, 1968.

[71] J. Hubbard. *Proc. Roy. Soc.*, A277:237, 1964.

[72] E. H. Lieb and F. Y. Wu. *Phys. Rev. Lett.*, 20:1445, 1968.

[73] M. C. Gutzwiller. *Phys. Rev.* , 137, 1965.

[74] W. F. Brinkman and T. M. Rice. *Phys. Rev. B*, 2(10):4302, 1970.

[75] M. Dzierzawa, D. Baeriswyl, and L. M. Martelo. *Helv. Phys. Acta*, 70:124, 1997.

[76] D. Baeriswyl and W. Von Der Linden. *Int. J. Mod. Phys. B*, 5:999, 1991.

[77] D. Baeriswyl. In A. R. Bishop et al., editor, *Nonlinearity in Condensed Matter*, volume 69. Springer Series in Solid State Sciences, 1987.

[78] F. Mancini. *Europhys. Lett.*, 50:229, 2000.

[79] K. Hashimoto. *Phys. Rev. B*, 31(11):7368, 1985.

[80] D. Baeriswyl. *Foundations of Physics*, 30(12):2033, 2000.

[81] M. A. Continentino. *Europhys. Lett.*, 9(1):77, 1989.

[82] D. J. Scalapino, S. R. White, and S. C. Zhang. *Phys. Rev. Lett.*, 68(18):2830, 1992.

[83] S. R. White, D. J. Scalapino, R. L. Sugar, E. Y. Loh, J. E. Gubernatis, and R. T. Scalettar. *Phys. Rev. B*, 40(1):506, 1989.

[84] A. Georges, G. Kotliar, W. Krauth, and M. J. Rozenberg. *Rev. Mod. Phys.* , 68(1):13, 1996.

[85] R. M. Noack and F. Gebhard. *Phys. Rev. Lett.*, 82:1915, 1999.

[86] M. J. Rozenberg, R. Chitra, and G. Kotliar. *Phys. Rev. Lett.*, 83:3498, 1999.

[87] A. Y. Matsuura, Z.-X. Shen, D. S. Dessau, C.-H. Park, T. Thio, J. W. Bennett, and O. Jepsen. *Phys. Rev. B*, 53(12), 1996.

[88] D. S. Jin, Y. V. Zastavker, T. F. Rosenbaum, X. Yao, and J. M. Honig. *Science*, 274:1874, 1996.

[89] X. Yao, J. M. Honig, T. Hogan, C. Kannewurf, and J. Spałek. *Phys. Rev. B*, 54(24):17469, 1996.

[90] X. Yao, Y.-K Kuo, D. K. Powell, J. W. Brill, and J. M. Honig. *Phys. Rev. B*, 56(12):7129, 1997.

[91] K. Kobayashi, T. Mizokawa, A. Fujimori, M. Isobe, Y. Ueda, T. Tohyama, and S. Maekawa. *Phys. Rev. Lett.*, 82(4):803, 1999.

[92] R. Neudert, M. Knupfer, M. S. Golden, J. Fink, W. Stephan, K. Penc, N. Motoyama, H. Eisaki, and S. Uchida. *Phys. Rev. Lett.*, 81(3):657, 1998.

[93] J. S. Ahn, J. Bak, H. S. Choi, T. W. Noh, J. E. Han, Y. Bang, J. H. Cho, and Q. X. Jia. *Phys. Rev. Lett.*, 82(26):5321, 1999.

[94] S. Lefebvre, P. Wzietek, S. Brown, C. Bourbonnais, D. Jérome, C. Mézière, M. Fourmigué, and P. Batail. *Phys. Rev. Lett.*, 85(25):5420, 2000.

[95] H. J. Schulz and C. Bourbonnais. *Phys. Rev. B*, 27(9):5856, 1983.

[96] C. Bourbonnais and L. G. Caron. *Phys. Rev. B*, 29(9):5007, 1984.

[97] M. Takahashi. *Prog. Theor. Phys.*, 47:69, 1972.

[98] X. Wang and T. Xiang. *Phys. Rev. B*, 56(9):5061, 1997.

[99] S. Fujimoto and N. Kawakami. *J. Phys. A: Math. Gen.*, 31:465, 1998.

[100] A. Klümper. *Eur. Phys. J. B*, 5:677, 1998.

[101] F. H. L. Eßler, V. E. Korepin, and K. Schoutens. *Phys. Rev. Lett.*, 67(27):3848, 1991.

[102] A. A. Ovchinnikov. *Sov. Phys. JETP*, 30:1160, 1970.

[103] A. Auerbach. *Interacting Electrons and Quantum Magnetism*. Springer, 1998.

[104] V. L. Berezinskiĭ. *Sov. Phys. JETP*, 32(3):493, 1971.

[105] J. M. Kosterlitz and D. J. Thouless. *J. Phys. C*, 6:1181, 1973.

[106] J. M. Kosterlitz. *J. Phys. C*, 7:1046, 1974.

[107] P. Minnhagen. *Rev. Mod. Phys.* , 59(4):1001, 1987.

[108] P. Gupta and S. Teitel. *Phys. Rev. B*, 55(5):2756, 1997.

[109] H. J. Schulz. Fermi liquids and non-fermi liquids. In et al. E. Akkermans, editor, *Proceedings of Les Houches Summer School LXI*. Elsevier (Amsterdam), 1995.

[110] H. J. Schulz, G. Cuniberti, and P. Pieri. Fermi liquids and Luttinger liquids. In G. Morandi et al., editor, *Field Theories for Low-Dimensional Condensed Matter Systems*. Springer, 2000.

[111] T. Giamarchi. *Phys. Rev. B*, 44(7):2905, 1991.

[112] T. Giamarchi. cond-mat. 9609114.

[113] F. D. M. Haldane. *Phys. Rev. Lett.*, 45(16):1358, 1980.

[114] J. Sólyom. *Advances in Physics*, 28(2):201, 1979.

[115] J. Voit. *Eur. Phys. J. B*, 5:505, 1998.

[116] S.-T. Chui and P. A. Lee. *Phys. Rev. Lett.*, 35(5):315, 1975.

[117] C. N. Yang and C. P. Yang. *Phys. Rev.* , 147(1):303, 1966.

[118] J. des Cloizeaux. *J. of Math. Phys.*, 7(12):2136, 1966.

[119] J. des Cloizeaux and M. Gaudin. *J. of Math. Phys.*, 7(8):1384, 1966.

[120] B. S. Shastry and B. Sutherland. *Phys. Rev. Lett.*, 65(2):243, 1990.

[121] G. Spronken, R. Jullien, and M. Avignon. *Phys. Rev. B*, 24(9):5356, 1981.

[122] R. Assaraf, P. Azaria, M. Caffarel, and P. Lecheminant. *Phys. Rev. B*, 60:2299, 1999.

[123] M. Nakamura. *Phys. Rev. B*, 61(24):16377, 2000.

[124] C. Itoi, S. Qin, and I. Affleck. *Phys. Rev. B*, 61(10):6747, 2000.

[125] M. Nakamura, A. Kitazawa, and K. Nomura. *Phys. Rev. B*, 60(11):7850, 1999.

[126] M. Nakamura, K. Nomura, and A. Kitazawa. *Phys. Rev. Lett.*, 79(17):3214, 1997.

[127] R. Roth and U. Schollwöck. *Phys. Rev. B*, 58(14):9264, 1998.

[128] S. R. White and I. Affleck. *Phys. Rev. B*, 54(14):9862, 1996.

[129] J. L. Black and V. J. Emery. *Phys. Rev. B*, 23(1):429, 1981.

[130] S. Fujimoto and N. Kawakami. *Phys. Rev. B*, 54(16), 1996.

[131] H. J. Schulz. *Phys. Rev. B*, 53(6), 1996.

[132] G. I. Japaridze and A. P. Kampf. *Phys. Rev. B*, 59(20):12822, 1999.

[133] A. A. Aligia, K. Hallberg, C. D. Batista, and G. Ortiz. *Phys. Rev. B*, 61:7883, 2000.

[134] S. A. Bulgadaev. hep-th. 9808115.

[135] S. A. Bulgadaev. hep-th. 9906091.

[136] S. A. Bulgadaev. hep-th. 9907195.

[137] C. Itoi and H. Mukaida. *Phys. Rev. E*, 60(4):3688, 1999.

[138] J. von Delft and H. Schoeller. cond-mat. 9805275.

[139] D. Sénéchal. cond-mat. 9908262.

[140] S. P. Strong and J. C. Talstra. *Phys. Rev. B*, 59(11):7362, 1999.

[141] W. Hofstetter and D. Vollhardt. *Ann. Phys.*, 7:48, 1998.

[142] M. Fabrizio. *Phys. Rev. B*, 54(14):10054, 1996.

[143] K. Kuroki, R. Arita, and H. Aoki. *J. Phys. Soc. Jap.* , 66:3371, 1997.

[144] R. Arita, K. Kuroki, H. Aoki, and M. Fabrizio. *Phys. Rev. B*, 57(17):10324, 1998.

[145] S. Daul and R. M. Noack. *Phys. Rev. B*, 61(3):1646, 2000.

[146] H. Q. Lin and J. E. Hirsch. *Phys. Rev. B*, 35(7):3359, 1987.

[147] E. Koch, O. Gunnarsson, and R. M. Martin. cond-mat. 9912345.

[148] F. D. M. Haldane. *Phys. Rev. B*, 25(7):4925, 1982.

[149] K. Nomura and K. Okamoto. *J. Phys. A: Math. Gen.*, 27:5773, 1994.

[150] R. J. Bursill and F. Gode. *J. Phys.: Condens. Matter*, 7:9765, 1995.

[151] S. Eggert. *Phys. Rev. B*, 54(14), 1996.

[152] P. Lecheminant, T. Jolicoeur, and P. Azaria. *Phys. Rev. B*, 63:174426, 2001.

[153] K. G. Wilson. *Rev. Mod. Phys.* , 47:773, 1975.

[154] S. R. White and R. M. Noack. *Phys. Rev. Lett.*, 68(24):3487, 1992.

[155] S. R. White. *Phys. Rev. Lett.*, 69(19):2863, 1992.

[156] S. R. White. *Phys. Rev. B*, 48(14):10345, 193.

[157] R. M. Noack and S. R. White. In I. Peschel et al., editor, *Density Matrix Renormalization Group: A New Numerical Method in Physics*. Springer (Berlin), 1999.

[158] M.-C. Chung and I. Peschel. *Phys. Rev. B*, 64:064412, 2001.

[159] S. Daul. *Eur. Phys. J. B*, 14:649, 2000.

[160] S.-W. Tsai and J. B. Marston. *Phys. Rev. B*, 62(9):5546, 2000.

[161] E. Jeckelmann, D. J. Scalapino, and S. R. White. *Phys. Rev. B*, 58:9492, 1998.

[162] W. H. Press, S. A. Teukolsky, W. T. Vetterling, and B. P. Flannery. *Numerical Recipes in C*. Cambridge University Press, 1994.

[163] H. Fukuyama, R. A. Bari, and H. C. Fogedby. *Phys. Rev. B*, 8(12):5579, 1973.

[164] A. Drzewiński and J. M. J. van Leuwen. *Phys. Rev. B*, 49(1):403, 1994.

[165] Ö. Legeza and G. Fáth. *Phys. Rev. B*, 53(21):14349, 1996.

[166] M. Andersson, M. Boman, and S. Östlund. *Phys. Rev. B*, 59(16):10493, 1999.

[167] M. N. Barber. Finite-size scaling. In C. Domb and J. L. Lebowitz, editors, *Phase Transitions and Critical Phenomena, vol. 8*. Academic Press, 1989.

[168] C. K. Majumdar and D. K. Ghosh. *J. of Math. Phys.*, 10:1399, 1969.

[169] C. K. Majumdar. *J. Phys. C*, 3:911, 1970.

[170] S. Maslov and A. Zheludev. *Phys. Rev. Lett.*, 80(26):5786, 1998.

[171] I. Affleck and S. Qin. *J. Phys. A: Math. Gen.*, 32:7815, 1999.

[172] V. Privman, P. C. Hohenberg, and A. Aharony. Universal critical-point amplitude relations. In C. Domb and J. L. Lebowitz, editors, *Phase Transitions and Critical Phenomena, vol. 14*. Academic Press, 1991.

[173] K. Kim and P. B. Weichman. *Phys. Rev. B*, 43(16):13583, 1991.

[174] V. Privman and M. E. Fisher. *Phys. Rev. B*, 30(1):322, 1984.

[175] T. R. Kirkpatrick and D. Belitz. *Phys. Rev. Lett.*, 79(16):3042, 1997.

[176] S. Jain and K. J. Hammarling. cond-mat. 9805141.

[177] E. Hofstetter and M Schreiber. *Phys. Rev. B*, 49(20):14726, 1994.

[178] I. Kh. Zharekeshev and B. Kramer. *Ann. Phys.*, 7:442, 1998.

[179] S. De Toro Arias and J. M. Luck. *J. Phys. A: Math. Gen.*, 31, 1998.

[180] D. N. Sheng and Z. Y. Weng. *Phys. Rev. Lett.*, 83:144, 1999.

[181] D. N. Sheng and Z. Y. Weng. *Phys. Rev. Lett.*, 80(3):580, 1998.

[182] E. Hofstetter. *Phys. Rev. B*, 57(20):12763, 1998.

[183] E. Cuevas. *Phys. Rev. Lett.*, 83(1):140, 1999.

[184] F. Iglói and E. Carlon. *Phys. Rev. B*, 59:3783, 1999.

[185] R. A. Monetti and J. E. Satulovsky. *Phys. Rev. E*, 57(6):6289, 1998.

[186] A. MacKinnon and B. Kramer. *Phys. Rev. Lett.*, 47(21):1546, 1981.

[187] F. M. Izrailev, T. Kottos, and G. P. Tsironis. *J. Phys.: Condens. Matter*, 8:2823, 1996.

[188] T. Kawarabayashi, B. Kramer, and T. Ohtsuki. *Phys. Rev. B*, 57(19):11842, 1998.

[189] M. Weiss, T. Kottos, and T. Geisel. *Phys. Rev. B*, 62:1765, 2000.

[190] B. Huckestein and B. Kramer. *Phys. Rev. Lett.*, 64(12):1437, 1990.

[191] D. Liu and S. Das Sarma. *Phys. Rev. B*, 49(4):2677, 1994.

[192] P. A. Rikvold, W. Kinzel, J. D. Gunton, and K. Kaski. *Phys. Rev. B*, 28(5):2686, 1983.

[193] A. Eilmes, U. Grimm, R. A. Römer, and M. Schreiber. *Eur. Phys. J. B*, 8:547, 1999.

[194] M. Henkel and U. Schollwöck. *J. Phys. A: Math. Gen.*, 34:3333, 2001.

[195] J. Voit. *Rep. Prog. Phys.*, 58(9):977, 1995.

[196] S. Kivelson, D.-H. Lee, and S.-C. Zhang. *Phys. Rev. B*, 46(4):2223, 1992.

[197] M. P. A. Fisher, G. Grinstein, and S. M. Girvin. *Phys. Rev. Lett.*, 64(5):587, 1990.

[198] D. C. Licciardello and D. J. Thouless. *Phys. Rev. Lett.*, 35(21):1475, 1975.

[199] A. A. Aligia, E. Gagliano, L. Arrachea, and K. Hallberg. *Eur. Phys. J. B*, 5:371, 1998.

[200] A. A. Aligia. *Europhys. Lett.*, 45(4):411, 1999.

[201] L. Balents and M. P. A. Fisher. *Phys. Rev. B*, 53(18):12133, 1996.

[202] M. Vojta, A. Hübsch, and R. M. Noack. *Phys. Rev. B*, 63:045105, 2001.

[203] S. Sachdev. cond-mat. 0108238.

[204] K. Park and S. Sachdev. cond-mat. 0104519.

[205] N. Read and S. Sachdev. *Phys. Rev. B*, 42(7):4568, 1990.

[206] N. Read and S. Sachdev. *Phys. Rev. Lett.*, 62(14):1694, 1989.

[207] M. Ogata and H. Shiba. *Phys. Rev. B*, 41(4):2326, 1990.

[208] N. Kawakami and S.-K. Yang. *J. Phys.: Condens. Matter*, 3:5983, 1991.

[209] J. Voit, Y. Wang, and M. Grioni. *Phys. Rev. B*, 61(12):7930, 2000.

[210] F. D. M. Haldane. *Phys. Rev. Lett.*, 47(25):1840, 1981.

[211] E. Melzer. cond-mat. 9410043.

[212] D. Controzzi, F. H. L. Eßler, and A. M. Tsvelik. cond-mat. 0011439.

[213] D. Controzzi, F. H. L. Eßler, and A. M. Tsvelik. *Phys. Rev. Lett.*, 86(4):680, 2001.

[214] E. Papa and A. M. Tsvelik. *Phys. Rev. B*, 63:085109, 2001.

[215] S. Lukyanov and A. Zamolodchikov. hep-th. 0102079.

[216] M. P. M. den Nijs. *Phys. Rev. B*, 23(11):6111, 1981.

[217] M. E. Fischer, M. Barber, and D. Jasnow. *Phys. Rev. A*, 8(2):1111, 1973.

[218] D. Nelson and J. M. Kosterlitz. *Phys. Rev. Lett.*, 39(19):1201, 1977.

[219] N. Schultka and E. Manousakis. *Phys. Rev. B*, 49(17):12071, 1994.

[220] K. Harada and N. Kawashima. *Phys. Rev. B*, 55(18), 1997.

[221] K. Harada and N. Kawashima. *J. Phys. Soc. Jap.* , 67:2768, 1998.

[222] H. J. Schulz. *Phys. Rev. B*, 22(11):5274, 1980.

[223] M. I. Salkola and J. R. Schrieffer. *Phys. Rev. Lett.*, 82:1752, 1999.

[224] C. A. Stafford. Private communication.

[225] F. H. L. Eßler, F. Gebhard, and E. Jeckelmann. cond-mat. 0103406.

[226] P. Brune, G. I. Japaridze, and A. P. Kampf. cond-mat. 0106007.

[227] T. Wilkens and R. M. Martin. *Phys. Rev. B*, 63:235108, 2001.

[228] S. Qin, J. Lou, T. Xiang, Z. Su, and G.-S. Tian. cond-mat. 0004162.

[229] Y. Takada and M. Kido. cond-mat. 0001239.

[230] N. Gidopoulos, S. Sorella, and E. Tosatti. *Eur. Phys. J. B*, 14:217, 2000.

[231] M. Fabrizio, A. O. Gogolin, and A. A. Nersesyan. *Phys. Rev. B*, 83:2014, 1999.

[232] K. Schoenhammer, O. Gunnarsson, and R. M. Noack. *Phys. Rev. B*, 52(4):2504, 1995.

[233] G. I. Japaridze. Private Communication.

[234] R. Zbinden. Diploma thesis, Université de Fribourg. 2001.

[235] A. Rabinovitch and J. Zak. *Phys. Rev. B*, 4(8):2358, 1971.

[236] A. Onipko and L. Malysheva. *Phys. Rev. B*, 63:235410, 2001.

[237] G. Bedürftig, B. Brendel, H. Frahm, and R. M. Noack. *Phys. Rev. B*, 58(16):10225, 1998.

Dielectric Catastrophe at the Mott Transition

C. Aebischer, D. Baeriswyl, and R. M. Noack*

Institut de Physique Théorique, Université de Fribourg, CH-1700 Fribourg, Switzerland

(Received 20 June 2000)

We study the Mott transition as a function of interaction strength in the half-filled Hubbard chain with next-nearest-neighbor hopping t' by calculating the response to an external electric field using the density matrix renormalization group. The electric susceptibility χ diverges when approaching the critical point from the insulating side. We show that the correlation length ξ characterizing this transition is directly proportional to fluctuations of the polarization and that $\chi \sim \xi^2$. The critical behavior shows that the transition is infinite order for all t', whether or not a spin gap is present, and that hyperscaling holds.

DOI: 10.1103/PhysRevLett.86.468 PACS numbers: 71.10.Fd, 71.30.+h, 75.40.Cx

A material's response to an applied electric field characterizes whether it is a metal or an insulator. One such response is the static electrical conductivity at zero temperature, which is finite for a metal (or infinite for an ideal conductor), but vanishes for an insulator [1]. The conductivity can therefore be used to probe the metal-insulator transition from the metallic side. A complementary quantity is the dielectric response to an electric field, the electric susceptibility, χ. This quantity is expected to diverge (for a continuous transition) when the transition is approached from the insulating side and to remain infinite in the metallic phase. This phenomenon, termed "dielectric catastrophe" by Mott [2], has been reported for doped silicon [3].

One possible origin of insulating behavior is the local Coulomb repulsion between electrons. This "Mott phenomenon" [4] leads to a metal-insulator transition which occurs either as the electron density, n, is varied for fixed electron-electron interaction strength or as a function of interaction strength at fixed electron density [2,5]. In this Letter, we concentrate on the transition as a function of interaction strength for fixed electron density. Experimentally, such a transition can be induced by applying isostatic or chemical pressure.

The prototype model for the Mott transition is the single-band Hubbard model with purely local interaction, whose Hamiltonian is

$$\hat{H} = -\sum_{ij\sigma} t_{ij} \hat{c}^{\dagger}_{i\sigma} \hat{c}_{j\sigma} + U \sum_{i} \hat{n}_{i\uparrow} \hat{n}_{i\downarrow} , \tag{1}$$

where $\hat{c}^{\dagger}_{i\sigma}$ creates an electron of spin σ at site i and $\hat{n}_{i\sigma} \equiv \hat{c}^{\dagger}_{i\sigma} \hat{c}_{i\sigma}$. The hopping matrix elements t_{ij} are short ranged. At half filling, $n = 1$, the Hamiltonian (1) maps onto a Heisenberg model with couplings $J_{ij} = 4t_{ij}^2/U$ for $U \to \infty$ and is thus insulating, while at $U = 0$, it describes a perfect metal. Therefore, a Mott transition must occur at some $U_c \geq 0$ [6].

In order to describe the dielectric response of such a system, one must consider the coupling to a static electric field. Taking the field in the x direction and neglecting overlaps between different Wannier functions (tight-binding approximation), we add the coupling term

$$\hat{H}_{\text{ext}} = -E\hat{X} = -E \sum_{i} x_i \hat{n}_i , \tag{2}$$

where $\hat{X}$ is the dipole operator (we have put $q = 1$), x_i is the x coordinate of the ith site, and $\hat{n}_i$ measures the occupation of this site. Here we have assumed that the finite lattice has *open boundary conditions,* i.e., the connections terminate at the lattice edges. We note that while this is the natural definition for experiments, the notion of response to an applied electric field has recently been generalized to periodic boundary conditions [7]. An applied electric field will induce a polarization at zero temperature given by

$$P = L^{-d} \langle X \rangle = -L^{-d} \frac{\partial E_0}{\partial E} \tag{3}$$

on a d-dimensional lattice with linear dimension L, where the average is taken with respect to the ground state of the full Hamiltonian $\hat{H} + \hat{H}_{\text{ext}}$, with corresponding energy E_0. The zero-field susceptibility is then defined as

$$\chi = \left. \frac{\partial P}{\partial E} \right|_{E=0} = -L^{-d} \left. \frac{\partial^2 E_0}{\partial E^2} \right|_{E=0} . \tag{4}$$

The examination of the properties of this susceptibility in the vicinity of the Mott metal-insulator transition is the principal aim of this Letter.

The susceptibility χ can be related to the eigenstates $|\Psi_n\rangle$ of $\hat{H}$ using elementary perturbation theory,

$$\chi = 2L^{-d} \sum_{n \neq 0} \frac{|\langle \Psi_0 | \hat{X} | \Psi_n \rangle|^2}{\Delta E_n} , \tag{5}$$

where ΔE_n is the excitation energy of the nth eigenstate. (Here we have chosen the origin of the coordinate system so that $\langle X \rangle = 0$ for $E = 0$.) This relation immediately yields a useful inequality in terms of the "charge gap," Δ (defined as the lowest excitation energy for which the dipole matrix element does not vanish):

$$\chi \leq \frac{2}{\Delta} L^{-d} \langle \Psi_0 | \hat{X}^2 | \Psi_0 \rangle . \tag{6}$$

It is thus instructive to consider fluctuations of the polarization, $\langle \Psi_0 | \hat{X}^2 | \Psi_0 \rangle$, which can be estimated as follows. We expand the ground state as a series $|\Psi_0\rangle = \sum_D |\Psi_0^{(D)}\rangle$, where D is the number of doubly occupied sites ("particles"). At large U the particles are located close to

 0031-9007/01/86(3)/468(4)$15.00

empty sites ("holes"). Each particle-hole pair represents an elementary dipole with essentially random orientations. Therefore our estimate is

$$\langle\Psi_0|\hat{X}^2|\Psi_0\rangle = \sum_D \langle\Psi_0^{(D)}|\hat{X}^2|\Psi_0^{(D)}\rangle \approx \langle D\rangle l^2, \quad (7)$$

where l is the average size of the dipoles. Comparing this result with the inequality in Eq. (6), we conclude that a diverging susceptibility requires either a diverging size of the dipoles or a vanishing charge gap or both. In one dimension, the quantity

$$\xi = \frac{1}{L}\langle\Psi_0|\hat{X}^2|\Psi_0\rangle \quad (8)$$

is a length characterizing the insulating phase [8,9]. We will show below that ξ is the *correlation length,* up to a dimensionless constant.

On regular lattices, one often faces the problem that the Mott phenomenon, which sets in at large values of U due to charge blocking, is masked by the opening of a charge gap at much lower values of U due to antiferromagnetic order induced by nesting or umklapp processes. In order to control such effects, we consider here a model that explicitly incorporates frustration of antiferromagnetism, namely, the one-dimensional Hubbard model with both nearest-neighbor t and next-nearest-neighbor t' hopping terms. We set $t = 1$ and consider only $t' \geq 0$ here because the sign of t' is irrelevant at half filling due to particle-hole symmetry. For $t' = 0$, the Bethe-ansatz solution allows one to calculate the charge gap [10], the charge stiffness, and the correlation length in the insulator [11] explicitly. The system is found to be insulating for all positive values of U. The metal-insulator transition occurs at $U_c = 0$ and is infinite order: the charge gap and, correspondingly, the inverse of the correlation length decrease exponentially as $U \to 0^+$. At the same time, the magnetic correlations show a power-law decay. For $t' > 0$, a weak-coupling renormalization group analysis [12] predicts the same behavior as long as there are two Fermi points: umklapp processes lead to an insulating state for $U > 0$, while the magnetic excitation spectrum remains gapless.

For $t' > 0.5$, there are four Fermi points in the noninteracting band structure and the picture becomes more complicated. In weak coupling, the lowest-order umklapp processes are marginally irrelevant [12], and the system is predicted to be metallic (vanishing charge gap) with a spin gap. At strong coupling, the model can be mapped to a frustrated Heisenberg chain, which develops a spin gap for $J'/J \sim t'^2 > 0.2412$ [13] and incommensurate antiferromagnetic order for $J'/J > 0.5$. This general picture has been confirmed numerically [14,15]. For a detailed phase diagram, we refer the reader to Fig. 3 of Ref. [15]. Here we will examine both the parameter regime with gapless magnetic excitations and $U_c = 0$ ($t' \lesssim 0.5$) and the one with gapped spin degrees of freedom and $U_c > 0$ ($t' \gtrsim 0.5$).

In order to numerically evaluate the electric susceptibility, Eq. (4), we use the density matrix renormalization group (DMRG) [16]. We apply a small electric field so that the system is in a linear response regime (as determined by a careful analysis of the E dependence, typically $EL = 0.001$) and measure

$$\chi = \frac{P}{E} = \frac{1}{LE}\sum_i x_i\langle\hat{n}_i\rangle. \quad (9)$$

We use the finite-size DMRG algorithm [16,17] on up to $L = 1000$ sites, retaining up to 2400 states for the system block. This allows us to keep the sum of the discarded density matrix eigenvalues to below 10^{-8}. We have performed extensive tests for $U = 0$, a difficult case to treat numerically, and find that we can reproduce analytic results to within less than 1%. The details of the calculations will be described more extensively elsewhere.

The electric susceptibility χ is shown in Fig. 1 as a function of the inverse system size for $t' = 0.7$ and a number of U values. There are two characteristically different behaviors: at small U, the system is metallic, and the susceptibility diverges with system size. A fit to a power law in L yields an exponent very close to 2 (within 5%) for the small U values. For $U = 0$, it can be shown analytically that $\chi \sim L^2$ for large L for all values of t'. We conjecture that such a L^2 divergence of χ is *generic* for a one-dimensional perfect metal. For larger U, χ extrapolates to a finite value as $L \to \infty$. While this is clear for the two

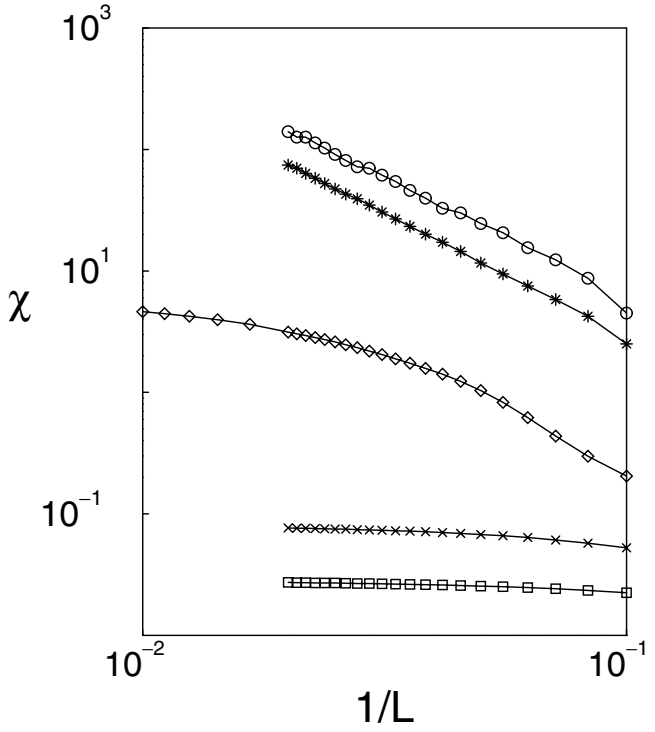

FIG. 1. Electric susceptibility, χ, as a function of $1/L$ for $t' = 0.7$ and $U = 1$ (circles), $U = 2.5$ (stars), $U = 4$ (diamonds), $U = 5.5$ (crosses), and $U = 7$ (squares).

larger U values in Fig. 1, care must be taken near the transition because the system appears metallic up to a length scale on the order of the correlation length which diverges at the transition. Such a crossover from metallic to insulating behavior is evident in the $U = 4$ curve, for which we have taken lattice sizes of up to $L = 100$ to show that χ scales to a finite value, i.e., that the system is insulating.

In the insulating regime, we expect χ to be analytic in $1/L$. We therefore perform finite-size scaling for large L using a linear fit and extrapolating to $1/L = 0$. The result, χ_∞, is shown in Fig. 2 for $t' = 0$, 0.7, and 0.8 as a function of U. Calculations for additional values of t' (0.3, 0.4, 0.5, 0.6, 0.75, 0.85, 0.9, and 1) are consistent with Fig. 2. For $t' = 0$, the transition takes place at $U_c = 0$, as discussed previously. Although we could not obtain a reliable finite-size extrapolation for $U \lesssim 2$ because the correlation length becomes much larger than the system sizes we were able to reach, we could observe numerically that $\chi \sim \Delta^{-2}$ (for $U \lesssim 10$), where Δ is the charge gap given in Ref. [10]. The extrapolation to $\Delta \to 0$ confirms that $U_c = 0$. Alternatively, we can fit to the low-U form for Δ^{-2},

$$\chi_\infty(t' = 0) = \frac{A}{U - U_c} \exp\left[\frac{B}{(U - U_c)^\sigma}\right], \qquad (10)$$

with the exactly known values $B = 4\pi = 12.566, \ldots,$ and $\sigma = 1$; here the prefactor $1/(U - U_c)$ comes from the logarithmic correction. This yields $U_c \simeq 0.058$ and we effectively find that $U_c = 0$ to within error bars. A fit to the form without the logarithmic correction would yield $U_c \simeq 0.209$, which is also consistent with zero, but to within a larger error bar.

It is clear from Fig. 2 that the bigger t', the larger the U at which χ diverges. However, one must perform careful fitting in order to accurately determine U_c and the form of the divergence at $t' > 0$, as an analytical result for the charge gap exists only at $t' = 0$. For $t' = 0.7$, we have calculated χ at many U values near the transition and have fitted to both power law, $\chi \sim (U - U_c)^\gamma$ and exponential forms [Eq. (10)], but without the logarithmic correction. The logarithmic corrections are, in general, nonuniversal, i.e., t' dependent. Leaving these corrections out, as argued above, will only make the determination of U_c less precise. We find that the fit to the power-law form yields $U_c \simeq 3.4$, a point at which careful finite-size scaling of χ yields a finite value of χ_∞. Therefore, this U_c is clearly too large. The exponential fit yields $\sigma \simeq 1.049$, $B \simeq 12.45$, and $U_c \simeq 2.67$, a more reasonable value of U_c. Note that the values for σ and B are again very close to the ones obtained for $t' = 0$. The inset of Fig. 2 shows a semilog plot of χ_∞ vs $1/(U - U_c)$ as well as the fit itself, illustrating its good quality. We therefore find that the exponential form, Eq. (10), expected in an infinite-order transition, characterizes the transition at *all* t', irrespective of whether a spin gap exists or whether U_c is finite or zero.

If hyperscaling is valid, there is only one relevant length scale ξ_∞ (the correlation length for $L \to \infty$) in the vicinity of the quantum critical point. This length then determines the finite-size scaling of the singular part of the ground state energy density [18]

$$E_0^{\text{sing}}/L^d = \xi_\infty^{-(d+z)} f(L/\xi_\infty), \qquad (11)$$

where z is the dynamic critical exponent and f a universal scaling function. The quantity EL is an energy and therefore scales like ξ_∞^{-z}. Using Eq. (4), one obtains the scaling behavior of the electric susceptibility

$$\chi = L^{2+z-d} C \Phi(L/\xi_\infty), \qquad (12)$$

where C is a nonuniversal constant that depends on microscopic details, and Φ is a universal function [19]. The hyperscaling assumption also implies that Φ tends to a finite value as $L/\xi_\infty \to 0$. This is the region in which the

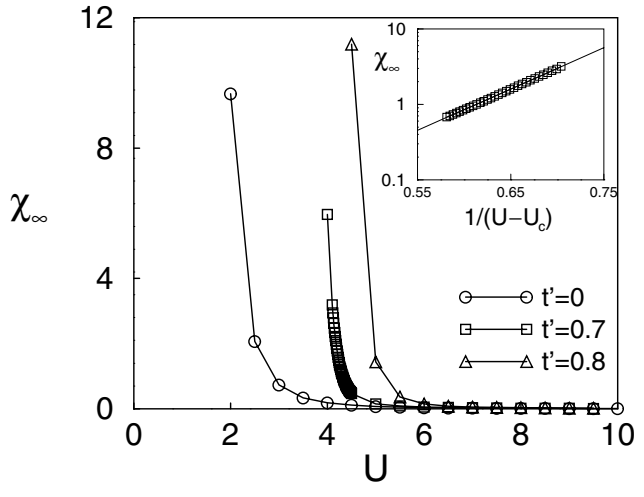

FIG. 2. Electric susceptibility $\chi_\infty(U, t')$ of the infinite-size system for $t' = 0$, 0.7, and 0.8, as a function of U; the lines are guides to the eye. Inset: $\chi_\infty(U, t' = 0.7)$ for $U = 4.1$ to 4.4 (squares) as a function of $1/(U - U_c)$, on a semilog scale. The line is a fit to an exponential form.

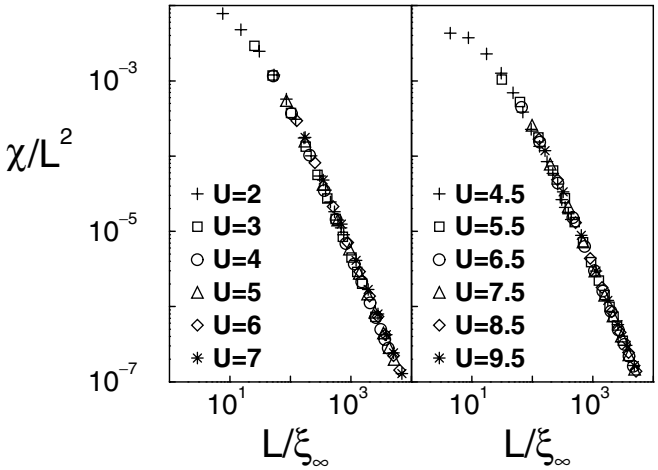

FIG. 3. Scaling plots of $\chi(L, U, t')/L^2$ vs $L/\xi_\infty(U, t')$ in a log-log scale: $t' = 0$ (left); $t' = 0.8$ (right).

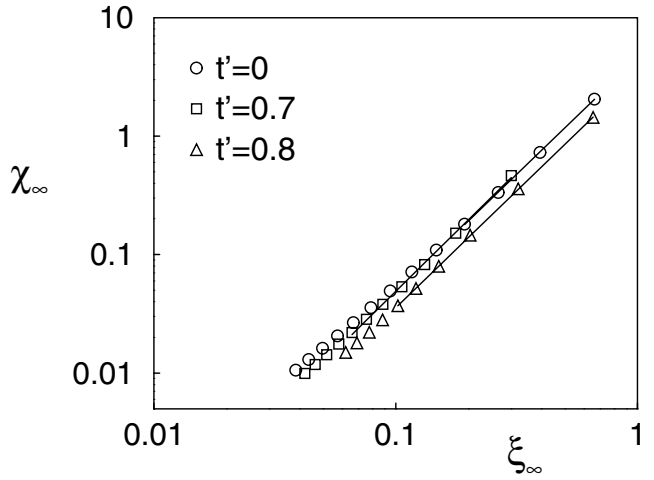

FIG. 4. Electric susceptibility χ_∞ versus correlation length ξ_∞ for different values of t'. Lines are power-law fits.

system appears metallic and in which χ tends to scale like L^2. Note that this is the same L dependence as that in the metallic phase. Thus $z = 1$ is the only consistent value in Eq. (12), in agreement with exact results for $t' = 0$ [11]. In the opposite limit, $L/\xi_\infty \to \infty$, the system behaves as an insulator for all sizes and χ tends to a finite value χ_∞. The scaling form (12) with $z = d = 1$ thus implies $\lim_{x\to\infty} \Phi(x) = A/x^2$ and

$$\chi_\infty = CA\xi_\infty^2, \tag{13}$$

where A is a universal constant.

In order to confirm the scaling form Eq. (12) for our model, we plot the DMRG results for χ/L^2 as a function of L/ξ_∞ in Fig. 3. The quantity ξ_∞ is obtained by calculating ξ on finite systems using Eq. (8) and then performing a finite-size extrapolation similar to that used to obtain χ_∞. Notice that *all* L and U points for a particular t' collapse onto the same curve, confirming hyperscaling. Therefore, ξ_∞ behaves as the correlation length, which we have checked by ascertaining that ξ_∞ is the same length (up to a constant) that characterizes the exponential decay of the density-density correlation function.

The results of the $1/L$ extrapolation for χ and ξ are shown in Fig. 4 for three different values of t'. A power-law fit to $\chi_\infty = C'\xi_\infty^{\tilde{\gamma}}$ yields $\tilde{\gamma}(t' = 0) \simeq 1.97$, $\tilde{\gamma}(t' = 0.7) \simeq 2.01$, $\tilde{\gamma}(t' = 0.8) \simeq 1.96$, and $C'(t' = 0.7)/C'(t' = 0) \simeq 1$, $C'(t' = 0.8)/C'(t' = 0) \simeq 0.7$. This confirms the scaling behavior (13). It also shows that the constant C depends weakly on t'.

In summary, our calculations for the $U - t - t'$ chain at half filling confirm that the electric susceptibility χ (and therefore also the dielectric constant $\varepsilon = 1 + 4\pi\chi$) diverge when approaching the Mott transition from the insulating side. The polarization fluctuations, which also diverge for $U \to U_c$ from above, have been found to be directly proportional to the correlation length ξ of the Mott insulating phase. In agreement with the hyperscaling hypothesis, the metallic or insulating behavior of the finite-size system depends only on the ratio L/ξ_∞. The finite-size scaling of χ can then be related to a universal scaling function and a dynamic exponent $z = 1$. The transition is found to be infinite order and to show the same critical behavior whether there is a spin gap or not. As to the origin of this dielectric catastrophe, we conclude, on the basis of both the inequality $\chi \le 2\xi/\Delta$ and the observed scaling $\chi_\infty \sim \xi_\infty^2$, that it involves both a diverging correlation length ξ (linked to the unbinding of dipoles) and a vanishing of the charge gap Δ.

We thank the Swiss National Foundation for financial support, under Grant No. 20-53800.98. Parts of the numerical computations were done at the Swiss Center for Scientific Computing. We thank F. F. Assaad, S. Daul, E. Jeckelmann, G. I. Japaridze, S. Sachdev, C. A. Stafford, and X. Zotos for valuable discussions.

*Present address: Institut für Physik, Johannes Gutenberg-Universität, D-55099 Mainz, Germany.

[1] W. Kohn, Phys. Rev. **133**, A171 (1964).
[2] N. F. Mott, *Metal-Insulator Transition* (Taylor & Francis, London, 1974).
[3] T. T. Rosenbaum *et al.,* Phys. Rev. B **27**, 7509 (1983).
[4] P. W. Anderson, in *Frontiers and Borderlines in Many-Particle Physics,* edited by R. A. Broglia and J. R. Schrieffer (North-Holland, Amsterdam, 1988), p. 1.
[5] F. Gebhard, *The Mott Metal-Insulator Transition,* Springer Tracts in Modern Physics Vol. 137 (Springer, New York, 1997).
[6] S. Sachdev, *Quantum Phase Transitions* (Cambridge University Press, Cambridge, England, 1999).
[7] R. Resta, Phys. Rev. Lett. **80**, 1800 (1998); R. Resta and S. Sorella, Phys. Rev. Lett. **82**, 370 (1999).
[8] E. K. Kudinov, Sov. Phys. Solid State **33**, 1299 (1991).
[9] I. Souza, T. Wilkins, and R. M. Martin, cond-mat/9911007 (to be published).
[10] A. A. Ovchinnikov, Sov. Phys. JETP **30**, 1160 (1970).
[11] C. A. Stafford and A. J. Mills, Phys. Rev. B **48**, 1409 (1993).
[12] M. Fabrizio, Phys. Rev. B **54**, 10 054 (1996).
[13] S. Eggert, Phys. Rev. B **54**, 9612 (1996); K. Okamoto and K. Nomura, Phys. Lett. A **169**, 422 (1992).
[14] R. Arita, K. Kuroki, H. Aoki, and M. Fabrizio, Phys. Rev. B **57**, 10 324 (1998).
[15] S. Daul and R. M. Noack, Phys. Rev. B **61**, 1646 (2000).
[16] S. R. White, Phys. Rev. Lett. **69**, 2863 (1992); Phys. Rev. B **48**, 10 345 (1993).
[17] R. M. Noack and S. R. White, in *Density Matrix Renormalization: A New Numerical Method in Physics,* edited by I. Peschel *et al.* (Springer-Verlag, Berlin, 1999).
[18] K. Kim and P. B. Weichman, Phys. Rev. B **43**, 13 583 (1991).
[19] V. Privman and M. E. Fisher, Phys. Rev. B **30**, 322 (1984).

Christophe Aebischer
Fontanettes, 9
1754 Rosé

tél.: (078) 766 99 91
e-mail: Christophe.Aebischer@unifr.ch

Curriculum Vitae

Données personelles

né le 28.1.1972 à Fribourg

8. 2. 2002	Bourse Thürler-Reeb

Etudes postgrades

1/1998-1/2002	Thèse de doctorat à l'Institut de Physique Théorique, Université de Fribourg: "Dielectric Catastrophe at the Mott Transition", investigations numérique et analytique de transitions de phase quantiques métal-isolant.
23.1.2002	Examen final de doctorat subi avec succès
16.3.2001	Examen intermédiaire de doctorat subi avec succès
5/2000	Department of Physics, University of Arizona, Tucson, USA. Collaborateur scientifique: universalité dans les transitions métal-isolant.
7/1997-11/1997	Séjour au Canada et aux Etats-Unis
10/1995-6/1997	Institut de Physique Théorique, Université de Fribourg: sous-assistant

Etudes

10/1991-3/1997	Etudes de physique à l'Université de Fribourg. Direction physique théorique, branches secondaires: mathématique et informatique
21.3.1997	Diplôme de physique, note: 6
3/1996-12/1996	Travail de diplôme: investigation numérique de la compétition entre la supraconductivité et le désordre, note: 6
15.10.1993	2ème Examen préliminaire de diplôme, note: 6
8.10.1992	1er Examen préliminaire de diplôme, note: 6

Collège

28.6.1991	Maturité latin–grec au Collège Sainte–Croix, Fribourg, note: 5.94
28.6.1991	"Prix de l'élève le plus méritant", Crédit Agricole et Industriel de la Broye

Expérience professionelle

Depuis 1/1998	Administration système Unix (12 PC linux et 3 stations de travail SGI)
Depuis 1/1998	Assistanat: direction des exercices et des travaux de diplômes

Connaissances informatiques

Systèmes d'exploitation	Linux, Unix (très bien)
Programmation	C, Perl, Mathematica, Pascal (très bien) Matlab, IDL (Interactive Data Language), Fortran (bien) C++, Java (connaissances de base)

Langues (écrites et parlées)

Francais	langue maternelle
Anglais	couramment
Allemand	très bien
Italien	très bien
Espagnol	bien
Arabe	connaissances de base

Publications

C. Aebischer, D. Baeriswyl, and R .M. Noack, "Dielectric Catastrophe at the Mott Transition", Phys. Rev. Lett. **86**, 468 (2001)

R. M. Noack, C. Aebischer, D. Baeriswyl, and F. Gebhard, "Studies of the Mott–Hubbard Transition in One and Infinite Dimensions", Proc. NATO Workshop on "Open Problems in Strongly Correlated Systems", Kluwer, Dordrecht, 2000

M.A.N. Araujo, M. Dzierzawa, C. Aebischer, and D. Baeriswyl, "Cooper–Pair Delocalization in Disordered Media", Physica B **244**, 9 (1998)

Présentations orales

21.5.2001	Fachbereich Physik, Universität Marburg, "Dielektrische Katastrophe an Metal–Isolator Übergängen"
17.5.2001	Institut für Physik, Universität Mainz, "Dielektrische Katastrophe an Metal–Isolator Übergängen"
15.2.2001	"Korrelationstage 2001", Max–Planck Institut, Dresden, "Dielectric Catastrophe at the Mott Transition"

24.11.2000 Institut de Physique Théorique, Université de Neuchâtel, "Dielectric Catastrophe at the 1D Mott Transition"

15.6.2000 Institut de Physique Théorique, Université de Fribourg, "Caractérisation de la transition de Mott à l'aide de la susceptibilité électrique et de la longueur de corrélation"

22.4.1999 Institut für Theoretische Physik III, Universität Stuttgart, "The Electric Susceptibility as a Tool to Study the Mott Metal–Insulator Transition"

12.11.1998 "Rencontre sur les Systèmes fortement corrélés", Neuchâtel, "DMRG Calculations of the Electric Susceptibility in the Hubbard and the U–t–t' chains"

Posters

4/2000 NATO Advanced Research Workshop "Open Problems in Strongly Correlated Electron Systems", Bled (Slovenia), "Characterizing the Mott Transition with the Electric Susceptibility and the Correlation Length"

3/2000 18th General Conference of the Condensed Matter Division of the European Physical Society, Montreux, "Characterizing the Mott Transition with the Electric Susceptibility and the Correlation Length"

10/1999 "Swiss Workhop on Superconductivity and Materials with Novel Electronic Properties", Les Diablerets, "Characterizing the Mott Transition with the Electric Susceptibility"

6/1999–7/1999 "Computational Techniques for Strongly Correlated Systems", Abdus Salam ICTP Trieste (Italy), "Investigating the Mott Transition with DMRG"

10/1996 "Swiss Workhop on Superconductivity", Les Diablerets, "The Cooper–Pair Problem with Non–Magnetic Disorder"